AUS DER ABTEILUNG
MOLECULAR CELL BIOLOGY LABORATORY
DEPARTMENT OF NEUROLOGY

DER FAKULTÄT FÜR MEDIZIN
DER UNIVERSITÄT REGENSBURG

POST-TRANSLATIONAL MODIFICATION AND REGULATION OF HUMAN SPIR PROTEIN

Inaugural – Dissertation
zur Erlangung des Doktorgrades
der Biomedizinischen Wissenschaften

der
Fakultät für Medizin
der Universität Regensburg

vorgelegt von

SREEJA LAKSHMI

2011

Dekan:	**Prof. Dr. Dr. Torsten E. Reichert**
1. Berichterstatter:	**Prof. Dr. Eugen Kerkhoff**
2. Berichterstatter:	**Prof. Dr. Jens Schlossmann**
Tag der mündlichen Prüfung:	**13/12/2011**

Erklärung

Hiermit versichere ich, dass ich die vorliegende Arbeit selbständig angefertigt und keine anderen als die hier angegebenen Quellen und Hilfsmittel verwendet habe.

……

Sreeja Lakshmi

To my loving parents

&

Preetham

Abstract

Spir proteins are the primodial members of the emerging group of actin nucleation factors, which initiate actin polymerization by binding monomeric actin to one or multiple Wiskott-Aldrich Syndrome protein (WASp) homology-2 domains. Spir proteins are implicated in diverse cellular processes including actin dynamics, vesicle trafficking as well as *Drosophila* and mammalian oogenesis. Despite the biological roles of Spir was interpreted to an extent in the fields of protein and membrane interactions, the exact mechanisms by which the protein is regulated is still exists to be unknown. A previous study by Otto *et al.,* (2000) disclosed Drosophila p150-Spir as a direct link between JNK (c-Jun N-terminal kinase) and actin organization, by being a downstream target of JNK function. The p150-Spir was phosphorylated by a constitutively active form of JNK, JNK-MKK7, both *in vivo* and *in vitro*. This finding came up with a new proposal for the regulatory mechanism for the Spir proteins, through the phosphorylation by Mitogen-activated protein kinases, eventhough a comprehensive phosphorylation profile was not convincingly uncovered.

Phosphorylation of proteins being one of the most relevant and ubiquitous post-translational modification, it carries interest as well as importance to gain more insights into the influence phosphorylation on the biological activities of Spir. In analogy with the previous finding, the present study is directed to elucidate the phosphorylation profile of mammalian Spir proteins, which has not been addressed yet. Precise identification of phospho-residues was carried out by combining biochemical and contemporary mass spectrometry analysis.

Mammals exhibit two Spir proteins, Spir-1 and Spir-2. Using nano LC-MS/MS (nano-Liquid Chromatography Tandem Mass spectrometry), the present study could localize the phosphorylated aminoacids in peptide sequences with three phospho-moieties reliably. Following the identification and characterization of phosphorylation sites, description of the biological events following the phosohorylation was depicted. Formin proteins are well known to be the prominent interaction partners of the Spir. Recently, it was identified that both mammalian Spir proteins interact with both mammalian Fmn subgroup proteins, formin-1 and formin-2 and the interaction is mediated by the KIND domain of Spir and and the Formin Spir Interaction (FSI) sequence at the very C-terminus of the Fmn proteins. (Pechlivanis *et al.,* 2009). Concomitantly, the autoregulatory interaction mediated by the N-terminal KIND domain and the C-terminal FYVE domain was also characterized by the phopshorylation. The study will generate a unique knowledge regarding the influence of post-translational modification on the regulatory events of Spir proteins by analysing inter and intra molecular interactions with the accompaniment of protein interaction studies.

Zusammenfassung

Spir Proteine sind primodiale Elemente einer neuen Gruppe von Aktin-Nukleations-Faktoren, die Aktin Polymerisation initiieren, indem sie Aktin Monomere an ein oder mehrere Wiskott-Aldrich-Syndrom Protein Homologie-2 Domänen (WASp) binden. Spir Proteine werden mit diversen zellulären Prozessen in Verbindung gebracht, einschließlich Aktin-Dynamik, Vesikel-Transport und Oogenese in Drosophila und Mammalia. Obwohl die biologische Rolle von Spir bezüglich Protein und Membran-Interaktionen zu einem gewissen Ausmaß untersucht wurde, sind die genauen Mechanismen der Protein Regulation immer noch unbekannt. Eine vorangegangene Studie von Otto *et al*., (2000) deckte Drosophila p-150 Spir als direkten Link zwischen JNK (c-Jun- N-terminale Kinase) und Aktin Organisation auf und identifizierte p-150 Spir als *downstream target* von JNK. Das p-150 Spir wurde sowohl *in vivo* als auch *in vitro* von einer konstitutiv aktiven Form von JNK, JNK-MKK7 phosphoryliert. Durch die Phosphorylierung Mitogen- aktivierter Proteinkinasen erkannte man einen neuen Ansatz für Mechanismen zur Regulation von Spir Proteinen, obgleich ein umfassendes Phosphorylierungsprofil nicht beschrieben werden konnte. Da es sich bei der Phosphorylierung von Proteinen um eine der wichtigsten und universellsten Formen der posttranslationalen Modifikation handelt, ist es sowohl von Interesse als auch von Bedeutung mehr Einblicke zu bekommen, wie Phosphorylierung von Spir die biologische Aktivität des Proteins beeinflusst. Analog zu den vorherigen Erkenntnissen hat die vorliegende Studie die Aufklärung des Phosphorylierungsprofils der Spir Proteine in der Klasse der zum ziel Mammalia. Phosphorylierungsstellen wurden mit Hilfe biochemischer und modernster massenspektrometrischer Methoden präzise identifiziert. Die Klasse der Mammalia weist zwei Spir Proteine auf, Spir- 1 und Spir-2. Die vorliegende Untersuchung konnte durch den Einsatz von LC-MS/MS (nano-Liquid Chromatography Tandem Mass spectrometry) die phosphorylierten Aminosäuren in der Peptid Sequenz mit drei Phosphorresten zuverlässig identifizieren. Nach Identifizierung und Charakterisierung der Phosphorylierungsstellen wurde eine Beschreibung der biologischen Ereignisse, welche auf einer Phosphorylierung beruhen, dargestellt. Formin Proteine sind bedeutende Interaktionspartner von Spir. Kürzlich wurde herausgefunden, dass beide Säuger-Spir- Proteine mit beiden Säuger-Fmn-Untergruppen Proteinen, formin-1 und formin-2, interagieren und dass die Interaktion über die KIND Domäne von Spir und der Formin Spir Interaction (FSI) Sequenz des C- Terminus der Fmn Proteine erfolgt. (Pechlivanis *et al*., 2009) Begleitend wurde die autoregulierte Interaktion, die durch die N-terminale KIND Domäne und die C-terminale FYVE Domäne vermittelt wird, durch die Phosphorylierung charakterisiert. Die Studie wird wichtige Erkenntnisse über den Einfluss posttranslationaler Modifikationen von Spir Proteinen generieren, indem inter-und intramolekulare Interaktionen zusammen mit Protein Interaktionsstudien durchgeführt werden.

Table of Contents

1. Introduction

The cellular cytoskeleton is an intricate network of filamentous proteins. The cytoskeleton confers upon the cells to resist deformation, to change shape during movement and act as a scaffolding for the attachment of many organells. Actin filaments, microtubules and intermediate filaments are equally involved in making up the cytoskeleton as well as undergo continual reorganization as a necessary requirement for cellular and morphological dynamics and motility.

1.1. Biology of Actin

Actin is a universal protein expressed in all organisms of the present day world. Since it´s discovery in 1942 (Bruno.F.Straub), actin has seen a long and fruitful period of investigations. It is manily located in the cytoplasm of the cells but is also present in nucleus (Dos Remedios *et al*., 2003). Until a short time ago, actin was thought to have only evolved in eukaryotic cells. Recently, prokaryotic proteins, like Murein formation cluster E B (MreB) and Partitioning M (ParM), with structural similarities to eukaryotic actin assemble into filaments have been discovered indicating their representment as ancestral actin cytoskeleton (Campellon and Welch, 2010).

Actin filaments are major components of at least 15 distinct structures in metazoan cells. They get assembled in response to different stimuli into a multifarious higher-order cellular structures ranging from lamellipodia to microvilli, each exicuting diverse cellular functions. The most cited assemblies of actin include muscle sarcomeres, synapses, membrane protrusions like-lamellipodia/lamella, ruffles, phagocytic cups, podosomes and invadopodia, filopodia and microvilli, stress fibers and the contractile ring (Higgs and Chabbra, 2007; Welch and Mullins, 2002; Small, Rottner and Kaverina, 1999). Thus the actin cytoskeleton participates in many important cellular processes like muscle contraction, cell motility, cell division and cytokinesis, vesicle and organelle movement, cell signalling and the establishment and maintenance of cell junctons and cell shape.

To perform all these functions, the constitution of actin cytoskeleton must be tightly regulated, which comprise the organization of actin monomers into actin polymers and further to filamentous network. A large repertoire of interacting partners that are still increasing in number, orchestrate spatial and temporal control of these phenomena which attribute versatile functions to actin.

1.2. Actin : Structure and Dynamics

1.2.1. Actin structure

Actin is one of the most abundant and highly conserved protein in eukaryotic cells that fall into three broad classes: α, β and γ-isoforms.

Actin, the chief component of the actin cytoskeleton, exist in two forms in the cell: monomers (G-actin or globular actin; Figure 1A) and filaments (F-actin or filamentous actin; Figure 1B).

Monomeric actin (G-actin) is composed of a single polypeptide chain of about 375 aminoacids resulting in an approximately 43 KDa protein. The first atomic-resolution 3D structure of G-actin in complex with DNase I was proposed by Kabsch *et al*., in 1990. G-actin has two main domains each of which is subdivided into 4 subdomains (here they are represented as I -IV). N- and C- termini are both present in subdomain I. The main domains are seperated by a deep cleft, which occupies a tightly bound adenosine-derived nucleotide with a divalent cation (Mg^{2+} or Ca^{2+}) (Kabsch *et al*., 1990). The bound nucleotide contacts residues from all four subdomains and functions as the coordinating center of the molecule (Page *et al*., 1998). The most favourable state for actin filament assembly is Mg-ATP-G-actin in the physiological state since Mg-ATP-actin nucleates about three orders of magnitude faster than Ca-ATP-actin (Estes *et al*., 1992). The actin molecule can undergo conformational changes according to the nucleotide and cation state or depending on the actin binding proteins (Schüler *et al*., 2001).

Filamentous actin (F-actin) is formed by the reversible endwise polymerization of monomeric G-actin. The first high-resolution structural model of the actin filament at a resolution of 8 A° was proposed by Holmes *et al*., in 1990. The filaments are of approximately 7-10 nm in diameter. F-actin appears morphologically as either a single-start left-handed helix or two right-handed helices that slowly rotate each other (Chabbra. D and Dos Remedios, 2010). Actin filaments are polar structures with two ends that are differentiated by their structural and biochemical characterestics (Welch and Mullins, 2002). This polarity is key to the mechanism of actin assembly in cells. The fast growing end is called the barbed or (+) end and the slow growing end is the pointed or (-) end. The nomenclature of the filament is based on the arrowhead-like appearance of the F-actin when decorated with myosin subfragment I (S-I). These ends correspond to subdomains I and III and subdomains II and IV, respectively (Dos Remedios *et al*., 2003).

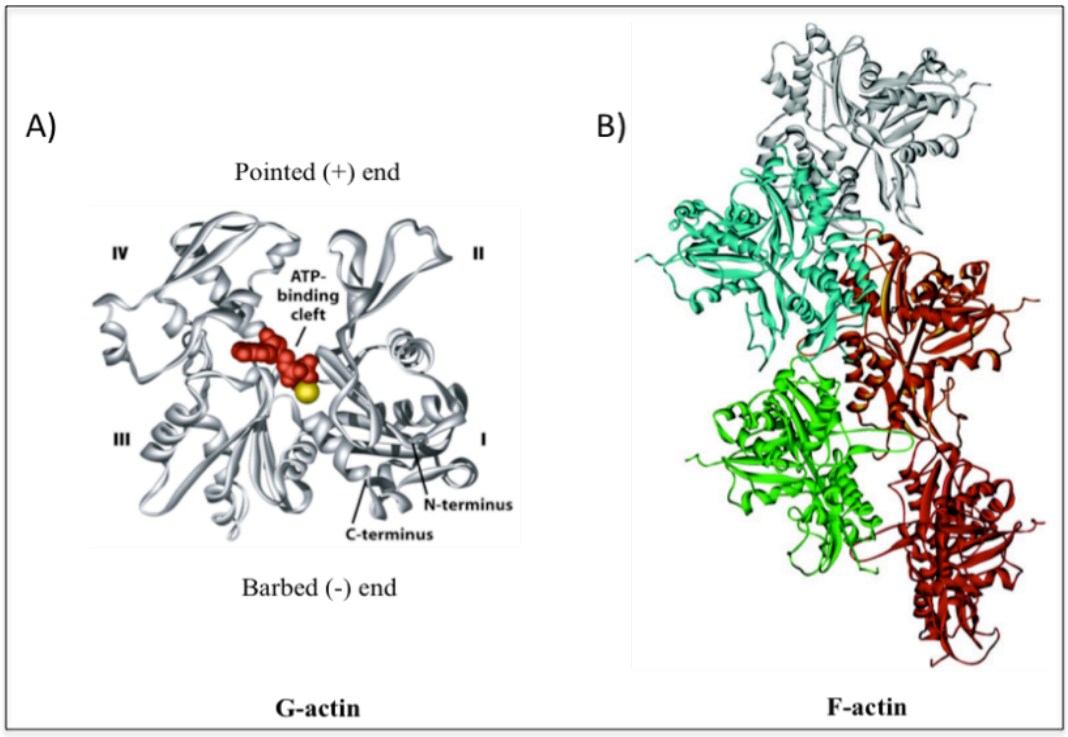

Figure 1. Ribbon representations of molecular structures of naturally occuring forms of actin. A) Crystal structure of monomeric G-actin (PDB code:1J6Z) with nucleotide binding cleft (ATP in G-actin and ADP in F-actin) (red) and divalent cation (gold). Locations of the subdomains marked and numbered from I-IV (Kabsch *et al.,* 1990). Exposed subdomains I and III, and II and IV represent barbed and pointed ends respectively. B) Holmes model of F-actin (Holmes *et al.,* 1990) with individual actin monomers in five different colours.

1.2.2. Actin dynamics

Actin polymerization is a classic example of self assembly and the cells regulate all aspects of actin assembly through a fascinating repertoire of proteins (Pollard, 2007). Polymerization involves three main features: 1) a slow initial association of actin monomers to a dimer that is more likely to rapid dissociation to monomers than association, (kinetics place the dissociation equilibrium constant for an actin dimer as high as 4-5 M (Welch and Mullins, 2002)); 2) The formation of a stable trimer that represents the nucleus of polymerization, a state where actin assembly is more likely than disassembly; and 3) the elongation phase during which actin monomers are rapidly assembled (Dos Remedios *et al*., 2003) (Figure 2).

The relative instablity of polymerization intermediates and the actin monomer binding proteins (ABPs), that buffer the large pool of actin monomers in the cells, supress the spontaneous actin polymerization. This makes nucleation as the rate limiting step in filament formation. Actin nucleation is the assembly of a stable F-actin like “seed“ from ATP actin (Winkler and Schafer, 2007). A minimum of three actin molecules need to be assembled to

form a polymerization-competent nucleus (Qualmann and Kessels, 2009). The factors that help to overcome the kinetic barrier to filament nucleation and elongation are called actin nucleation factors, which control the time and location of polymerization and influence the structures of actin networks they generate (Pollard, 2007; Chesarone and Goode, 2009; Dominguez and Holmes, 2010).

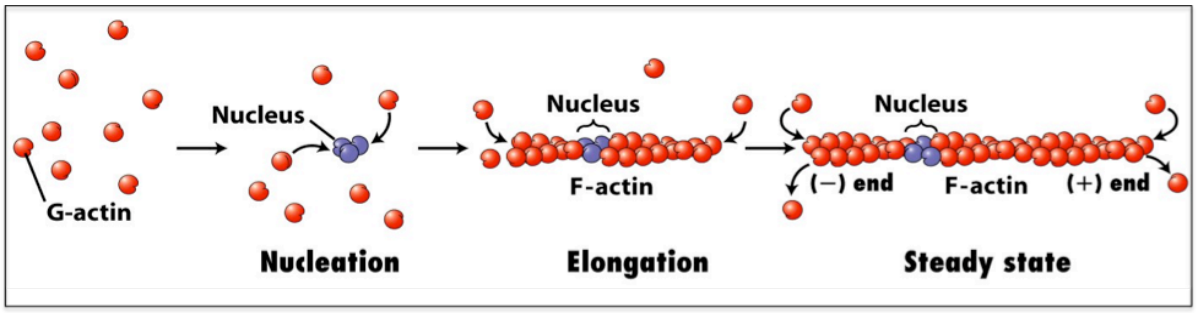

Figure 2. The stages in the polymerization of monomeric G-actin to form filamentous actin. G-actin carrying ATP will form a stable nucleus in the process, nucleation, which enable the binding of succeeding actin monomers and undergo elongation to give rise to filamentous, F-actin. Addition of G-actin take place at the barbed end. As the filament ages, ATP get hydrolysed to ADP and depolymerization of ADP-G-actin take place at the pointed end of the filament. The released ADP is exchanged for ATP to take another G-actin inorder to start a new cycle of polymerization. (Adapted from Molecular Cell Biology, 6th Edition).

An actin filament is structurally assymmetric which is reflected in a difference in rate of addition of G-actin at two ends- elongation at the barbed end is 10-20 times faster than that at the pointed end. Subunit addition at the barbed end is determined by the Critical concentration (C_c) of G-actin. Under physiological conditions in the cell, C_c of Mg-ATP actin is lower at the barbed end (0.1μM) and than at the pointed end (0.7μM) (Weber A. 1999). Thus polymerization take place by the preferential addition of ATP-loaded actin monomers primarily at the barbed end since the critical concentration of the actin monomers, is lower at the barbed end than at the pointed end. Hydrolysis of ATP by polymerized actin and dissociation of the γ-phosphate appear to be an internal timer that indicates the age of a filament and triggers processes that disassemble actin filaments in cells (Pollard, 2003). As the filament ages, ATP is hydrolyzed to ADP and inorganic phosphate (Pi) is released. ATP hydrolysis is irriversible and fast with a half time of about 2s and phosphate dissociation is much slower with a half time of 350s, so ADP-Pi-actin is relatively long-lived intermediate in freshly assembled filaments. The different rates of monomer association and dissociation at the two ends eventually developes a “steady state“ where the pointed end depolymerization replenishes the G-actin for the barbed end polymerization enabling the filament to perform “treadmilling“. The process will result in the net incorporation of ATP-actin at the (+) end

which equalizes the loss of ADP-actin at the (-) end. The released ADP-actin gets recharged with ATP for another round of polymerization (Qualmann and Kessels, 2009; Dos Remedios *et al*., 2003; Baum and kunda, 2005; and Pollard, 2003).

In vivo, all steps in actin dynamics are controlled and modulated by actin-binding proteins. Efficient exchange of ADP for ATP is ensured by G-actin binding protein, profilin. Thymosin β4 control the pool of non-filamentous actin in cells by binding to actin monomers. Capping proteins, at the pointed end, serves protection from depolymerization and at the barbed end, stop actin polymerization reactions, therefore prevent excessive actin filament polymerization.

1.3. Actin nucleation machinary

Current knowledge on the complexity of nucleation mechanisms has tremendously increased with a vast array of nucleators and nucleation mechanisms. They can be divided into three principal groups, the Arp2/3 complex and it´s large family of nucleation promoting factors, formins and WH2 domain - containing nucleators. Apart from the short description of Arp2/3 complex and formins, the rest of this thesis book gives a close-grained illustration of the novel class of actin nucleation factor, Spir, a WH2 domain - containing nucleator, that may allow a better understanding of it´s functions and localization.

1.3.1. The Arp2/3 complex

Arp2/3 complex, the founding member of actin nucletaion factors, was first isolated from *Acanthamoeba castellanii* (Machesky *et al.,* 1994). The 220 KDa complex is composed of seven stably associated polypeptides that are highly conserved in virtually all eukaryotic organisms (Goley and Welch, 2006). The polypeptides comprise two name giving actin-related proteins, Arp2 and Arp3, held together by five additional Arp2/3 complex components (ARPC), ARPC1 (p41-Arc), ARPC2 (p34-Arc), ARPC3 (p21-Arc), ARPC4 (p20-Arc) and ARPC5 (p16-Arc). Metazoans, fungi, amoeba and plants express all of these subunits (Pollard, 2007). The crystal structure of bovine Arp2/3 complex at 2.0 A° was solved by X-ray crystallography giving insights to it´s organization and functions (Robinson *et al*., 2001).

Among the known nucleators, Arp2/3 complex is unique in it´s ability to nucleate filaments as well as to organize them into branched networks. Arp2/3 complex is referred to as the primary nucleator of actin filaments in most crawling cells owing to their localization in lamellipodia and pseudopodia in the leading edge of the motile cells. The complex is also functionally important for actin polymerization during phagocytosis (May *et al*., 2000).

The actin-related proteins Arp2 and Arp3 are postulated to mimic an actin dimer and serves as a nucleation site. Upon binding to an existing filament, Arp2 and Arp3 likely

reorient into a dimer that acts as the first two subunits of the new filament. The ARPC2–ARPC4 heterodimer provides the main surface for interaction of the complex with the mother filament and anchors Arp3, the first subunit of the daughter filament (Campellone and Welch, 2010). Arp2/3 complex has only a very moderate actin nucleation capacity on it´s own, but can be activated by binding to nucleation-promoting factor (NPF) proteins (Goley and Welch, 2006). In presence of nucleation promoting factors, Arp2/3 complex catalyzes the actin polymerization by binding to the sides of an existing (mother) filament and initiates the assembly of a new (daughter) filament in a Y-branch configuration with a 70° branch angle (Campellon and Welch, 2010) (Figure 3). This will generate highly branched actin filaments that form entangled ´dendritic` networks and is central to it´s functions *in vivo*. Although actin filaments are flexible, branch junctions appear to be very rigid (Blanchoin *et al*.,2000). Potent nucleation also requires phosphorylation of Thr or Tyr residues in Arp2 (LeClaire III *et al*., 2008).

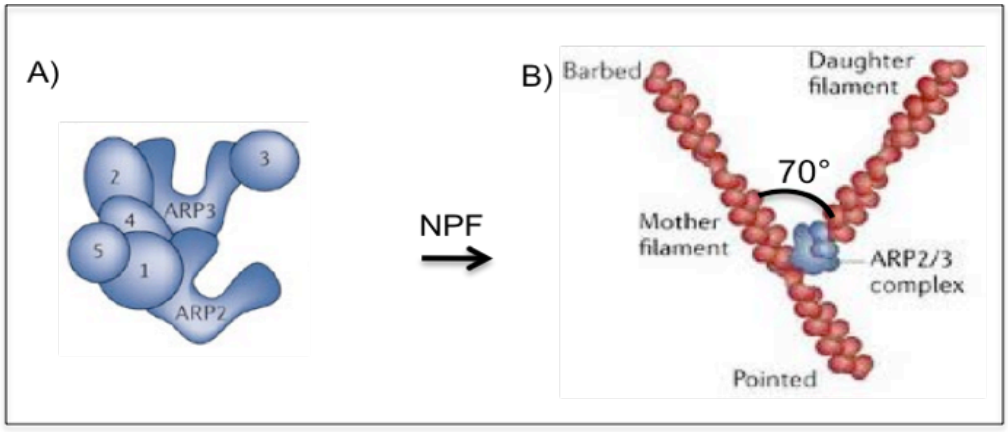

Figure 3. Schematic representation of Arp2/3 complex and the actin filament elicited by the complex. A) Cartoonic representation of Arp2/3 complex- a seven subunit protein complex containing Arp2, Arp3 and five additional subunits, ARPC1-5. **B)** When activated by nucleation promoting factors (NPF) the Arp2/3 complex initiates the formation of new actin filaments from the sides of existing mother filaments in a Y-branch configuration with a regular branch angle of 70° (Goley and Welch, 2006).

NPFs, are classified into Class1 and Class II based on the mechanism by which they activate Arp2/3 complex and their effect on the Y- branching reaction (Goley and Welch, 2006). Class 1 NPFs- bacterial protein ActA, WASP (Wiskott-Aldrich syndrome protein), WASP family verproline homologue (WAVE; also known as SCAR), WASP and SCAR homologue (WASH), WASP homologue associated with actin, membranes and microtubules (WHAMM) and junction-mediating regulatory protein (JMY). All proteins of WASP family possess a common c-terminal WCA domain with a W (WH2) domain binding to G-actin, amphipathic connector (C) region and an acidic (A) peptide that collectively bind Arp2/3

complex and thus activate the complex to polymerize branched actin filaments (Campellon and Welch, 2010). Class II include *S.cerevisiae* actin binding protein-1 (Abp1) (Goode *et al*., 2001), Pan1 (Duncan *et al*., 2001) as well as metazoan cortactin (Weaver *et al*., 2001), possessing an F-actin binding region rather than the G-actin binding W domain in Class 1 NPFs. NPFs are typically found associated with membranes, and they specify the front of a cell, ensuring that the nucleation of new filaments in a dendritic actin-filament network occurs only from filaments growing towards the membrane (Fletcher and Mullins, 2010). The activities of NPFs, in turn, are tightly regulated by the Rho-family GTPases, Cdc42 and Rac (Higgs and Pollard, 2000). Improper functioning of the ARP2/3 complex and its regulators can lead to disease like WAS, X-linked genetic disorder, caused by mutation in WASP encoding gene (Goley and Welch, 2006). The complex disfunction might also be associated with cancer metastasis (Wang *et al*.,2005) and might represent targets for the therapeutic invention.

1.3.2. Formins

Formins are a group of recently emerged key regulators of actin polymerization, which promote not only nucleation but also processive barbed-end elongation (Goode and Eck, 2007). Formins catalyze the formation of unbranched (linear) actin filaments involved in actin-based processes including polarized cables in budding yeast, contractile rings and interphase cables in fission yeast and stress fibers and filopodia in animal cells (Paul and Pollard, 2009 ; Dahlgaard *et al*., 2007).

Formins are named for the mouse *limb deformity* (ld) gene, the first formin gene identified (Zigmond, 2004). Even though much of knowledge regarding the structure and biochemical activity of formins were originated from the studies in yeast homologue Bni1 (Schönichen and Geyer, 2010), nucleation activity has since been observed for vertebrates. Phylogenetic analysis have classified the fifteen distinct mammalian formin genes into 7 subfamilies– Diaphanous formins (Dia 1, -2 and -3), Dishevelled-associated activator of morphogenesis (DAAM-1 and -2), formin-related proteins identified in leucocytes (FRL-1, -2 and -3; also called FMNL-1, -2 and -3), `Inverted` formins (INF-1,-2), Formin homology domain proteins (FHOD-1,-2), Delphilin and formin sub family of Formins (Fmn-1 and Fmn-2) (Higgs and Peterson, 2005; Goode and Eck, 2007).

Formins are large multidomain proteins of > 1000 aminoacid residues that are composed of various combinations of different functional domains. Formins are defined by a unique and highly conserved C-terminal formin homology 2 (FH2) domain usually flanked by formin homology 1 (FH1) domain, N-terminal to FH2 domain (Figure 4) (Faix and Grosse, 2006). The N-terminal part is very divergent within the formin protein family.

FH2 domain typically ~ 400–500 amino acids long, is necessary and sufficient for actin nucleation. The domain mediates actin binding, actin nucleation and processive capping. The FH2 domains form homodimers, which assume a ring-like structure that encircles the elongating actin filament at its fast-growing end, promoting its elongation and protecting it from other capping proteins. Thus FH2 domain appears to be a processive cap that walks with the barbed end of the filament as it elongates. FH2 domains are active as dimers (Moseley *et al,* 2004) and mutations that disrupt the dimerization abolish actin polymerization activity (Xu *et al,* 2004).

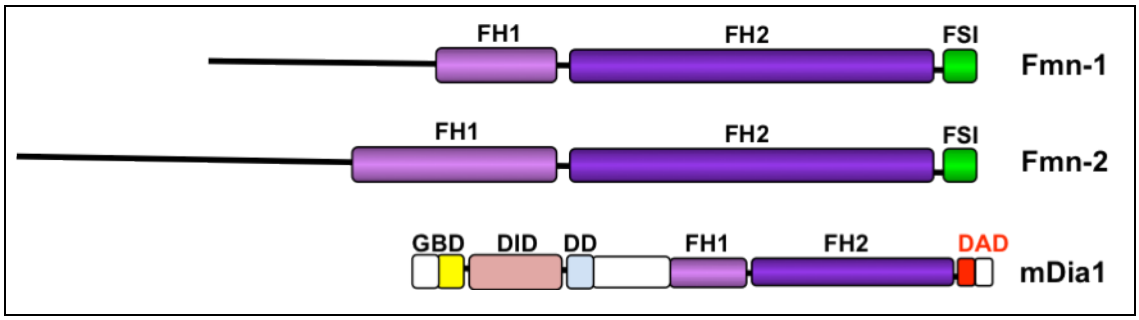

Figure 4. Domain array of mammalian formin proteins, Fmn-1, Fmn-2 and mDia1. Mammalian formin-1 (mm formin-1), mammalian formin-2 (mm formin-2) proteins correspond to Swiss-Prot entry numbers Q05860 and Q9JL04 are shown. Proline rich FH1 domain is succeeded by actin binding FH2 domain. FH1 domain of Fmn-2 has extensively repeated proline motifs. At the very C- terminus a conserved sequence motif, FSI is depicted, which is unique for Fmn subfamily of formins. Several members of the formin superfamily contain an autoregulatory peptide (DAD) in their C-termini at the position where the FSI sequence is located. In Diaphanous family formins (the structure of mDia1 protein is shown) the intramolecular interaction between the C-terminal DAD domain and a N-terminal DID results in an autoinhibited conformation of the formin proteins. Abbreviations: FH1, Formin homology 1 ; FH2, Formin homology 2; FSI, Formin Spir Interaction sequence; GBD, GTPase binding domain; DID, Diaphanous inhibitory domain; DD, Dimerization domain; DAD, Diphanous autoregulatory domain.

The FH1 domain is a proline-rich region that binds to profilin–actin complexes and enhances the delivery of new actin monomers onto the growing filaments (Paul and Pollard, 2008). Two principal roles of the FH1 domain is appeared to be, 1) the FH1 domain is required for formins to efficiently use profilin-bound actin to build filaments; 2) FH1-profilin interactions increase the rate of filament elongation. In short, FH2 domain is sufficient in catalyzing the filament nucleation where as FH1 domain in stimulating filament elongation.

Mammalian Fmn subgroup of formins possess a FSI (Formin Spir Interaction) sequence at the very C-terminus of the protein which mediate the interaction with the KIND domain of mammalian Spir proteins (Figure 4) (Pechlivanis *et al*., 2009).

Formins govern two distinct phases of actin assembly: nucleation and elongation (Figure 5). The mechanism of actin assembly primarily involves the high affinity binding of their dimeric donut-shaped FH2 domains to the barbed ends of actin filaments. Since FH2 domain lacks detectable affinity for actin monomers, it has been hyothesised that they catalyze polymerization by binding and stabilizing spontaneously formed actin dimers or trimers and thus defeating the kinetic hurdle (Pring *et al*., 2003). These interactions depend on the ability of FH2 domains to dimerize. Each functional half of the FH2 dimer is called a `hemi-dimer`or bridge and contains two F-actin-binding sites (Ottomo *et al*., 2005). During the filament elongation FH2 dimer exists in alternating morphologies at the barbed end – `open` and `closed` structural states. In closed conformation, both FH2 monomers bind the two terminal actin subunits at the filament end, blocking further actin incorporation. In open conformation, actin incorporation is enabled and the barbed end can assoiate with a new actin subunit (Campellone and Welch, 2010). Once a filament is nucleated, the dimeric FH2 domain moves processively with the growing barbed end, shielding it from capping proteins terminating the elongation, while permitting the rapid addition of new subunits.

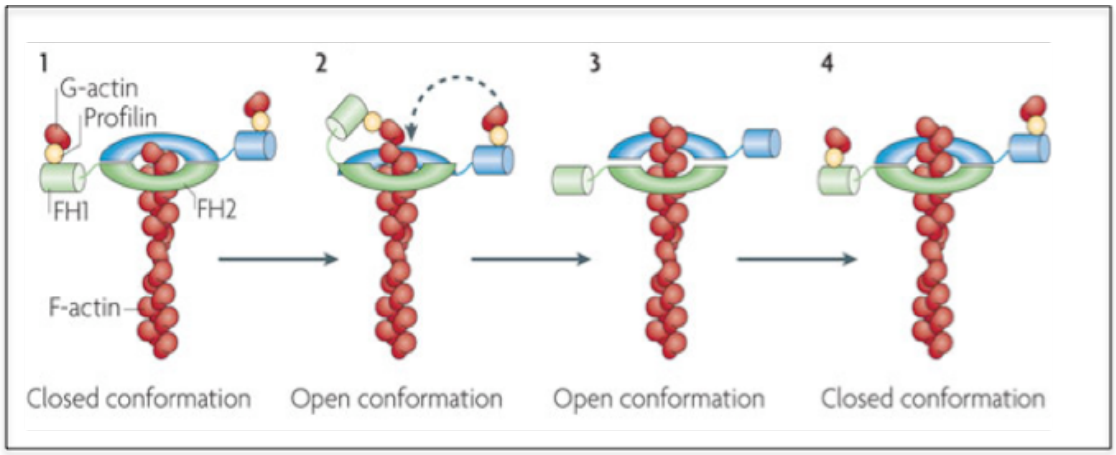

Figure 5. Actin nucleation by formins. Formins are large multidomain proteins that initiate the polymerization of unbranched actin filaments. The formin homology-2 (FH2) domain initiates filament assembly and remains associated with the fast-growing barbed end, enabling further addition of actin subunits while protecting the end from capping proteins. Proline rich formin homology-1 (FH1) domain, recruits profilin–G-actin complexes to the barbed ends of the growing filament (Pieta K. Mattila & Pekka Lappalainen, 2008).

Following nucleation, the adjecant Pro-rich FH1 domain comes in action for the subsequent elongation of the filament. Profilin is a ubiquitous actin monomer binding protein with separate binding sites for monomeric actin and polyproline tracts. Therefore, the interaction between profilin and the FH1 domain are crucial for the recruitment of new ATP-

G-actin residues from profilin-actin complexes to the FH2 domain for incorporation into the growing filaments at their barbed ends (Chesarone, DuPage and Goode, 2010; Faix and Grosse, 2006). FH1-FH2 dependent acceleration of barbed end elongation is as much as 5-fold over the rate of elongation at the free barbed ends (Kovar *et al.*, 2006).

Regulation of formins appears significantly different for every formin family (Schönichen and Geyer, 2010). Many formins `rest` in an autoinhibited state in the cytosol and must be activated by specific ligands. Rho family GTPases are known to play an important role in activating both mammalian and yeast systems (Heasman and Ridely, 2008).

The best understood mechanism of regulation is the autoinhibitory interaction which was well studied in Diaphanous-related formins (DRFs), a conserved subfamily of formins and known to be the direct effectors of Rho-family GTPases as well. The DRFs include the Dia, DAAM and FRL formins in mammals and Bni1, Bnr1 and SepA in yeast (Goode and Eck, 2007). Formin autoinhibition is mediated by interactions between the N- and C-terminal functional halves. The actin assembly apparatus in the C-termini encompass FH1-FH2 module and the Diaphanous auto-regulatory domain (DAD). The N-termini is the regulatory region which include GTPase binding domain (GBD), which binds to Rho family GTPases, Diaphanous inhibitory domain (DID), that participate in autoinhibition, the dimerization domain (DD) and a coiled-coil region (Li and Higgs, 2003; Ottomo *et al*., 2005). The binding of DAD to the GBD-DID is obstructing the actin polymerizing activity of FH2 domain (Wallar et al., 2006). This inhibitory interaction is disrupted by the binding of RhoA to the GBD-DID resulting in the activation of FH2 (Lammers *et al*., 2005). For other metazoan formins, auto-inhibitory sequences are less clear. Formins of FHOD group possess DAD regions but not DID and that of FMN, INF and Delphilin groups contain neither DID or DAD (Higgs H N, 2005). The differences in the diversity of domains attributed to regulatory mechanisms underscores the importance of their structural analysis.

1.3.2.1. Formin-2

The *Fmn-2* genes in mouse and humans share conservation of sequence and genomic location, and are expressed throughout the brain and spinal cord (Leader B and Leder P, 2000). Human and mouse formin-2 share 90% identity over the C-terminus and 79% identity over most of the N-terminus. Also, human formin-2 showed 74.7% total-amino-acid identity with mouse Fmn2, and 31.9% total-amino-acid identity with human formin-1 (Katoh and Katoh, 2004). Formin-2 is also similar to *Drosophila* Cappuccino with 37% identity in the C-terminus. The high similarity among formin-1, formin-2 and Cappuccino bring them all together in the Fmn group of formins. Formin-2 contains both the FH1 and the FH2 domains. The FH1 domain of formin-2 possess the most extensively repeated proline motif yet described in the family (Leader and Leder, 2000). Recently, a new conserved sequence

motif namely FSI (Formin Spir Interaction sequence) have been identified in the very C-terminus of formin-2 protein adjecant to FH2 which is unique among the members of Fmn subgroup of formins from flies, fish, birds and mammals. The FSI region of both mammalian formin (formin-1/2) proteins is mediating the interaction with KIND domain of both mammalian Spir (Spir-1/2) (Figure 4). (Pechlivanis *et al.,* 2009).

Formin-2 is preferentially expressed in developing Central Nervous System (CNS) during embryogenesis. The expression begins in the developing spinal cord and brain structures and continues in neonatal and adult brain structures including the olfactory bulb, cortex, thalamus, hypothalamus, hippocampus and cerebellum. The similar expression pattern of mouse and human *formin-2* in the developing and mature CNS suggests a similar role for the human and mouse genes. It also shares similar expression pattern with a distinct actin nucleation factor, Spir-1 which has predominant expression in brain. Both genes were found to be expressed in the developing nervous system. The expression of both the genes was again identical in the adult brain, with the highest expression in CA1, CA2 and CA3 fields in the hippocampus, garanular layer of dentate gyrus and in the Purkinje cells in cerebellum. The strong overlapping expression patterns of two distinct classes of actin nucleators, Spir-1 and Formin-2, suggests a strong functional correlation between the two (Schumacher *et al*, 2004). Even though *formin-*2 is predominantly expressed in the nervous system, the corresponding deficient mice have no abnormalities in the nervous system. Fmn-2 deficient mice exhibit hypofertility due to a failure in correct metaphase spindle positioning during meiosis I. In 2002, Leader B *et al.* showed that Fmn2 is expressed in the developing mammalian oocyte and required for DNA-spindle positioning during meiosis I. Later, Schuh and Ellenberg (2008) showed in live mouse oocytes that spindle relocation, which is essential for fertility, requires a continuosly reorganizing cytoplasmic actin network nucleated by Fmn-2.

1.3.3. WH2 domain-containing nucleators

Following the buzz of Arp2/3 complex and formin family into the world of actin polymerization, a new genere of nucleating proteins were launched that contain one or multiple actin binding WH2 motifs, as their signature. They include Spir (4 WH2) (Quinlan *et al*., 2005), Cordon-Bleu (Cobl) (3 WH2) (Ahuja *et al*., 2007), Leiomodin (Lmod) (1 WH2) (Chereau *et al*., 2008) as well as bacterial nucleators– VopF/VopL (3 WH2) (Liverman *et al*., 2007) and TARP (1 WH2) (Jewett *et al*., 2006). Even though the WH2 domain is shared by NPFs of ARP2/3 complex, WASP, and the amino-terminal portion of Thymosin β4 (Paunola *et al*., 2002), neither can trigger the actin nucleation on its own and this feature put Spir proteins in the world of it´s own as a versatile actin nucleation factor.

Spir Proteins

Spir proteins are the primodial member of the emerging group of actin nucleation factors with tandem cluster of WH2 domains. In 2005, Quinlan *et al.* revealed a fillip to give a new lease on actin nucleation machinary catalyzed by Spir proteins which were about to complete the trio of factors, along with Arp2/3 complex and Formins.

Spir gene was first identified in *Drosophila* together with *Capuccino, Drosophila* formin, in a *Drosophila* screen to elucidate their requirement for proper development of oocytes and embryos. Mutations in either gene resulted in the failure of the egg, and later the developing embryo, in establishing the polarity (Manseau and Schüpbach, 1989). Since then Spir proteins have been exclusively identified in metazoans.

Vertebrate genome encode two *spir genes, Spir-1 and spir-2* (Schumacher *et al*., 2004) and the corresponding proteins Spir-1 and Spir-2 have a high similarity. *Spir-1* expression was identified in developing nervous system as well as in adult brain. In the adult brain, high expression was found in the Purkinje cells of cerebellum, neuronal cells of hippocampus and dentate gyrus. In addition to the nervous system, *Spir-1* was also detected in fetal liver and adult spleen (Schumacher *et al*., 2004). *Spir-2 gene* possess broader expression pattern when compared to *Spir-1 gene*, which was detected throughout the digestive tract, brain, testis and kidney with no significant expression in spleen, lung and liver (Pleiser *et al*., 2010). Until now, the class of Spir proteins comprises – *Drosophila* Spir (dSpir), vertebrate Spir-1 and Spir-2, the sea squirt *Ciona Savignyi* PEM-5 (posterior end mark-5) (Wellington *et al*., 1999) and pEg6 of the African clawed frog *Xenopus* (Le Goff *et al*., 2006).

Spir has a unique mechanism in actin nucleation and polymerization, sharing only limited functional hallmarks with the Arp2/3 complex and formins. Similar to formins but unlike Arp2/3 complex Spir induce unbranched, linear actin filaments (Quinlan *et al*., 2005). Spir resembles Arp2/3 complex in that it remains bound to the pointed end of newly formed actin filaments whereas formins processively move along with the barbed ends of the actin strutures. But, a recent study put direct evidence in front showing that Spir binds to the barbed end of the actin filament, under conditions where Spir accelerates actin polymerization (Takuto *et al*., 2011). Otherwise Spir has no sequence homology to the formin family of proteins or to the subunits of Arp2/3 complex (Quinlan *et al*., 2005).

Spir proteins form a well-conserved family in animals. They are single polypeptides with multiple domains starting from the N-terminus to C-terminus: KIND, a cluster of four WH2 domains, Spir box and FYVE domain (Figure 6).

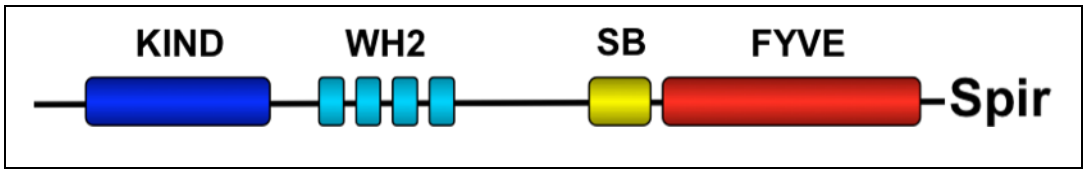

Figure 6. Domain architecture of Spir proteins: All known Spir proteins share a common structural array with an N-terminal Kinase non-catalytic C-lobe domain (KIND) followed by a cluster of four WASP homology-2 (WH2) domains in the center. The C-terminus comprises Spir Box and modified FYVE-Zn-finger domain.

KIND (Kinase non-catalytic C-lobe domain) was first identified by Ciccarelli *et al*., as a conserved region in the N-terminal half of Spir proteins and named the region based on its sequence similarity to the C-lobe of the protein kinase fold (Ciccarelli *et al*., 2003). The KIND domain is found only in metazoa. The region significantly matched various catalytic domains of protein kinases but the best similarity was found to p21-activated kinase (PAK), a serine threonine phosphotransferase (Ciccarelli *et al*., 2003). Multiple sequence analysis of different protein kinases defined a characterestic eukaryotic protein kinase catalytic domain, `a kinase fold`, with about ~ 200-350 amino acids, with 11 major conserved motifs (Hanks and Quinn, 1991). The fold harbours two structurally independent subdomains connected by a short linker region: a short N lobe formed by a β sheet and an α helix that contributes to the binding of ATP, and a larger and mainly helical C-lobe that contains the catalytic residues and the activation loop. Spir protein has the entire C-lobe of the kinase domain without the essential catalytic residues required for the kinase activity, which names the novel region as Kinase non-catalytic C-lobe domain. Also Spir proteins are devoid of the N-lobe as well as the linker region of the kinase domain (Ciccarelli *et al*., 2003). But the KIND domain evolved from a functional kinase turned into an interaction module since the substrates of the protein kinases interacts with the α helical regions in the C-lobe. This fact was initially characterized by the discovery of the specific interaction between the Spir-KIND domain and Fmn subgroup of Formin superfamily, prominent interaction partners of Spir (Quinlan *et al*., 2007). The first atomic structure of KIND domain was revealed recently (Zeth K *et al.,* 2011). The crystal structure of KIND domain was determined at 2.05 A° and showed an almost complete α-helical fold with a small three-stranded β-sheet (Zeth K. *et al.,* 2011).

The central region of Spir proteins encodes a cluster of four **WH2 repeats**- the name derived from the WASP (Wiskott-Aldrich syndrome protein) homology domain 2. They comprise 17-27 amino acid long actin binding motifs. The actin nucleation activity of Spir proteins resides in the WH2 domains (Figure 7). These WH2 domains, designated A, B, C, and D (from N- to C-terminal) connected together through intervening sequences, linker 1 through to linker 3 (L-1, L-2, L-3) (Quinlan *et al*., 2005). The sequence allignments revealed

that the four WH2 domains, especially WH2-B and WH2-D (Wellington *et al*., 1999), and the linker regions are conserved in Spir proteins belonging to different species (Kerkhoff, 2006). The C-terminal half of the WH2 cluster with WH2-C, L-3 and WH2-D, are crucial for nucleating actin assembly (Quinlan *et al.,* 2005). A stabilized actin dimer is formed by the close coordinated activity of WH2-C and WH2-D through L-3, in that each taking an actin monomer. Afterwards, WH2-B and WH2-A add the third and fourth monomer to the initial dimer. Mutational studies indicate that among the four WH2 domains of Spir, the C and D domains have the strongest nucleation potential and removal of the C-D fragment and the replacement of L-3 nearly abolish the nucleation activity (Quinlan *et al*., 2005).

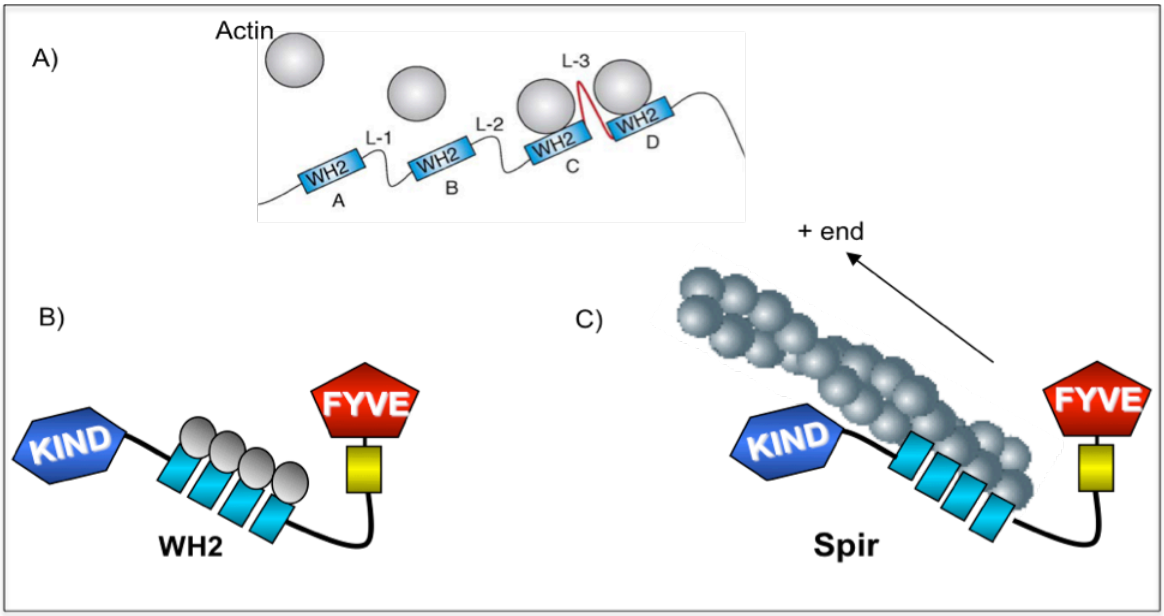

Figure 7. Mechanism of actin nucleation by Spir proteins: A) The tandem WH2 domains are designated as A, B, C and D, and the coresponding linker regions as L-1, L-2 and L-3. First two actin monomers get bound to WH2-D and WH2-C to initiate the formation of an actin dimer and are stabilized by L-3. Subsequently G-actin is added to WH2-B and WH2-A to form trimers and tetramers. **B)** Four actin monomers are bound to the cluster of four WH2 domains. **C)** Further polymerization occurs at the barbed end whereas Spir proteins remain bound to the ponted end of the actin filament, (Kerkhoff, 2006).

Spir localization at the intracellular membrane structures is attributed to the integrity of the C-terminal half of the protein encompassing- **modified FYVE zinc finger domain** and **Spir box (SB)** located N-terminal to the FYVE domain.

Spir box (SB) is a highly conserved region among Spir family proteins sharing sequence homology to α-helical domain of rabphilin-3A, also located adjacent to its FYVE finger-related zinc finger motif (Ostermeier and Brunger, 1999). The rabphilin-3A α helix N-terminal to its FYVE-related zinc-finger motif mediates the interaction with GTP loaded

Rab3A and Rab3A GTPase. The homology of the Spir-box and the rabphilin-3A α helix suggested a role for the Spir-box in mediating the association of the Spir actin organizers with Rab GTPase (Kerkhoff *et al*., 2001). Spir proteins colocalize with Rab11 GTPase, at the trans-Golgi network, post-Golgi vesicles and the recycling endosomes. Still, a direct interaction of Spir with Rab GTPase has not been shown yet.

The modified FYVE zinc finger domain (mFYVE) is named after the four cysteine-rich proteins: Fab 1 (yeast orthologue of PIKFYVE), YOTB, Vac 1 (vesicle transport protein), and EEA1 (Early Endosomal Antigen 1), in which it has been found. FYVE domains are membrane binding modules. The FYVE finger has eight potential zinc coordinating cysteines. The structure forms a `turret loop` which helps in penetrating the membrane (Hurley, 2006). A hallmark of FYVE domains is the cluster of basic amino acids between cysteines 2 and 3 of the consensus sequence, mediating the interaction with phosphatidylinositol 3-phosphate (Stenmark, 2005). The Spir zinc finger motif is a modified version of the FYVE domains (mFYVE), lacking the basic cluster between cysteines 2 and 3 and having a loop insertion between cysteines 6 and 7. The Spir actin organizers are targeted to intracellular mambranes by their modified FYVE zinc finger domain and is involved in vesicle transport processes (Kerkhoff, 2001 and Morel *et al*., 2009).

WH2- domain containing actin nucleators other than Spir include:

Cobl, has three WH2 domains for actin binding and promote nonbundled, unbranched actin filaments. It seems to be a vertebrate-specific nucleator (Qualmann and Kesels, 2009) with restricted expression in brain (Ahuja *et al*., 2007). Even if the cellular functions of Cobl are just beginning to be explored, it has been found out that in neurones Cobl is crucial for neuritogenesis and dendritic branching (Ahuja *et al*., 2007).

Lmod is a muscle specific actin nucleation factor (Chereau *et al*., 2008), with isoforms, Lmod-1 expressed in smooth muscles, Lmod-2, latest actin nucleator to be characterized, expressed in cardiac muscles and the uncharacterized Lmod-3, fetal leiomodin (Conley *et al*., 2001). The domain organization of Lmods has resemblence to tropomodulins (Tmods), proteins that cap actin filament pointed ends (Chereau *et al*., 2008). Unlike Cobl, Lmod has only one WH2 motif in the C-terminus and elicites unbranched actin filaments. The Lmod is localized to the middle of muscle sarcomeres and the knock down of the protein severely affects the sarcomere assembly in cultured muscle cells.

Recently two remarkable bacterial actin nucleators have been found out- **VopF** in *Vibrio cholerae* and **VopL** in *Vibrio parahaemolyticus*, each with three WH2 domains for accelerating the actin polymerization and both nucleate the actin filaments that grow from the barbed end (Tam *et al*., 2007). **TARP** (translocated actin recruiting phosphoprotein) from *Chlamydia trachomatis* also contains one WH2 domain (Jewett *et al*., 2006). These

observations suggest that pathogens adopted Spir-like actin nucleation mechanism to manipulate host cytoskeleton.

1.4. Synergy amongst two distinct nucleators, Spir and formin

Formins are the known prominent interaction partners of Spir (Quinlan *et al*., 2007; Pechlivanis *et al*., 2009). Cappuccino (Capu; in *Drosophila*) and formin-1 and formin-2 (Fmn-1 and fmn-2 in mammals) belong to the formin (Fmn) subgroup of formins. Like formins, mammals have two homologous Spir proteins, Spir-1 and Spir-2. Progressive studies to elucidate the interaction between Spir and formin was revealed by the finding that the actin nucleation factors, Spire and Capu, are required to construct as well as to maintain the polarity in developing Drosophila oocytes using both actin and microtubule systems (Theurkauf et al., 1992). Both proteins cooperate in the generation of a dynamic actin mesh in the oocyte that prevents premature ooplasmic streaming and loss of either have an identical phenotype in early Drosophila oogenesis (Dahlgaard et al., 2007), inducing premature cytoplasmic streaming, loss of oocyte polarity, and female sterility (Theurkauf *et al*., 1992; Emmons *et al.,* 1995; Wellington *et al.,* 1999). Analogous to Drosophila counterparts, *Spire and Cappu*, mammalian *formin-2* and *spir-1* genes are coexpressed in the developing and adult nervous system, and the corresponding proteins interact each other (Schumacher *et al*., 2004; Quinlan *et al*., 2007; Pechlivanis *et al.,* 2009). Recently it was found that a dynamic actin mesh, as during Drosophila oogenesis, is also required for mouse oogenesis. The correct localization of the meiotic spindle during mouse oogenesis and the resulting asymmetric division depends on an actin mesh that is built up by formin-2. Myosin-2 generates the pulling forces required for spindle movement (Schuh and Ellenberg, 2008).

Quinlan *et al*. (2007) observed the interaction between Spir and Capu both *in vivo* and *in vitro* which showed that the Spir-KIND/Capu-FH2 has more affinity in interaction at a stoichiometry of 2:2 (two KIND monomers to one FH2 dimer) when compared to that in between Spir-WH2/Capu-FH2. Subsequently the interaction inhibits actin nucleation by Capu but enhances that by Spir (Quinlan *et al*., 2007). The interaction was also studied with mammalian isoforms, Spir-1 and formin-2. The KIND-FH2 interaction is evolutionarily conserved. Further anatomization of this interaction by Pechlivanis *et al*., (2009) revealed high affinity Spir binding site at the very C-terminus of formin-2, designated as Formin Spir Interaction (FSI) sequence adjacent to its core FH2 domain. The FSI sequence was found to be highly conserved within the Fmn subfamily of formin proteins and absent in other formin subfamilies. Both mamalian Spir proteins Spir-1/2 interact with both mammalian formin proteins Fmn-1/2 and FSI interacts with the KIND domains of both Spir-1 and Spir-2 with a similar affinity (Pechlivanis *et al*., 2009).

1.5. Spir- regulation

The regulation of Spir proteins can be proposed on the basis of protein interaction and protein phosphorylation even though a better understanding is necessary. An approach towards the regulation of Spir was proposed on the basis of the phosphorylation of *Drosophila* p150-Spir proteins by the mitogen-activated protein kinase (MAPK), JNK (c-Jun N-erminal kinase) (Otto et al., 2000). MAPKs are specific serine/threonine kinases which respond to various stimuli and control a variety of cellular activities including gene expression, mitosis, cell differentiation and cell survival/apoptosis. Signal transduction occurs by a series of three kinases that form a phosphorylation relay. The activated MAPKKK, by the phopshorylation of Ser and Thr residues, phosphorylates MAPK-kinase (MAPKK), which then becomes active and phosphorylates the MAP kinase (MAPK). MAPKK is a "dual specific" enzyme, phosphorylates Thr-X-Tyr motif located in the kinase activation loop (Davis R J, 2000). Studies of a large number of MAPKs demonstrate that this mechanism of activation is conserved in many organisms, including plants, yeast, nematodes, insects, and mammals (Cathy Tournier *et al*., 2001). This phosphorylation enables the MAPK to translocate to nucleus and phosphorylate their target protein(s) (Cavigelli *et al.,* 1995). Three best characterised subfamilies in vertebrates are named, extracellular-signal regulated kinase (ERK), c-Jun N-terminal kinase (JNK) and p38. Two different MAP kinases, MKK4 and MKK7, are implicated in the activation of JNK group of kinases (Wang *et a*l., 2006). Although both MKK4 and MKK7 are dual-specificity protein kinases that can phosphorylate JNK on Tyr and Thr, *in vitro* experiments indicate that these sites are phosphorylated selectively by MKK4 and MKK7, respectively (Cathy Tournier *et al*., 2001). And of these two, MKK7 selectively activates only JNK (Jacobs *et al*., 1999 and Cathy Tournier *et al*., 2001).

C-terminal region of p150-Spir with a smallest fragment comprising 53 amino acids at the DEJL motif (docking site for Erk and JNK containing LXL motif), which is not highly conserved within the Spir-family proteins, mediates the interaction between *Drosophila* p150-Spir and JNK (Otto *et al.,* 2000). Colocalization studies in NIH 3T3 cells transiently transfected with both p150-Spir and JNK, revealed that JNK translocated to and colocalizes with p150-Spir at discrete spots around the nucleus. Moreover, C-terminal sequences of p150-Spir were shown to get phosphorylated both *in vitro* and *in vivo* by JNK-MKK7, a constitutively active JNK. Since Erk and JNK MAP kinases are recruited to substrate proteins via docking sites, enabling the kinases to phosphorylate serine or threonine residues adjacent to prolines (S/TP motifs) (Jacobs D *et al*., 1999) and as p150-Spir contains a JNK docking site (the DEJL motif) with several potential S/TP phosphorylation motifs, electrophoretic mobility shift exhibited by p150-Spir supports the fact that p150-Spir is a phosphorylation target of JNK. Colocalization of p150-Spir with F-actin and induction of clustering of F-actin around the nucleus following the co-expression with p150-Spir, observed

in mouse fibroblasts led to the conclusion that besides being a downstream target of JNK function, p150-Spir also provides a direct link between JNK and actin organization (Otto et al., 2000). In analogy to the p150-Spir, this part of the study points on the post-translational modification (phosphorylation) of mammalian Spir proteins.

1.6. An overview on Post-translational modifications and Mass spectrometry

1.6.1. Post-translational modifications (PTMs)

The term post-translational modification refers to the addition or removal of a functional group from an aminoacid, resulting in reversible modification of the protein activity. PTMs of a protein can determine its activity state, localization, turnover, and interactions with other proteins (Mann and Jensen, 2003). About 300 types of post-translational modifications of proteins are known to occur physiologically (Jensen, 2004). However, only some of them have been reported to play crucial roles in protein function in general.

Of all known post-translational protein modifications, protein phosphorylation has turned out to be one of the most biologically relevant and ubiquitous PTM, since the isolation of phosphoserine (first described as serine phosphoric acid) in 1932 by Phoebus A.Levene and Fritz A.Lipmann (Pradela and Albar, 2007). It is estimated that one-third of eukaryotic proteins are phosphorylated as a result of carefully regulated protein kinase and protein phosphatase activities, which differ in their kinetic properties, substrate specificities and cellular or tissue distribution. Phosphorylation and dephosphorylation catalyzed by these counteracting enzymes can modify the function of a protein. Thus protein phosphorylation has been shown to be the key regulator in cell division, signal transduction etc. The simplicity, flexibility and reversibility of phosphorylation, coupled with the ready availability of ATP as a phosphoryl donor, explain its selection as the most general regulatory device adopted by eukaryotic cells (Cohen P, 2002). Among the aminoacids that can be phosphorylated, O-phosphates are the most common class and are mostly attached to serine (Ser), threonine (Thr) and tyrosine (Tyr) residues. The occurence of phosphorylation on Ser and Thr residues is more frequent than on Tyr residues, with the ratio of pSer/pThr/pTyr in the order of 1800:200:1 (Reinders and Sickmann, 2005; Witze *et al*., 2007). Protein phosphorylation events are detected by increase in aminoacid residue mass of +80Da, which report the addition of HPO_3 (Witze *et al,* 2007).

Despite its relevance, the analysis of protein phosphorylation has been revealed as one of the most challenging tasks due to its highly dynamic nature and low stoichiometry. A comprehensive study of protein phosphorylation should include the identification of phosphoproteins and sites of phosphorylation, identification of proteins involved in the process (kinases and phosphatases) and description of the biological events following the phosphorylation (Pradela and Albar, 2008).

Identification of sites of post-translational modification is crucial for elucidating the biological roles of any given protein. Low stoichiometry of many PTMs makes characterization of the sites of modification challenging. Several approaches can be employed for the identification of PTMs of proteins like Mass spectrometry, 2D gel analysis, sequencing by Edman´s degradation and computational prediction (Johnson and Eyers, 2010; Hjerrild and Gammeltoft, 2006). Due to it´s sensitivity and specificity, Mass spectrometry (MS) has become a powerful analytical strategy in proteomics and a method of choice for unbiased analysis of protein phosphorylation.

1.6.2. Mass spectrometry

A mass spectrometer produces ions from the substance under investigation, seperates them according to their mass-to-charge ratio (m/z), and records the relative abundance of each ionic species present. MS measurements are carried out in gas phase.
A Mass spectrometer can be divided into three fundemental parts,

- Ionisation source
- (m/z) analyzer and
- Detector

Individual components of a mass spectrometer are shown in Figure 8. MS analysis of the sample can be performed in two ways: bottom-up and top-down. In the bottom-up approach, proteins are enzymatically digested into peptides prior to MS analysis, whereas in a top-down method an intact protein is analyzed. Of these bottom-up approach is the most popular one for the protein identification by peptide sequencing. In this approach, digestion of protein is carried out by proteolytic enzymes (usually Trypsin) to obtain peptide mixtures which are further fractionated by reversed-phase liquid chromatography (RP-LC) followed by mass spectrometry. The obtained peptides are fragmented preferentially via collision induced dissociation and the corresponding tandem mass spectra are collected. The peptide sequence information from the resulting fragment ions are then searched in a database using appropriate algorithms.

The mass spectrometer used for the study is Tandem Mass Spectrometer (Tandem MS or MS/MS) namely QTOF-mass spectrometer (QStar XL, Applied Biosystems GmbH, Darmstadt, Germany) directly coupled to nano-HPLC system (Agilent Technologies GmbH, Boeblingen, Germany). A tandem MS is used to determine structural features of a compound (here protein) comprising the aminoacid sequence, site of attachment and the type of PTM. In this case, detailed structural features of the peptides can be obtained from the analysis of the masses of the resulting fragmented ions inside the mass spectrometer.

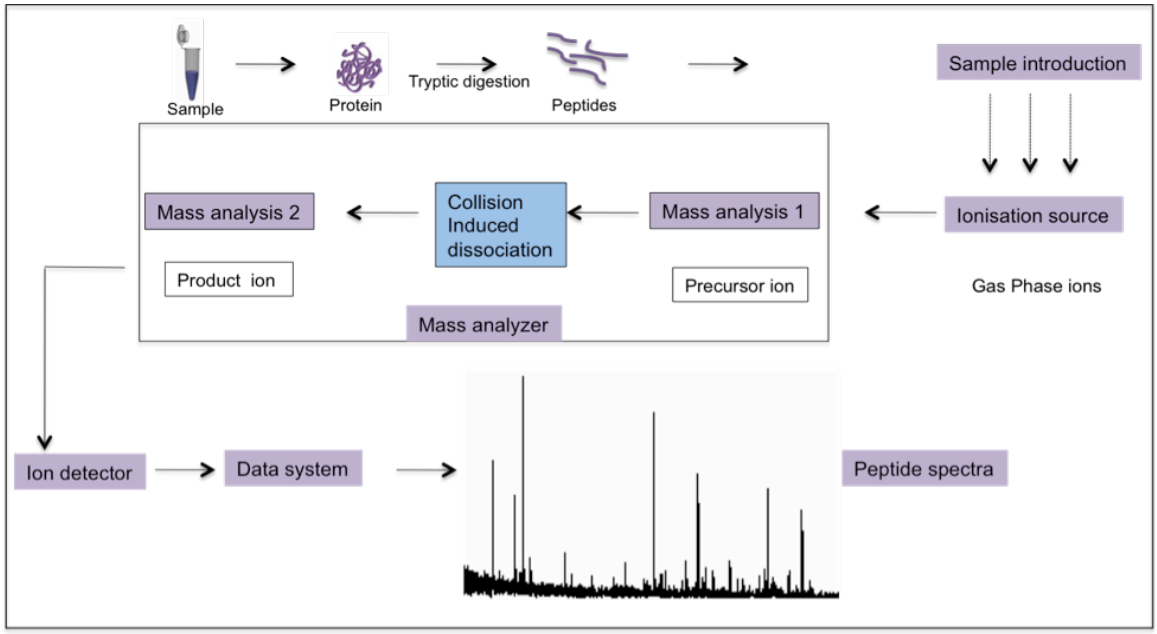

Figure 8 . Components of a Mass spectrometer.

Outline of the working of Mass spectrometer.

1. Sample introduction

The method of sample introduction to the ionisation source often depends on the ionisation method being used, as well as the type and complexity of the sample.

The sample can be inserted directly into the ionisation source, or can undergo some type of chromatography en route to the ionisation source. This latter method of sample introduction usually involves the mass spectrometer being coupled directly to a high pressure liquid chromatography (HPLC), gas chromatography (GC) or capillary electrophoresis (CE) separation column, and hence the sample is separated into a series of components which then enter the mass spectrometer sequentially for individual analysis. The current study uses reversed phase liquid chromatography (RP-LC). The outlet of a RP column can be directly coupled to the inlet of the MS to analyze complex peptide mixtures, a method known as LC–MS. In a typical LC–MS experiment, the peptides are eluted from a RP column according to their hydrophobicity, are ionized via ESI and, then, transferred with high efficiency into the MS for analysis.

2. Ionization

For analyzing biomolecules by MS, the ability to transfer large and polar analytes of interest into gas-phase ions are taken in credit. The development of soft ionization methods like, MALDI and ESI, have enabled the transfer of polar, nonvolatile, and thermally unstable proteins and peptides into the gas phase without extensive degradation. The study employs

ESI, a technique used to produce gas-phase ions from the analyte in solution. During ESI, the analyte is dissolved in volatile solvent and is passed through a high voltage needle at atmospheric pressure over which a voltage of 3-5 kV is applied. As a consequence of this strong electric field, the sample emerging from the tip of the needle is dispersed into aerosol of tiny charged droplets assisted by nebulising gas. Solvent from the droplet is evaporated and the droplet gets smaller. The process of repeated evaporation ultimately release multiply charged individual gas phase analyte ions and make their way to the analyzer of the MS.

3. Mass analyzers

Mass analyzers are an integral part of each instrument because they can store ions and separate the ions formed in the ionisation source of the mass spectrometer according to their m/z ratios. Among the numerous mass analyzers, the better known of which include:

- Time-of-flight (TOF) mass analyzers
- Quadrupole (Q) mass analyzers
- Ion trap (Quadrupole ion trap, QIT; linear ion trap, LIT or LTQ) mass analyzers
- Fourier-transform ion cyclotron resonance (FTICR) mass analyzers
- Orbitrap mass analyzers

Mass analyzers mainly differ in how they determine the m/z ratios of the peptides.

The tandem MS employed in this study uses Quadrapole-Time-of-flight geometry (QTOF). Since the analysers are of two different types, the respective MS is a hybrid one. The two analyzers are seperated by a collision cell into which an inert gas is admitted to collide with the selected sample ions and bring about their fragmentation.

3.1. Fragmentation methods (Peptide sequencing by tandem mass spectrometry)

Within an MS, individual proteins or peptides are separated and fragmented for sequencing and for the localization of post-translational modification site(s). The fragment mass data can then be used to search the database for peptide identification.

Collision-induced dissociation (CID), also called collision-activated dissociation (CAD), is the most common peptide fragmentation method. There are three different types of bonds that can fragment along the amino acid backbone: the NH-CH, CH-CO, and CO-NH bonds. Each bond breakage gives rise to two species, one neutral and the other one charged, and only the charged species is monitored by the mass spectrometer. The charge can stay on either of the two fragments depending on the chemistry and relative proton affinity of the two species. Figure 9 shows a peptide with four aminoacids having six possible fragment ions for each amino acid residue and are labelled with the a, b, and c ions having the charge retained on the N-terminal fragment, and the x, y, and z ions having the charge retained on the C-terminal fragment. The most common cleavage sites are at the CO-NH bonds which give rise to the b and/or the y ions. The mass difference between two adjacent

b ions, or y ions, is indicative of a particular amino acid residue.

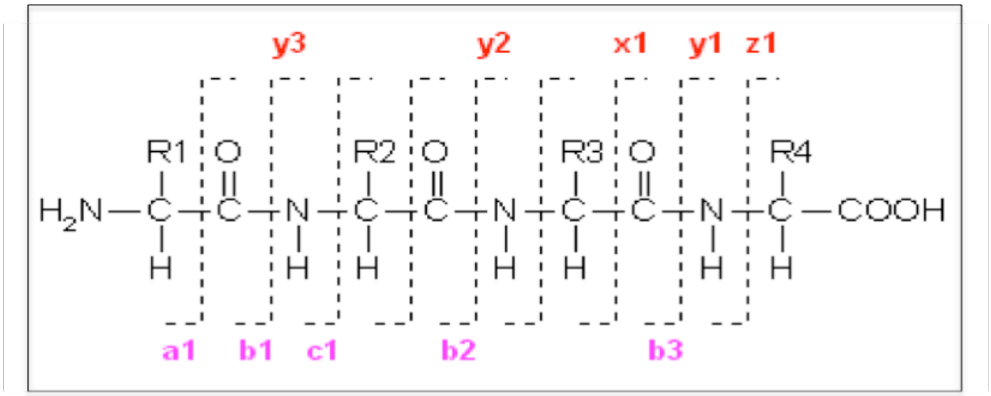

Figure 9. Fragmentation of a peptide containing four aminoacids. The cleavage can happen at different positions. If the charge remains on the N terminal fragment, the ion is named as either a, b or c. If the charge remains on the C terminal fragment, the ion type is either x, y, or z. The cleavage of the peptide bond is very common for a CID process. In the MS/MSspectrum, most ions are detected as y and b ions.

4. Detection and recording of sample ions.

The detector monitors the ion current, amplifies it and the signal is then transmitted to the data system where it is recorded in the form of mass spectra. The m/z values of the ions are plotted against their intensities to show the number of components in the sample, the molecular mass of each component, and the relative abundance of the various components in the sample. The type of detector is supplied to suit the type of analyser; the more common ones are the photomultiplier, the electron multiplier and the micro-channel plate detectors.

5. Computational algorithms for peptide identification

The profiling of proteins in a sample can be achieved by search programmes that match the MS/MS spectra of peptides recorded during sample analysis with the theoretical spectra. A series of computational methods for the assignment of peptide sequences based on automated interpretation of the MS/MS spectra and protein sequence database searching have been developed. The search programmes calculate a similarity score that evaluates the degree of match between the experimental MS/MS spectrum and a theoretical spectrum (e.g., SEQUEST, Thermo Corp., http://www.thermo.com/) or uses a statistical approach to evaluate the probability of observing the MS/MS fragment ions (e.g., Mascot, Matrix Science, http://www.matrixscience.com/).

2. Materials

2.1. Chemicals

Agarose UltraPure™	Invitrogen, Molecular Probes	15510-027
Agar select	Sigma-Aldrich	A5054
Acrylamide(30%)/ Bisacrylamide(0,8%)(37.5:1)	Carl-Roth	3029.1
Ammonium persulfate (APS)	Sigma-Aldrich	A3678
Ampicillin; Sodium crystalline	Sigma-Aldrich	A9518
Ammonium bicarbonate	AppliChem	A3689.0500
Acetonitrile	VWR	83640.320
ß-Mercaptoethanol	Carl-Roth	4227.3
Bovine serum albumin, Cohn V fraction	Sigma-Aldrich	A4503
Boric acid	Sigma-Aldrich	B0252
Bromophenol blue	Carl-Roth	A512.1
Calcium chloride	Carl-Roth	A119.1
Chloramphenicol	Sigma-Aldrich	C0378
Complete, Mini, EDTA-free; Protease inhibitor	Roche	11836170001
Coomassie Blue G	Carl-Roth	9598.1
1,4-Dithioerythritol (DTE)	Sigma-Aldrich	109K1022
EDTA	Sigma-Aldrich	E5134
Ethanol >99.8%, p.a.	Carl-Roth	9065.2
Ethanol denatured (+1% Mek)	Carl-Roth	K928.1
Ethidiumbromide	Carl-Roth	HP46.1
Formic acid	MERCK	KGaA 1.00264.1000
Glutathione	Sigma-Aldrich	G4251
Glutathione Sepharose beads	GE/Healthcare	17-0756-01
Glycerine	Carl-Roth	3783.1
Glycine	Sigma-Aldrich	G7126

Hydrochloric acid	Carl-Roth	6331.1
IPTG	Sigma-Aldrich	I9003
Isopropanol	AppliChem	A0900
LB	Sigma-Aldrich	L3022
Lipofectamine	Invitrogen, Molecular Probes	18324012
Magnesium chloride, hexahydrate	Carl-Roth	2189.2
Milk powder, blotting grade	Carl-Roth	T145.2
Methanol, 99.9%	Carl-Roth	4627.2
Nonidet P-40	Biochemica; distributed by A. hartenstein Laborbedarf	A1694,0500
PBS buffer (10x Dulbecco´s) powder	Applichem	A0965
Ponceau S	Sigma-Aldrich	P3504
Protein-G-Agarose beads	Roche	11243233001
Sodium chloride	Sigma-Aldrich	S3014
Sodium dodecyl sulfate	Sigma-Aldrich	L4390
Sodium hydroxide pellets	Merck	106462
TEMED	Sigma-Aldrich	T9281
Triton X 100	Carl-Roth	3051.3
Tween 20	AppliChem	A1389
Tris	AppliChem	A1086, 1000
Trypsin (Trypsin Gold; MS grade)	Promega	V5280
Trifluoroacetic acid	Merck	KGaA 1.08178.0050

2.2. Analytical Kits

Kit	Supplier	Order Number
NucleoTrap DNA Gel extraction Kit	Macherey-Nagel	740609.50
DNA Plasmid Maxi Kit	Qiagen	12163
DNA Plasmid Mini Kit	Qiagen	12123
ECL Western Blotting Detection	GE/Healthcare	RPN2109

2.3. Bacterial Strains

Strain	Supplier	Description	Order number
NEB10	NEB	Genotype:araD139Δ(ara,leu)7697 fhuA lacX74 galK16 galE15 mcrA f80d(lacZΔM15) recA1 relA1 endA1 nupG rpsL rph spoT1Δ(mrr hsdRMS mcrBC)	C3019H
E. coli Rosetta	Novagen /Merck	Increased protein expression rate by providing tRNAs rarely used in E.coli. Genotype: F- ompT hsdSB(rB- mB-) gal dcm pRARE (CamR)	70953

2.4. Eukaryotic cell line

Cell line	ATTC number	Annotation
HEK 293	CRL-1573	Human embryonic kidney 293 cells

2.5. Expression vectors

Vector	Supplier	Annotation
pGEX-4T-1	GE/Healthcare	Bacterial expression vector. Genes cloned into the MCS will be expressed as fusions to the C-terminus of GST
pProEX HTb	Invitrogen, Molecular Probes	Bacterial expression vector. Genes cloned into the MCS will be expressed as fusion proteins with an N-terminally 6xHis tag.
pcDNA3	Invitrogen, Molecular Probes	Mammalian expression vector
pEGFP-C1	Clontech	Mammalian expression vector. Genes cloned into the MCS will be expressed as fusions to the C-terminus of eGFP

2.6. Enzymes

Enzyme	Supplier	Order number
Pfu -Polymerase	Promega	M774B
Restriction enzymes	NEB	-
T4 DNA ligase (supplied with 10XReaction Buffer)	NEB	M0202
Calf Intestinal phosphatase (CIP)	NEB	0531005

2.7. Molecular weight standards

Standards	Supplier	Order number
DNA ladder 1 Kb	PeqLab	25-2031
DNA ladder 100 bp	PeqLab	25-2010
Precision Plus Protein dual colour standard	Bio-Rad	1610374

2.8. Antibodies

2.8.1. Primary Antibodies

Antigen	Antibody	Species	Supplier	Order number	Working dilution
Anti-myc	Myc 9E10	mouse monoclonal	Santa Cruz	sc-40	1:500
Anti-EGFP	Living-colors EGFP A.v PeptideAntibody	Rabbit polyclonal	Clontech	632376	1:100
Anti-Spir-2	Anti-Spir-2 antibody	Rabbit polyclonal	Lab source	-	1:1000

2.8.2. Secondary Antibodies

Antigen	Antibody	Species	Supplier	Order number	Working dilution
Anti-mouse	anti-mouse IgG horseradishperoxidase linked	Sheep polyclonal	Amersham Pharmacia biotech	NA 9310	1:5000
Anti-rabbit	anti-rabbit IgG horseradishperoxidase linked	sheep polyclonal	Amersham Pharmacia biotech	NA 9340	1:5000

2.9. Cell culture media and suppliments

Material	Supplier	Order number
DMEM	Invitrogen, Molecular Probes	41965039
L-Glutamine 200 mM	Invitrogen, Molecular Probes	25030024
Poly-L-Lysine; 0,01% solution	Sigma-Aldrich	P 4707
Trypsin 0,05% EDTA	Invitrogen, Molecular Probes	25300054
PBS	Invitrogen, Molecular Probes	14190094
Fetal calf serum Fetalclone III	Thermo Scientific; Hyclone	SH30109.03

2.10. Plastic ware and other materials

Item	Supplier	Order number
Blotting papers Grade 3 MM Chr	Whatman	3030.917
Cell culture flask (T75)	Sarstedt	83.1813.002
Cell culture plates 6-Well	Greiner Bio-One	657160
Cell culture glass bottom dish	Willco wells	GWSt-5040
Conical reaction tubes (15 ml)	Greiner Bio-One	188271
Parafilm® □`M`□ Laboratory Film	Pechiney Plastic Packaging	PM-996
Pasteur pipettes	distributed by A. Hartenstein Laborbedarf	PP07
PCR-tubes (0.2 ml)	Axygen, distributed by Abimed	PCR-0208-CP-C
Pipette tips (0.5-10 µl)	Axygen, distributed by Abimed	T-300
Pipette tips (100-1000 µl)	Axygen, distributed by Abimed	T-1000-B
Pipette tips (2-20 µl) and (20-200 µl)	Sarstedt	70.760.002
Petri dishes (94 x 16 mm)	distributed by A. Hartenstein Laborbedarf	PP90
Reaction tubes (1.5 ml)	distributed by A. Hartenstein Laborbedarf	RK1G
Reaction tubes (2.0 ml)	distributed by A. Hartenstein Laborbedarf	RK2G
Syringe (1 ml) with needle 0.45 x 10 mm	Becton-Dickinson	300015
Syringe (10 ml)	Braun	4606108V
Syringe (50 ml)	Dispomed	22050
Syringe filter (0.2 µm)	Sartorius Stedim Biotech	17597
X-ray film	FujiFilm	47410 08379

2.11. Equipments

Apparatus	Supplier
Autoclave tape (180°C)	distributed by A. Hartenstein Laborbedarf
Autoclave tape (120°C)	distributed by A. Hartenstein Laborbedarf
Neubauer counting chamber	Brand
Centrifuges	Eppendorf
Computer	Apple
Incubator	Heraeus, Thermo electron corporation
Thermocycler	Eppendorf
Gel Documentation system	Image Quant 4000, GE Healthcare
Photometer	GeneQuant 1300, GE Healthcare
Nano-HPLC system	Agilent 1100, (Agilent Technologies GmbH, Boeblingen, Germany)
C18 columns (for nano seperations)	Nieuwkoop, The Netherlands
Q-TOF-Mass spectrometer	QstarXL, Applied BiosystemsGmbH, Darmstadt, Germany

2.12. Media, Buffers and Solutions

Cell culture medium for HEK 293

- 10% FCS
- 100 U/ml Penicillin
- 100 µg/ml Streptomycin
- 0.2 mM L-glutamate in DMEM

LB Medium for Bacterial propagation

20g LB broth (with 10g/L Trypton, 5g/L NaCl and 5 g/L Yeast extract) in 1L of dH_2O
Autoclave for 15 minutes at 121°C.

Buffers and solutions for Protein SDS-PAGE and Western blotting

Seperating Gel

	6.5 %	**7.5%**	**10%**	**11%**	**12%**
Dist.Water	6.7 mL	5.7mL	4.8mL	4.5mL	4.1mL
3M Tris-HCl, pH-9.0	1.3mL	1.3mL	1.3mL	1.3mL	1.3mL
Acrylamide 30	2.3mL	2.6mL	3.5mL	3.9mL	4.2mL
20% SDS	50µL	50µL	50µL	50µL	50µL
TEMED	10µL	10µL	10µL	10µL	10µL
10% APS	50µL	50µL	50µL	50µL	50µL

Stacking Gel

Dist.water	2.6 mL
1M Tris-HCl,pH-6.8	420µL
Acrylamide 30	550µL
20%SDS	17µL
TEMED	5µL
10% APS	33µL

10x Running Buffer

- 250 mM Tris (base)
- 190 mM Glycine
- 0.1% (w/v) SDS
- H_2O dest

Blotting (Transfer) Buffer (1.5L)

- 25 mM Tris (base)
- 192 mM Glycine
- 20% (v/v) Methanol

Ponceau S

- 0,2 % (w/v) Ponceau S
- 3 % (w/v) Trichloroacetic acid

1X PBS

- 9.5 g 10x PBS powder in 1L H_2O dest

PBS-Tween

- 0.05% (v/v) Tween 20 in 1x PBS

Blocking solution (5% Dried milk solution)

- 5 g Dried milk powder in 100 ml 1x PBST

Stripping buffer

- 62,5 mM Tris
- 2 % (w/v) SDS
- pH 6,7

1x SDS sample buffer (Protein sample buffer)

- 60 mM Tris-HCl pH 6,8
- 10 % (v/v) Glycerin
- 3 % (w/v) SDS
- 5 % (v/v) ß-Mercaptoethanol
- 0,005 % (w/v) Bromophenolblue

5x SDS sample buffer (Protein sample buffer)

- 300 mM Tris-HCl pH 6,8
- 50 % (v/v) Glycerin
- 15 % (w/v) SDS
- 25 % (v/v) ß-Mercaptoethanol
- 0,025 % (w/v) Bromophenolblue

Immunoprecipitation buffer

- 25 mM Tris, pH 7.4
- 150 mM NaCl
- 1 mM EDTA
- 0.1% (v/v) NP 40
- 10% (v/v) Glycerin

Purification of GST-tagged proteins

Binding buffer

- 2.5 mM Tris pH 7.4
- 1X PBS

Elution buffer

- 20 mM Tris pH 7.8
- 100 mM NaCl
- 20 mM Glutathione
- 5 mM DTE

GST Pull down assay

Lysis buffer

- 25 mM Tris pH 7.4
- 150 mM NaCl
- 1 mM EDTA
- 0.1% (v/v) NP40
- 10% (v/v) glycerol
- 1 mM PMSF
- Roche-Protease inhibitor cocktail

Washing buffer

- 20 mM Tris pH 7.6
- 50 mM NaCl
- 1 mM EDTA
- 5% (v/v) glycerol
- 1 mM DTE
- 0.1% Triton-X-100
- Roche-Protease inhibitor cocktail

Lysis buffer, without EDTA (for GST-Spir-1-KIND/ Myc-Spir-1-CT pull down)

- 25 mM Tris pH 7.4
- 150 mM NaCl
- 5 mM $MgCl_2$
- 0.1% (v/v) NP-40
- 10% (v/v) glycerol
- 1 mM PMSF
- Roche-Protease inhibitor cocktail

Washing buffer without EDTA (for GST-Spir-1-KIND/ Myc-Spir-1-CT pull down)

- 20 mM Tris pH 7.6
- 50 mM NaCl
- 5 mM $MgCl_2$
- 5% (v/v) glycerol
- 2 mM DTE
- 0.1% Triton-X-100
- Roche-Protease inhibitor cocktail

6x DNA loading buffer

- 9 mM Tris-HCl pH 7,4
- 0,45 mM EDTA
- 46 % (v/v) Glycerin
- 0,2 % (w/v) SDS
- 0,05 % (w/v) Bromophenolblue

TBE buffer

- 0.89 M Tris –Base, pH 8.3
- 25 mM EDTA
- 0.89 M Boric acid

CIP buffer

- 50 mM Tris-HCl pH 7,9
- 10 mM $MgCl_2$
- 100 mM NaCl
- 1 mM DTT

Coomassie (G-250) solution

- 0.1% Coomassie Brilliant Blue G-250
- 2% Phosphoric acid
- 5% Aluminium sulphate
- 20% Methanol

3. Methods

3.1. Molecular Biology

3.1.1. DNA amplification by polymerase chain reaction (PCR)

PCR is a powerful technique used for the amplification of a specific DNA sequence of interest using a DNA polymerase enzyme, like *Pfu* polymerase and two sequence specific oligonucleotide primers that bind to the sense and antisense strands of the DNA template. The PCR is commonly carried out in an automated Thermal cycler (Eppendorf) which put the reaction through a series of 20-40 cycles of denaturation of DNA template, annealing of primers to the DNA template, elongation of the primer catalyzed by the polymerase and the final elongation, with three different temperatures. The denaturation temperature is in the range of 94-96°C. The annealing temperature is about 3-5 degrees below the Tm (melting temperature) of the primers used. The time requred for the elongation is dependent on the length of the desired PCR product. For *Pfu* polymerase 1 minute elongation was sufficient for 1kb of plasmid length.

3.1.2. Agarose Gel Electrophoresis

Agarose gel electrophoresis is a technique used to identify and separate DNA fragments based on their size. Agarose gel with a concentration of 0.8% is prepared by dissolving Agarose (w/v) in 0.5x TBE buffer and boiled in microwave until the agarose is dissolved. Afterwards the solution is cooled to 50°C, and supplimented with 0.5 µg/ml of the fluorescent DNA-intercalating ethidium bromide. This was poured into the gel trays and the combs were inserted. After the soldification of the gel, the trays were put into the electrophoresis chamber and the combs were removed. DNA samples were mixed with 6x DNA loading buffer, loaded onto the gel and electrophoresis was conducted at 120 volts for 35 minutes until the blue dye reaches the front of the gel. 1Kb DNA ladder was used to determine the size of the DNA fragments which were visualised using a UV transilluminator. The fragments were excised and recovered from the gel using NucleoTrap Gel Extract Kit (Macherey & Nagel) following the manufacturers´ instructions.

3.1.3. DNA digestion

DNA fragment with specific restriction sites was incubated with restiction endonucleases (NEB) following the manufacturers´ recommendations. The exact digestion was verified by agarose gel electrophoresis.

3.1.4. Transformation

Uptake of plasmid DNA into a bacterium is called transformation and the bacterial cells that are capable of transformation are called competent cells. Competent cells are prepared by treating them with Rubedium chloride (RbCl), which promotes the binding of the plasmid DNA to the cell surface which further pass into the cell.

Competent *E.coli* (NEB 10) cells, kept as glycerol stocks, were initially thawed on ice. 100 µl of the cell suspension was mixed with the DNA sample, gently mixed and kept on ice for 45 minutes. The cells were heat shocked for 55 seconds at 42°C and chilled on ice for 2 minutes. 900µl LB was added and incubated at 37°C for 1 hr with shaking. The cells were collected by centrifugation at 6000 rpm for 10 minutes at room temperature. Supernatent was discarded and the pellet was resuspended in 150µl LB. 50 and 100µl were plated out on LB agar plates containing appropriate antibiotic selection marker and incubated overnight at 37°C.

3.1.5. Plasmid DNA preparation

A single bacterial colony from the overnight transformants was added to LB medium supplimented with appropriate antibiotic were incubated at 37°C for overnight. The cells were pelleted and the DNA was isolated using Plasmid Mini Kit and Plasmid Maxi Kit (Qiagen). The purified DNA was digested with the desired restriction enzymes. The digested sample was loaded on 0.8% agarose gel and conducted electrphoresis for verification.

3.1.6. Sequencing

DNA plasmids were sequenced by Eurofins MWG/ Operon (Ebersburg).

3.1.7. Site-directed Mutagenesis

Serine136 in pcDNA3-Myc-hs-Spir-2 (Spir-2 full length) and S150 in pGEX-4T1-NTEV-hs-Spir-1-KIND were mutated to Ala and Glu using QickChange Site-directed Mutagenesis Kit. This method is performed using *PfuTurbo*® DNA polymerase. The basic procedure utilizes a supercoiled double stranded DNA (dsDNA) vector with an insert of interest and two synthetic oligonucleotide primers containing desired mutation. The primers, each complimentary to opposite strands of the vector, are extended during temperature cycling by *PfuTurbo*® DNA polymerase. Incorporation of oligonucleotide primers generates mutated plasmid containing staggered nicks. PCR was carried out in 50µl containing, 50ng of DNA to be mutated, 125ng each of 5´ and 3´ primers, 5µl Pfu 10x buffer, 1µl of 10mM dNTPs and 1.5µl of *PfuTurbo*® DNA polymerase in autoclaved water. Thermal cycler carry out the reaction through the following settings:

1. 95°C for 30sec for the first denaturation of the double stranded DNA template
2. 95°C for 30sec for the denaturation of the DNA template
3. 67°C for 1 min for annealing of the primer to the DNA template
4. 68°C for 1 min/kb of plasmid length elongation.

The following primers (primer sequence 5´to 3´) were used for Myc-Spir-2- S136A: gag agc gag gag cgc gaa ctc **gcc** cct cag ctg gag cgg ctc atc ; Myc-Spir-2- S136E: gag agc gag gag cgc gaa ctc **gaa** cct cag ctg gag cgg ctc atc ; Myc-Spir-1-KIND-S150E : aag gag aat gaa gaa agg gaa tta **gag** cct ccc cta gag cag ctt atc.

The non-mutated methylated DNA template was selectively degraded by *Dpn*I endonuclease by adding 1 µL *Dpn*I (10 U/µL) per reaction mixture and incubated at 37°C for 1 hour. The non-methylated amplified mutation-harboring plasmid was then transformed into NEB10. Plasmid DNA was isolated from the transformed colonies by Plasmid Mini and Maxi kits and mutations were verified by sequencing.

3.2. Cell biology

3.2.1. Cell culture

HEK 293 cells were grown in Dulbecco´s modified Eagle´s medium supplimented with 10% fetal calf serum, 2mM L-glutamate, 100U/ml Penicillin and 100µg/ml Streptomycin in a humidified atmosphere of 10% CO_2 and at a temperature of 37°C.

3.2.1.1. Poly-L-Lysine coating of culture plates

Poly-L-lysine is a synthetic aminoacid widely used as a coating to enhance cell to improve cell attachment even in reduced and serum free conditions. Culture plates were incubated with 10% Poly-L-Lysine solution in H_20 dest. for 2-3 minutes at room temperature. Afterwards, the solution was removed and wells were allowed to get dried. Before culturing the cells in the plates, washing 2 times with 1x PBS is performed.

3.2.1.2. Transfection

Transient transfections were carried out by using Lipofectamine according to manufacturers´recommendations. Cells were seeded approximately 24 hours before transfection in DMEM full medium (10% FCS, Pen/Strep, L-Glu). At the day of transfection the cells reached a confluency of 80-90%. DNA and transfection reagent were suspended in DMEM without FCS, Pen/Strep and L-Glu. Appropriate amount of Lipofectamine solution was incubated with corresponding concentrations of DNA, for 20 minutes before being added to the cells. After 5-6 hr, the medium was changed to DMEM containing FCS, Pen/Strep and L-Glu. Cells were allowed to express proteins for 24-36 hours prior to harvesting.

3.3. Protein biochemical methods

3.3.1. Electrophoretic seperation of proteins

Polyacrylamide gel electrophoresis (PAGE) is applied to separate protein mixtures based on their migration in solution in response to an electric field. Proteins are amphoteric compounds. Therefore their net charge is determined by the pH of the solution. Throughout the course of this study, protein samples were separated under denaturing conditions using anionic detergent, SDS (Sodium dodecyl sulphate), which denature the proteins without breaking the peptide bonds. SDS disrupts the secondary and tertiary structure of the proteins and confers a negative charge to the polypeptides. Proteins charged negatively by the binding of SDS separate within a matrix of polyacrylamide gel in an electric field according to their molecular weights.

Gels were casted using casting chambers. The casting chamber was filled with seperating gel solution and overlaid by isopropanol. Formation of the polyacrylamide matrix was done by polymerization reaction of the monomers acrylamide and bisacrylamide induced by adding N, N, N', N'- tetraethylmethylendiamine (TEMED) and the polymerization starter, ammonium persulfate (APS). After polymerization, isopropanol was removed and the separating gel was overlaid by the stacking gel solution and the combs were inserted. Different concentrations of acrylamide were used for separating gels. Gels were placed in gel chambers and 1x SDS electrophoresis buffer (Running buffer) was added in the buffer chamber. Prior to loading, protein samples were boiled with 1x, 2x or 5x SDS-loading buffer and boiled for 5 minutes at 90°C. Electrophoresis was performed at 45 mA at room temperature until the bromphenol blue dye reached the bottom of the gel. Protein sizes were analyzed using the pre-stained Protein Ladder (*Bio-Rad*) as molecular weight marker.

3.3.2. Coomassie staining

To visualise the proteins with Coomassie staining, Coomassie Brilliant Blue G-250 or R-250 is employed. The former differ from the latter in having two additional methyl groups. This staining method is fast but much less sensitive (about 100 ng per protein band) than silver staining. After electrophoresis, the gels were dipped in the stain for 15 min with shaking and excess stain is removed by gentle agitation with dH_2O until the clear band of desired protein is viewed. Coomassie Brilliant Blue G-250 is highly compatible with mass spectrometry and is therefore employed for staining the gels for the purpose of identification of phosphorylation sites by mass spectrometry. Coomassie Brilliant Blue G-250 is able to form colloids in acidic media containing ammonium sulfate (Neuhoff *et al.,* 1988) i.e., there is a very low concentration of free dye resulting in minimal background staining. The colloids act as a reservoir of dye molecules, so that enough dye is present to occupy all binding sites

of the proteins, provided that staining is prolonged to the steady state. The electrophoresed gel was stained with Coomassie Brilliant blue G250 for overnight and washed with distilled water for 4-5 times with gentle shaking.

3.3.3. Ponceau S staining

To control the efficient transfer of the proteins to the nitrocellulose membrane, the membrane was incubated in Ponceau solution for 1 minute and gently washed with PBST buffer. Afterwards, the membrane was destained in PBST buffer for several times until the red colour was completely removed.

3.3.4. Western blotting and Immunodetection

Proteins were transferred efficiently from a polyacrylamide gel to a nitrocellulose membrane by electroblotting (western blot) using a Sigma blotting tank. The transfer was carried out for 1.5 hours at 150 mA at room temperature in blotting buffer. Protein transfer was verified by staining the nitrocellulose membrane with Ponceau S solution for 1 minute at room temperature followed by rinsing the membrane with distilled water 2-3 times to reveal the protein distribution on the nitrocellulose membrane. Thereafter, the membrane was destained with PBS-Tween (PBST) until staining faded away completely. For immunodetection, the nitrocellulose membrane was blocked over night in blocking buffer (5% Milk solution) at 4°C. After blocking, the membrane was incubated in blocking buffer containing the corresponding primary antibody for 1.5 hour at room temperature. Subsequently, the membrane was washed 3 times with PBST for 10 min at room temperature with shaking. Further the membrane was incubated in PBST: blocking buffer 3:1 (v/v) containing the secondary HRP-linked antibody for 35 minutes at room temperature, followed by a second washing as described above. Detection was performed with an ECL reagent kit (Enhanced Chemiluminescence, GE Healthcare) and experimental datas were digitalized with an ImageQuant LAS 4000 CCD camera imaging system and a PeqLab gel documentation system which was further processed with Adobe Photoshop.

3.3.5. Blot stripping

Membrane stripping is the removal of primary (1°) and secondary (2°) antibodies from a western blot membrane to allow the incubation of new 1° and 2° antibodies for the assay of new protein by western blot. Western blot stripping buffer removes both the antibodies without removing or damaging the immobilized antigen. This allows blots to be stripped and reprobed. Blot stripping buffer is prewarmed at 50°C. The nitrocellulose membrane to be stripped, is incubated with stripping buffer for 15 minutes at 50°C. This is repeated for 2 more times. After the third incubation, the membrane is washed with 0.05% PBST, 4 times for 10

minutes and blocked in blocking solution overnight before being reprobed by corresponding antibodies.

3.3.6. Recombinant protein expression in prokaryotes

The expression of the fusion protein may be affected by a variety of factors such as the (a) *E. coli* strain, (b) cell growth conditions (e.g. temperature, aeration, cell density, IPTG concentration, etc.), (c) toxicity of the target protein, (d) codon usage and (e) structure and stability of mRNA. For the prokaryotic expression of proteins, the *E.coli* strain Rosetta (Novagen) has been used. Rosetta strains are BL21 derivatives designed to enhance the expression of proteins that contain codons rarely used in *E.coli.* These strains supply tRNAs for AGG/AGA (Arginine), AUA (Isoleucine), CUA (Leucine), CCC (Proline) and GGA (Glycine), codons on a compatible chloramphenicol-resistant plasmid, pRARE. By supplying rare codons, the Rosetta strains provide for ″universal″ translation, where translation would otherwise be limited by the codon usage of E.coli. Protein expression is under the control of the lacZ promotor and is induced by the lactose analog isopropyl-ß-D-thio-galactoside (IPTG). IPTG binds to the repressor and inactivates it, but is not a substrate for β-galactosidase. As it is not metabolized by E. coli, its concentration remains constant. Therefore the expression rate of the recombinant protein is also constant.

3.3.6.1. Expression and purification of GST-tagged recombinant proteins

Glutathione-S-transferase (GST) from *Schistosoma japonicum* is used as tag for proteins for expression and purification applications. GST is a 26 KDa protein which binds to glutathione with high affinity and specificity. Recombinant proteins fused to GST can then be selectively purified based on its high affinity for immobilized glutathione (glutathione sepharose). Sepharose is a bead form of agarose. The binding occurs under nondenaturating conditions since GST loses its ability to bind glutathione sepharose when denatured. The cDNA of interest cloned into pGEX-4T1-NTEV was used.

Procedure : Expression and purification of GST-fusion proteins for GST-pull down assay (GST-Fmn2-eFSI, GST-Spir-1-KIND and GST-Spir-1-KIND-S150E)

Escherichia coli Rosetta pLysS bacteria were transformed with plamid encoding GST-tagged Spir and formin constructs. Initially, the recombinant bacteria were grown in LB medium with 10% Ampicillin (1:1000) and 34 mg/liter Chloromphenicol (1:1000) at 37° C with shaking (160 rpm). The next day 200 ml of LB medium with 10% Ampicillin (1:1000) and 34 mg/liter Chloromphenicol (1:1000) was inoculated with primary culture (10:1) and incubated at 37°C with shaking at 160 rpm until A_{600} ~ 0.5 – 0.6 is reached. When the desired OD is reached, the temperature was lowered to 21°C and protein expression was

induced with 120µM IPTG and allowed to proceed at 21°C for overnight. Cells were harvested at 4000 x g for 20 minutes at 4° C and the pellet were resuspended in buffer A (2.5 mM DTE in 1x PBS, pH 7.4). Bacteria were lysed by ultrasonication and centrifuged at 20000 x g for 30 minutes at 4°C. The high speed supernatant were incubated with 300 µL GSH- Sepharose 4B resin (GE Healthcare) for 2h-overnight at 4°C on a rotating wheel. The beads were washed 5 times with buffer A and proteins were eluted with 600 µL of elution buffer (20 mM Tris, pH 7.8, 100 mM NaCl, 20 mM glutathione and 5 mM DTE). Proteins were concentrated by ultrafiltration using Amicon Ultra-4 ultracentrifugation devices with molecular mass cut offs of 10000 Da (Millipore). Protein concentration was measured by Bradford method using bovine serum albumin as standard. Fractions were collected, stored at – 20°C. Aliquots of the fractions were analyzed by SDS-PAGE followed by Coomassie staining.

3.3.7. Methods for the detection of protein-protein interactions

Since protein-protein interactions are intrinsic to every cellular processes and carries extreme relevance, there are a multitude of methods to detect them. Each approaches has its own advantages and disadvantages regarding the sensitivity and specificity. The study make use of two methods: Pull down assays and Immunoprecipitation.

3.3.7.1. GST fusion protein pull-down technique.

As a relatively easy and straightforward method to confirm the known protein-protein interactions and to map the interaction sites, it is worthwhile to employ pull-down assays. Glutathione-S-transferase (GST) fusion proteins have had a range of applications since their introduction as tools for synthesis of recombinant proteins in bacteria. GST pull-down experiments are used to identify interactions between a probe protein and unknown targets and to confirm suspected interactions between a probe protein and a known protein. The probe protein is a GST fusion protein whose coding sequence is cloned into an IPTG – inducible expression vector. This fusion protein is expressed in bacteria and purified by affinity chromatography on GSH-Sepharose beads. The target proteins are usually lysates of cells. The cell lysate and the GST fusion protein are incubated together with GSH-Sepharose beads. Complexes recovered from the beads are resolved by SDS-PAGE and analyzed by western blotting or staining.

For GST Pulldown experiments with the GST-Fmn2-eFSI / Myc-hs-Spir-2 and GST-Spir-KIND domains / EGFP-tagged Spir-1-FYVE. 50µg of purified GST/GST fusion protein bound to 13µl of GSH-Sepharose 4B resin (GE Healthcare) were used. Cell lysates were prepared by lysing ~36 x 10^5 HEK 293 cells in 900 µl of Lysis buffer (25 mM Tris pH 7.4, 150 mM NaCl, 1 mM EDTA, 0.1%(v/v) NP40, 10%(v/v) Glycerol, 1 mM PMSF ; which was also

supplemented with one tablet of Protease inhibitor mixture (Roche Applied Science) per 7ml of buffer) at 4°C. Care should be taken to avoid EDTA from lysis and washing buffer when dealing with HEK 293 transfected with Spir-CT. The lysate was centrifuged at 20,000×g for 20 minutes at 4°C. 50µg of GSH-Sepharose 4B- bound GST fusion proteins were incubated with the high speed supernatant of the cell lysate for 2 hours at 4°C. Beads were gently washed 4 times with Washing buffer (20 mM Tris pH 7.6, 50 mM NaCl, 1 mM EDTA, 5% (v/v) Glycerol, 1mM DTE, 0.1% (v/v) Triton X- 100; supplemented with 1 tablet of Protease inhibitor mixture per 7 ml of buffer) and boiled in 2x SDS protein sample buffer. The samples were subjected to SDS-PAGE followed by Western blot analysis. c-Myc-9E10 mouse monoclonal antibody (1:500 ; Santa Cruz Biotechnology, Inc.) and anti-Spir-2 antibody (1:1000 ; Lab stock), rabbit A.V- living colors antibody (1:100; Takara/Clontech) were used as primary antibodies, which were detected with horseradish peroxidiase- conjugated anti-mouse and anti-rabbit secondary antibodies (1:5000 ; GE Healthcare) respectively, and visualized with the enhanced chemiluminescence kit (GE Healthcare). Experimental datas were digitalized with an ImageQuant LAS 4000 CCD camera imaging system and a PeqLab gel documentation system which was further processed with Adobe Photoshop.

3.3.7.2. Immunoprecipitation (IP)

IP is a technique of precipitating a protein antigen out of solution using an antibody that specifically binds to that particular protein. The present study makes use of the indirect method of IP in which antibody that is specific for the particular protein are directly added to the mixture of proteins. The Protein G agarose beads are then added to the mixture of antibody and the protein, so that antibody bound to the targets will stick to the beads. One of the major technical hurdles with IP is the difficulty in generating an antibody that specifically target a single known protein which can be overcome by using tags onto either N- or C-terminal end of the protein of interest. Target proteins used in the study is Myc-tagged and to immunoprecipitate them anti-Myc 9E10 antibody is used. HEK293 cells (3 x 10^5 per well) were seeded in a 6-well plate one day before transfection. Cells were transfected with Myc-Spir-2 alone and together with Myc-JNK-MKK7. 24 hours post-transfection the cells were lysed with 333µl immunoprecipitation buffer (25 mM Tris, pH- 7.4, 150 mM NaCl, 1 mMEDTA, 0.1% (v/v) NP40 and 10% glycerol). The cell lysate was centrifuged for 5 minutes at 40,000 rpm at 4°C. Anti-myc-9E10 antibody was added to the cleared supernatent to a final concentration of 4 µg/ml and incubated for 1 h on ice. 30µl of Protein- G-Agarose (Roche) beads was added, and the sample was rotated for 2 hours at 4°C. The beads were washed three times with IP buffer and the reaction was stopped by boiling the beads in 1x SDS protein sample buffer. The samples were resolved by SDS-PAGE and detected by Western blotting.

3.3.8. Phosphatase assay

HEK 293 cells were transfected with Myc-Spir-2 in presence and absence of JNK-MKK7 using Lipofectamine following manufacturers´ ´instructions. After 24 hours post-tansfection, the cells were harvested in immunoprecipitation (IP) buffer and were further undergone immunoprecipitation with anti-Myc-antibody (4µg/ml) for 1hour in ice. The complex is incubated with 30 µl Protein-G-Agarose beads (Roche) for 2 hours at 4°C on a rotating wheel. The beads were washed 3 times with IP buffer and after the last washing the beads were resuspended in CIP buffer (50 mM Tris- HCl, pH-7.9, 10 mM MgCl2, 100 mM NaCl and 1 mM DTT). 10 units of Calf Intestinal Phosphatase (CIP; 10,000U/ml) was added to 25µl beads suspension and incubated at 37°C for 1 hour. Reaction was stopped by the addition of 40µl of 1X SDS sample buffer and heated for 5 mins at 90°C. The samples were subjected to 7.5% SDS-PAGE followed by western blotting using anti-Myc-antibody.

3.4. Fluorescence anisotropy

Anisotropy is a measure of the correlation between polarization aof fluoresence excitation and emission. The anisotropy is maximal when a fluorophore is absolutely fixed in space. Fluorescence anisotropy can be used for measuring the binding interaction between two molecules, to determine the binding constant (or the inverse, the dissociation constant) for the interaction. Protein interactions can be detected when one of the interacting partners is fused to a fluorophore. Upon binding of the partner molecule a larger, more stable complex is formed which will tumble more slowly (thus, increasing the polarization of the emitted light and reducing the "scrambling" effect). This technique works best if a small molecule is fused to a fluorophore and binds to a larger partner (this maximizes the difference in signal between bound and unbound states). If the fluorophore is attached to the larger protein in a binding pair, the difference in polarization between bound and unbound states will be smaller (because the unbound protein will already be fairly stable and tumble slowly to begin with) and the measurement will be less accurate. Fluorescence anisotropy measurements were performed in a Horriba Jobin Yvon Fluoromax-4 spectrophotometer in anisotropy buffer (10 mM Hepes, pH 7.0,100 mM NaCl) at 20 °C. Proteins for anisotropy measurements, were labelled on cysteines with the thiol reactive maleimidocaproyl-linked BodipyFL™-fluorophore (Probes). Proteins were buffer exchanged into labelling buffer (10mM Hepes, pH 7.0, 100mM NaCl, 0.25 mM Tris (2-carboxy-ethyl) phosphine) using Nap 10 columns (GE Healthcare). A 2-fold molar excess of the dye was coupled with the protein (1-5g/L) for 16-18 h at 4°C. Excess non-reacted dye was quenched with 20mM dithioerythritol and subsequently removed using Nap 10 columns. The BodipyFL™ fluorophore was excited at 495 nm, and emission was collected at 510 nm, with an integration time of 2s for the Bodipy-labelled

formin peptides (100 nM) and 4s for the BodipyFL™-labeled Spir-1-KIND domain (100 nM). The slit width of the emission and excitation monochromators was set to 2 nm for the Bodipy-FLTM-labeled formin peptides and 3 nm for the labeled Spir-1-KIND domain, respectively. Each data point of the binding curve which is the mean of at least eight collected polarization signals. Data analysis and processing was done with Sigma Plot 9.0 (Systat Software).

3.5. Mass Spectrometry measurements

Gel bands in the Coomassie staining (Coomassie Brilliant Blue G250) corresponding to the phosphorylated and non-phosphorylated fragments of Spir-2 protein, were excised and washed according to Shevchenko *et al*. (1996). Briefly, gel pieces were washed 3 times alternatively with 50µl of 50 mM ammonium bicarbonate and 25 mM ammonium bicarbonate in 50% acetonitrile. Subsequently, the gel slices were dried in vaccum centrifuge. 5µl of Trypsin solution (12.5 ng/µl in 50 mM ammonium bicarbonate) were added to each gel piece and incubated at 37°C overnight for in-gel digestion. The obtained peptides were eluted with 20µl of 5% formic acid and subjected to nano-liquid chromatography-MS/MS analysis. Therefore, an Agilent 1100 nano- HPLC system (Agilent Technologies GmbH, Boeblingen, Germany) was used. The samples were pre- concentrated on a 100 µm inner diameter, 2cm C-18 column (Nanoseperations, Nieuwkoop, The Netherlands) using 0.05% trifluroaceticacid with a flow rate of 8ml/minute. The peptides were then separated on a 75µm inner diameter, 15cm, ZorbaxSB300-C18-column (flow rate 300µl/minute; Agilent Technologies GmbH, Boeblingen, Germany) using a 2h binary gradient from 5-50% solvent B (Solvent A: 0.2% formic acid; Solvent B: 0.2% formic acid, 84% acetonitrile). The nano-HPLC was directly coupled to QTOF-mass spectrometer (QStar XL, Applied Biosystems GmbH, Darmstadt, Germany) acquiring repeatedly one full-MS and two tandem-MS spectra of the most intensive ions in the respective full MS scan. The tandem-MS spectra were searched against the SwissProt database using Mascot algorithm version 2.2 (Matrix Science Ltd., London, UK) using the following adjustments: trypsin as protease, one missed cleavage site, oxidation of methionine, phosphorylation of serine, threonine and tyrosine, pyroglutamic acid for N-terminal Gln as variable modifications, 0.2 Da tolerance for MS and MS/MS signals, and only doubly and triply charged ions.

4. Results

4.1. Phosphorylation of human Spir-2

4.1.1. Identification of phosphorylation sites in human Spir-2

Drosophila p150-Spir was found to be a phosphorylation target of JNK activity and it was also observed that JNK-MKK7, a constitutively active form of JNK, induces an electrophoretic mobility shift of p150-Spir as a result of protein phosphorylation (Otto *et al,* 2000). Still, the sites of phosphorylation were not known yet. In analogy to these facts, this study carries the interest to elucidate the phosphorylation profile of mammalian Spir proteins by employing a contemporary mass spectrometric (MS) approach. All the phosphorylation experiments are carried out with Myc tagged human-Spir-2 protein (Myc-hs-Spir-2) together with the constitutively active JNK-MKK7 kinase. As a prerequisite to get the Spir-2 protein for the MS analysis, Spir-2 was expressed in HEK 293 cells and subsequently pulled down using purified GST-tagged Fmn-2-eFSI in a conventional GST-pull down assay, which was performed based on the fact that mammalian Spir proteins (Spir-1/2) interact with mammalian formin proteins (Fmn-1/2) and the interaction is mediated by N-terminal Spir KIND domain and formin-2 formin Spir interaction sequence (FSI) with flanking sequences N-terminal to it (eFSI) (Pechlivanis *et al*., 2009). Later on, both the phosphorylated as well as non-phosphorylated fragments of Spir protein were identified in Coomassie staining as well as in Western blotting. Initially GST-Fmn-2-eFSI was expressed and purified to perform the pull-down experiment.

4.1.1.1. Expression and purification of GST-Fmn-2-eFSI

As a preliminary step for the GST pull-down assay, GST-Fmn-2-eFSI fusion protein was purified. *E.coli* Rosetta strain was transformed with a GST-Fmn-2-eFSI expression vector and expression was induced with 0.1mM IPTG at 21°C (→ 3.3.6.1). Cells were harvested, sonicated and the clear supernatent was incubated with Glutathione (GSH) – Sepharose 4B beads. The beads and associated proteins were undergone repeated spin down and resuspension cycles and afterwards the protein was eluted from the beads and concentrated via an Amicon Ultrafiltrate device. The concentration was determined by a Bradford assay and the purified GST-Fmn-2-eFSI protein corresponding to the size of 33KDa was identified in coomassie staining (Figure 4.1.1.1) which was further on used for the GSTpull-down assay with Spir-2 protein.

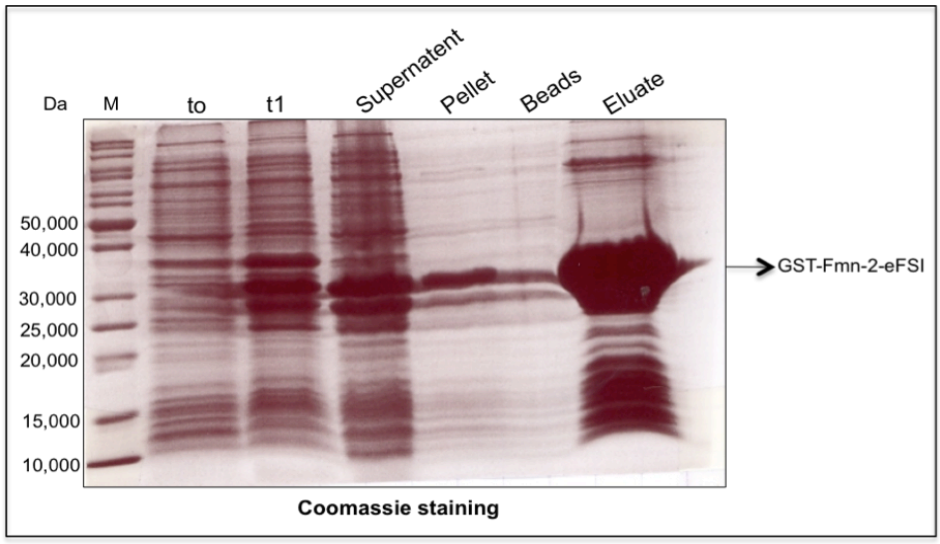

Figure 4.1.1.1 Expression and purification of GST-Fmn-2-eFSI. GST-Fmn-2-eFSI was expressed in Rosetta and the expression was induced using 0.1mM IPTG at 21°C. The cells were harvested, sonicated and centrifuged. Supernatent and pellet fractions are from the high speed centrifugation of the sonicated cell lysates. The clear supernatent was coupled to GSH-Sepharose beads. The beads were washed and the protein was eluted and concentrated via Amicon Ultra4 centrifugation devices. SDS-PAGE was conducted on a 10% Polyacrylamide gel and the protein was visualized using Coomassie staining. The band of GST-Fmn-2-eFSI protein is indicated.
Abbreviations: M, Marker; KDa, kilo Dalton; to, non-induced control; t1, induced control.

4.1.1.2. Interaction between Spir-2 and Fmn-2

To purify transiently expressed Spir-2 from HEK 293 cell lysates, a GST pull-down assay was performed. HEK 293 cells were transiently transfected with plasmid encoding Myc-hs-Spir-2 (pcDNA3-Myc-hs-Spir-2 (full length)). After 24 hours transfection, total cell lysates were made in 900µl of chilled pull-down buffer. The lysate was centrifuged at 20,000x g for 20 minutes at 4°C. 50 µg each of purified GST-Fmn-2-eFSI and GST (as control) proteins were allowed to get bound to 13µl of GSH-Sepharose 4B beads (→ 3.3.7.1) for 1 hour. Beads were gently washed with the pull down buffer and incubated with the high speed supernatant of the cell lysate for 2 hours at 4°C. Beads were again washed for 4 times at 4 °C at 500 x g and boiled in 2x SDS protein sample buffer at 95°C for 5 minutes. The pulled fractions were subjected to SDS-PAGE followed by western blotting using anti-Myc antibody as primary antibody and a horseradish peroxidase-conjugated anti-mouse secondary antibody. The bands were visualized with the Enhanced Chemiluminescence Kit (Amersham). The blot reveals the interaction between Spir-2 and Fmn-2 (4.1.1.2 B).

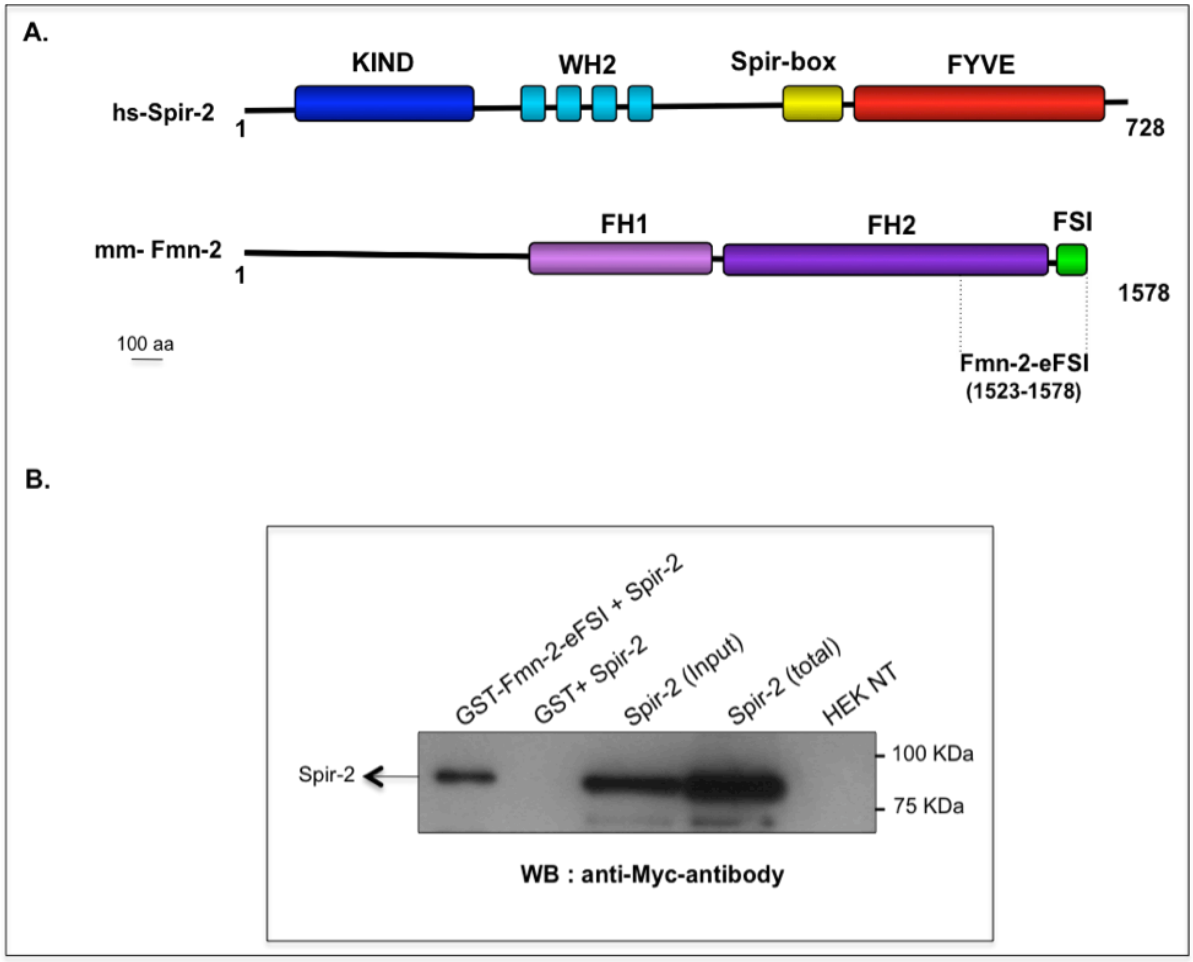

Figure 4.1.1.2. Interaction between Spir-2 and Fmn-2. A. Domain organizations of hs-Spir-2 (GenBank accession No: CAD19439.1) and mm-Fmn-2 (Swiss-Prot entry No: Q9JL04.2) Abbreviations: KIND, Kinase non-catalytic C-lobe domain; WH2, WASP homology-2 domain; FYVE, modified FYVE Zn finger; FH1, Formin homology 1 domain; FH2, Formin homology 2 domain; FSI, Formin-Spir Interaction sequence; eFSI, FSI with flanking sequences from FH2 (aa1523-aa1578); aa, aminoacid **B.** GST protein alone or GST-protein fused to Fmn-2-eFSI (GST-Fmn-2-eFSI) have been coupled to Glutathione-Sepharose beads and incubated with HEK 293 cell lysates expressing Spir-2. The proteins expressed in the cell lysates were pulled down in a GST pull-down experiment with purified GST-Fmn-2-eFSI and GST bound to GSH-Sepharose 4B beads, were detected by immunoblotting using anti-Myc antibody. HEK NT is HEK 293 cells non-transfected with Spir-2 and is used as control.

4.1.1.3. Spir-2 is phosphorylated by JNK-MKK7

The next step was to address the question, whether mammalian Spir is phosphorylated. To cross over this question, the same pull-down assay as above was employed but with the involvement of JNK-MKK7, so as to know the effect of JNK-kinase on phosphorylation. Briefly, HEK 293 cells were transiently transfected with Spir-2 alone and together with JNK-MKK7 in order to compare the electrophoretic mobility, if there is any. 24

hours post-transfection the cell lysates were collected, sonicated, centrifuged and the clear supernatent was incubated with purified GST and GST-Fmn-2-eFSI. Afterwards pull-down assay was conducted as above. The pulled fractions were resolved in SDS-PAGE followed by western blotting with Anti-Spir-2 antibody and horseradish peroxidase conjugated anti-rabbit antibody as primary and secondary antibodies respectively and visualized using Enhanced Chemiluminescence Kit.

JNK-MKK7 induced an electrophoretic mobility shift of Spir-2 indicating phosphorylation of Spir-2 (Figure 4.1.1.3 B). Two prominent bands were observed corresponding to the molecular weight of non-phosphorylated and phosphorylated fragments of Spir-2 protein which strongly suggests the phosphorylation of Spir-2 protein in response to JNK-MKK7. There was no interaction between Spir-2 and GST protein alone.

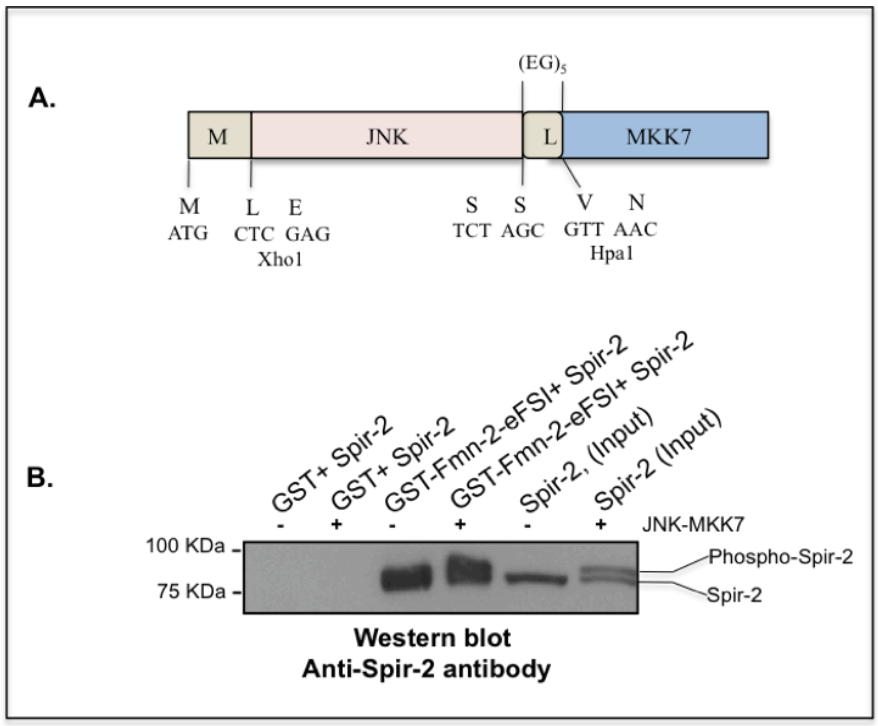

Figure 4.1.1.3. Phosphorylation of Spir-2 by JNK-MKK7. A. Structure of the JNK–MKK7 fusion protein. Amino acids 2–426 of rat JNK3 (GenBank accession No. ABD24063) were fused via an (EG)5 linker peptide (L) to amino acids 2–346 of mouse MKK7 (GenBank accession No: AF026216). In addition, a Myc epitope tag (aminoacids 410–419 of c-Myc; M) was fused to the amino terminus of the protein (modified from Otto *et al.,* 2000). **B.** GST protein alone or GST-protein fused to Fmn-2-eFSI (GST-Fmn-2-eFSI) have been coupled to Glutathione-Sepharose beads and incubated with HEK 293 cell lysates expressing Spir-2 alone and along with JNK-MKK7. The proteins expressed in the cell lysates were pulled down in the GST pull-down experiment with purified GST-Fmn-2-eFSI and GST bound to GSH-Sepharose 4B beads, were detected by immunoblotting using a rabbit polyclonal anti-Spir-2 antibody.

4.1.1.4 Identification of phosphorylated residues in Spir-2

To confirm the phopshorylation as well as to identify the phopshorylation sites, a mass spectrometrical approach was employed.

Gel electrophoresis of protein samples, trypsin digestion of target proteins and analysis of the resulting peptide fragments by Mass Spectrometry (MS) comprise a powerful method for protein identification and characterization. A fluorescent, coomassie or silver stain is necessary to visualize proteins that have been separated in 1-D or 2-D gels. Processing such samples for mass spectrometry necessitates first excising the protein spot of interest, removing the stain, digesting and eluting the protein in the gel piece using an in-gel tryptic digestion which is the most commonly used procedure.

Accordingly, the same pulled fractions which showed the phosphorylation status of Spir-2, were again subjected to SDS-PAGE followed by staining with Coomassie Brilliant Blue (CBB) G-250 (Figure 4.1.1.4) to visualize the protein fragments, followed by MS analysis to confirm the phosphorylation site assignment of the protein.

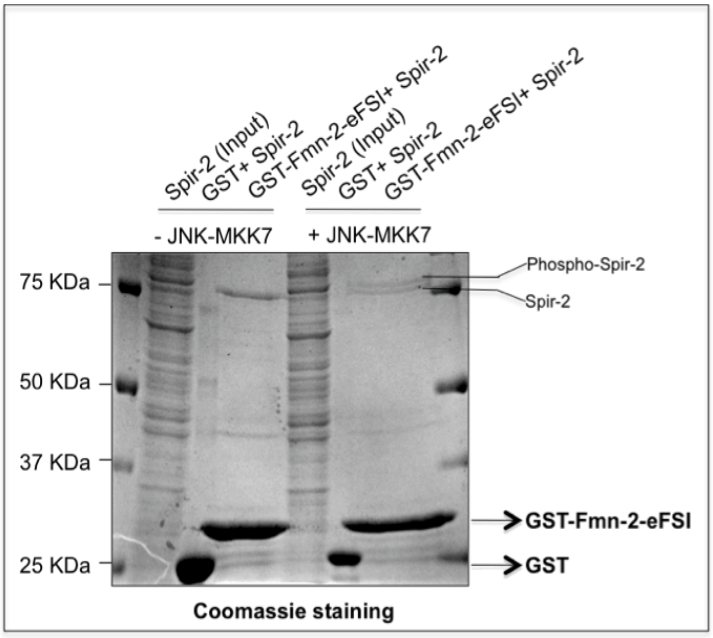

Figure 4.1.1.4 Coomassie staining of GST-Fmn-2-eFSI/Spir-2 (-/+JNK-MKK7) pull down.
SDS-PAGE gel of the pulled fractions comprising both phosphorylated and non- phosphorylated fragments of Spir-2, alone and along with JNK-MKK7, from the GST-pull down assay, stained with Coomassie Brilliant Blue G-250. Pull-down of Spir-2, with and without JNK-MKK7 from purified GST protein is also shown as a control.

Likewise the Westernblot from the pull down experiment, coomassie staining of the SDS-PAGE gel with the same pulled fractions came up with two sharp bands corresponding to the coexpression of Spir-2 protein along with JNK-MKK7 pulled from purified GST-Fmn-2-eFSI protein. On the otherhand, only a single sharp band is clearly visible which points to the pulled sample containing Spir-2 alone. These facts empower the study to move further with the MS analysis.

4.1.1.5. LC-MS/MS analysis of Spir-2 protein

MS has become a powerful technology for proteomics and is evolved as a method of choice for unbiased analysis of protein phosphorylation. To identify the phosphorylation sites, the study make use of nano-LC-MS/MS (Liquid chromatography-Tandem mass spectrometry) instrumentation which provide high sensitivity and good reproducibility.

Prior to the entry into MS, the gel bands corresponding to both the potentially phosphorylated and non-phosphorylated fragments of Spir-2 were excised carefully, washed and performed in-gel tryptic digestion (→ 3.5). The resulting peptide mixture is eluted with formic acid and further fractionated by nano-scale high performance liquid chromatography (HPLC) systems (Agilent 1100) that are directly linked to the inlet of the mass spectrometer which allows on-line detection and analysis of peptides. The liquid effluent containing the peptides eluted from the chromatography column is then electrostatically dispersed to multiply−charged analyte ions by Electrospray ionisation (ESI). Following ionization, the analyte ions are seperated by mass analyzer and finally detected.

The mass analyzer, QTOF (Quadrapole Time of Flight) enables the ions formed in the ionisation source of the mass spectrometer to get resolved according to their mass-to-charge (m/z) ratios. The detector monitors the ionic current, amplifies it and the signal is then transmitted to the data system where it is recorded in the form of mass spectra. For protein identification, acquired mass spectra are typically compared to a database that contains all possible protein sequences. The tandem-MS spectra were searched against the Swiss-Prot data base (human nr) using the Mascot algorithm version 2.2.

MS/MS spectra of the phosphopeptides obtained in the analysis identified three individual phosphorylated Serine residues, S136, S456 and S636 (Figure 4.1.1.5 B/C/D and Table 1). Assignment of phosphorylation sites was verified by manual inspection of the tandem mass spectra. The results established the phosphorylation of S136, S456, and S636 which were identified for the first time in Spir-2 protein.

To identify post-translational modifications, it is important to obtain good sequence coverage. The peptide sequence data correspond to an accumulated aminoacid sequence coverage of 67%, resulted after the tryptic digestion (cut at C-terminal of Lys and Arg residues) (Figure 4.1.1.5 A).

Figure 4.1.1.5 A. Illustration of Spir-2 sequence coverage by nano-LC-MS/MS analysis. MS/MS spectra files were searched against MASCOT search engine. Aminoacid sequence coverage (red colour) obtained by nano-LC-MS/MS analysis of peptide mixtures after the digestion with trypsin (cut at K-X or R-X; X is any aminoacid). The aminoacid sequence coverage was determined to 67%. Verified phosphopeptide regions in the tryptic digests are underlined.

The peptide, ^{134}EL[**pS**]PQLER^{141}, is found to be mono phopshorylated and the mass difference between y6 (711.325) and y5 (642.299) represents phopshoserine indicating S136 is phopshorylated. The prominent neutral loss (-97 Da) is a common phenomenon for the peptides those are phopshorylated on Ser or Thr. ´y´ ions containing phopshorylated Ser featured loss of 98 Da due to the elimination of phosphoric acid.

The above fact is applicable to the remainig two peptides as well. The peptide ^{454}SF[**pS**]EHDLAQLR^{464}, is monophosphorylated carrying a phosphorylated Ser residue at the site 456. The difference between b3 (304.100) and b2 (235.083) is an indication of Ser phosphorylation since the result is indicating the loss of 18Da (H_2O loss). The difference between y4 (470.00) and y3 (400.209) in the spectra ^{624}FGHIPVYTLGFE[**pS**]PQR^{639} also points to a loss of 18 Da from the molecular weight showing Ser phopshorylation.

Figure 4.1.1.5 B.

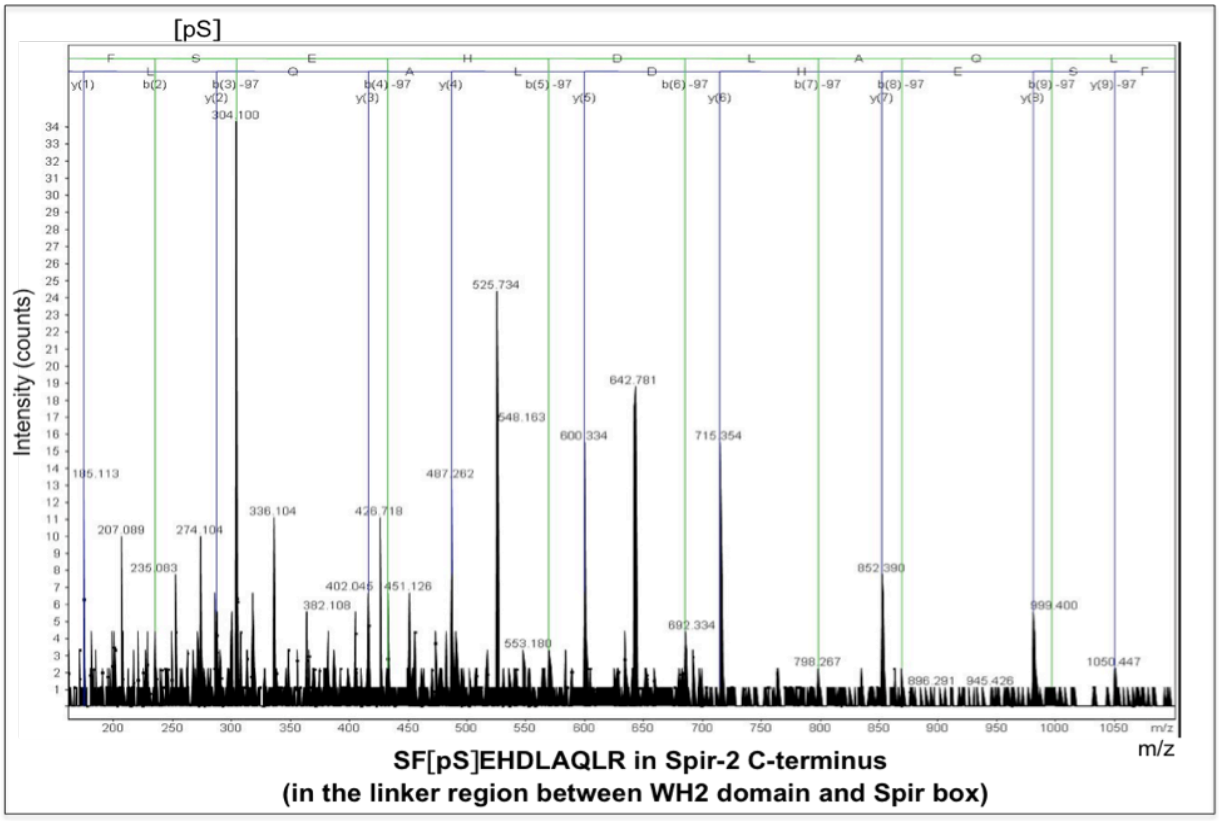

Figure 4.1.1.5 C

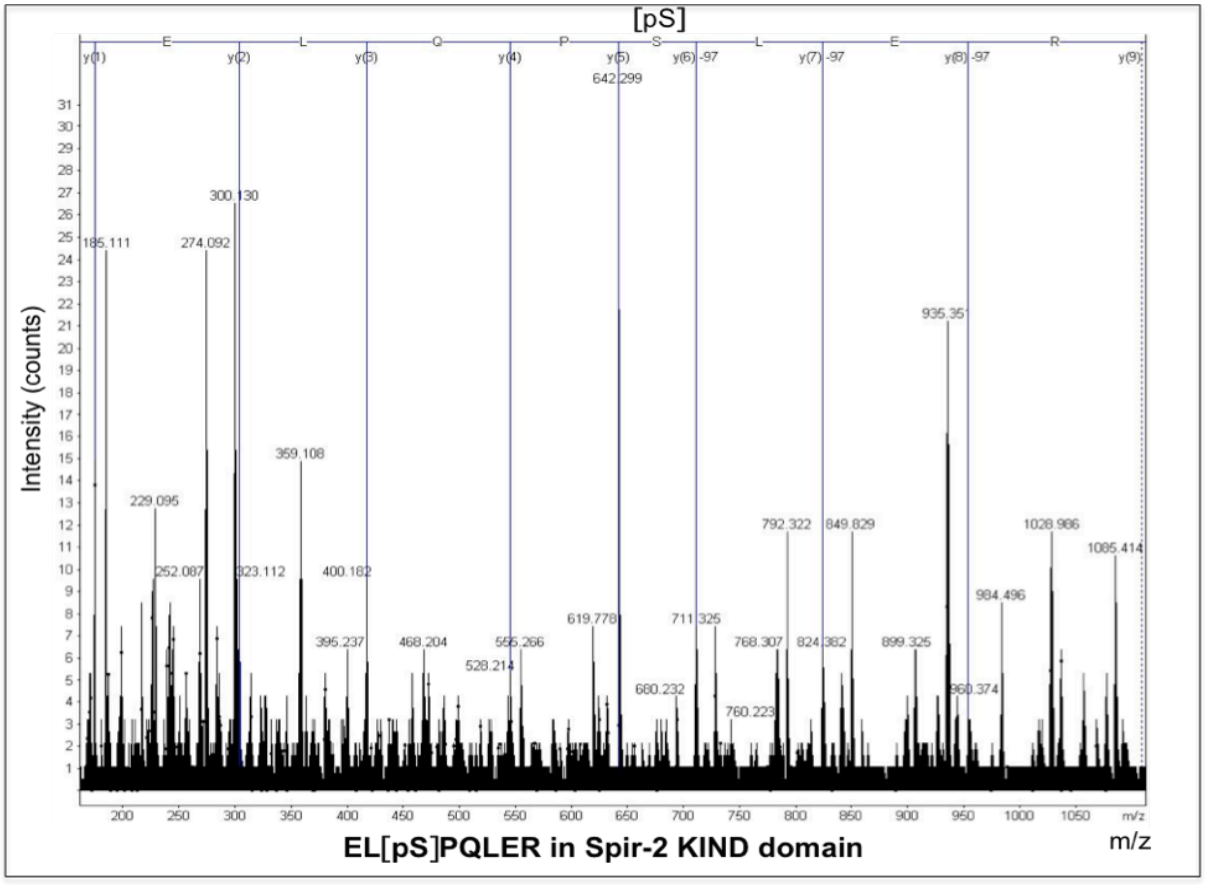

Figure 4.1.1.5 D

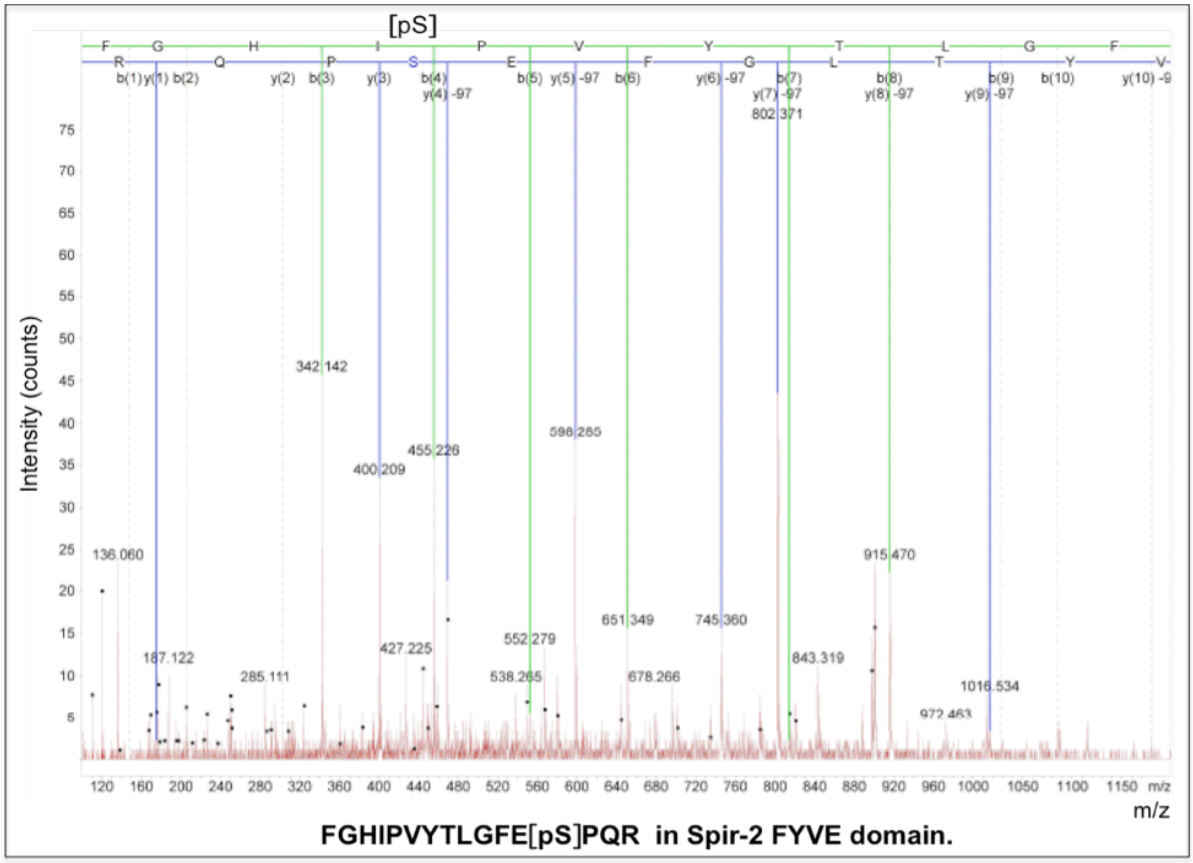

Figure 4.1.1.5 B/C/D Peptide Spectra of three phopshorylated peptides in Spir-2. Automatic nanoflow LC-MS/MS analysis of Spir-2 identified three phopshorylated peptides and three phopshorylation sites in each. MS/MS peptide sequence data established the presence of phosphate groups on S136, S456 and S636. N and C-terminal peptide fragment ions (b-ion (in green) and y-ion (in blue) series respectively) are indicated. ´y´ ions containing phosphorylated Ser, featured loss of 98 Da due to the loss of phosphoric acid are shown.

Conjointly, nano-LC-MS/MS analysis allowed the identification of three phospho-peptides with one in N-terminal KIND domain and the others in C-terminus of Spir-2 protein, locating one Ser phosphorylation sites in each peptides (Table 1).

Table 1. Phosphopeptides identified and sequences by mass spectrometry

Peptide sequence	Phosphorylation sites
1. 134- EL[**pS**]PQLER- 141	S136
2. 454- SF[**pS**]EHDLAQLR- 464	S456
3. 624- FGHIPVYTLGFE[**pS**]PQR-639	S636

Phosphopeptides identified in phosphorylated Spir-2 protein by nano-LC-MS/MS analysis of tryptic digests.

Among the three Ser phosphorylation residues, **S136** is found to be localized in the KIND domain of Spir-2, which is a putative protein interaction module. Interestingly, this site is conserved among the Spir family of proteins (Figure 4.1.1.5 E), raising the possibility that this site serve a functional guise.

```
Spir-1_human/1-756      139 YGLKENEERELSPPLEQLIDHMANTVEADGSNDEGYEAAEEGLGDED-EK 187
Spir-1_mouse/1-874      256 YGLKENEERELSPPLEQLIDQMANTVEADGSKDEGYEAADEGPEDEDGEK 304
Spir-2_human/1-728      125 WGLDESEERELSPQLERLIDLMANNDSEDSGCGAADEGYG-GPEEEEEAE 173
Spir-2_mouse/1-718      115 WGLDENEERELSPQLERLIDLMANSDCEDSSCGAADEGYV-GPEEEEEAE 163
Spir_Pem-5_/1-758        90 YGLGAHQEQEISLSLDDVISRMTAHLQTGADEEYHDEGYD----GDKPST 135
Drosophila_Spir/1-991   237 YNLPEDEECQVSQELENLFNFMTADETDDDCIDEGIDEGD--KRWDDESE 284
```

Figure 4.1.1.5 E Sequence alignment of a part of KIND domain of Spir family proteins mapping the S136 phosphorylation site. Sequence alignment of a portion of N-terminal KIND domain of Spir family members mapping the singly phosphorylated peptide ELpSPQLER in Spir-2 protein pointing S136 phosphorylation site which is conserved among Spir family proteins. In mammals S136 is immediately succeeded by Proline. The sequences were aligned by a ClustalW mutiple sequence alignment and manually realigned when necessary. Abbreviations : KIND, Kinase non-catalytic C-lobe domain; JNK, c-Jun-N terminal kinase; Ser, Serine and Thr, Threonine

JNK MAP kinases are recruited to substrate proteins via docking sites, enabling the kinases to phosphorylate serine or threonine residues adjacent to prolines (S/TP motifs) (Jacobs D *et al.,* 1999). Since S136 residue of Spir-2 is immediately followed by a proline in all mammalian Spir proteins, leads to the conclusion that S136 could be definitively assigned as a positive target motif for JNK in mammalian Spir proteins, whereas the respective site is not the highest confidence assignment in Drosophila and Ciona Spir (PEM-5), as the corresponding serine is not followed by a proline. Thus the residue following S136 of Spir-2

confirm JNK consensus sequence. The fact that, phosphorylation on S136 is specifically induced by JNK-MKK7 was confirmed using Extracted ion chromatogram, taking the peptide containing S136. Extracted ion chromatograms of the peptide containing S136, in presence and absence of JNK-MKK7 were integrated. The abundance of phosphorylation of S136 was found to be huge in presence of JNK-MKK7 when compared to that in the absence of the same kinase (Figure 4.1.1.5 F).

The above features reveals that the Ser136 found in the Spir KIND domain, which is typically involved in protein-protein interactions, and phosphorylation in this domain may regulate the ability of Spir proteins to bind to it´s interacting protein partners.

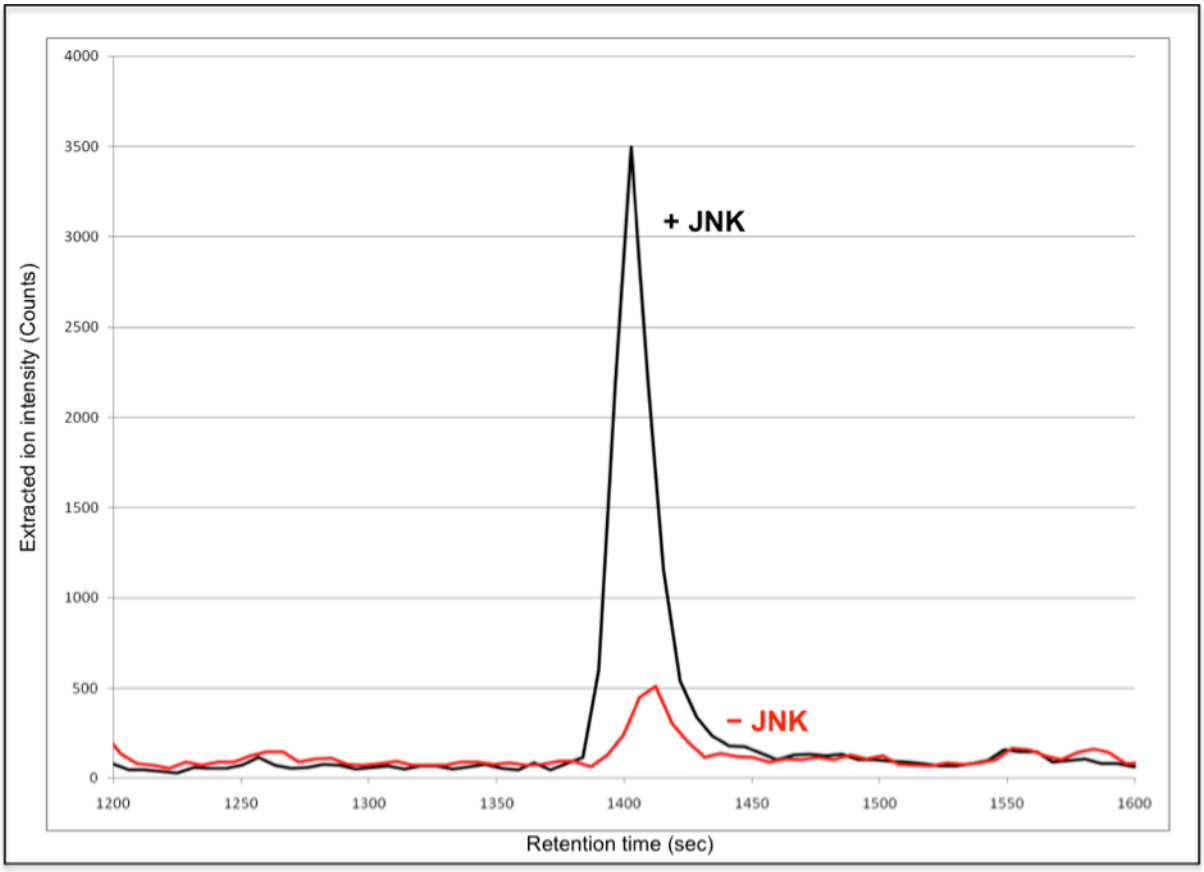

Figure 4.1.1.5 F Extracted ion chromatogram for S136 containing peptide. The extracted ion chromatogram showing the abundance of phopshorylation on S136 in the N-terminal KIND domain of Spir-2, in presence and absence of JNK. The chromatogram shows that the S136 exhibit a high rate of phosphorylation when Spir-2 is expressed together with JNK-MKK7.

The second identified phosphorylation site in Spir-2 protein, S456, is located in the C-terminal half of the protein, specifically in the linker region between the WH2 domain and the Spir-box. This site is found as not conserved among the Spir family proteins and is specific for mammalian Spir-2 proteins. However, theoretically, this site can not be assigned as

definitively assigned motif for JNK since it did not satisfy the consensus sequence residue (ST/P) following the S456 site (Figure 4.1.1.5 G, upper panel). Eventhough this site is outside of any described domains of the proteins, it may not imply a lack of functional significance.

The third Ser phosphorylation site is found to be Ser636, which resides in the FYVE Zn-finger domain. It is also not a conserved site and is specific for mammalian Spir-2 protein (Figure 4.1.1.5 G, lower panel). But in Spir-2 this site is immediately followed by Proline, which is not the case in mouse homologue. FYVE domains are membrane binding modules. The Spir proteins are specifically recruited to endosomal membranes by a FYVE zinc finger membrane localization domain which makes point to investigate the role of this phosphorylation site in the membrane targeting and intracellular membrane transport.

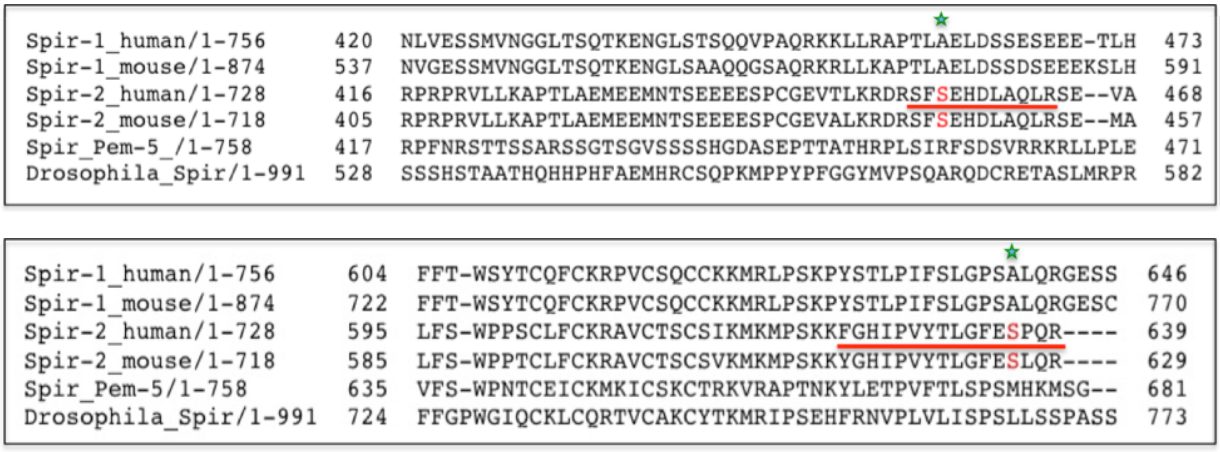

Figure 4.1.1.5 G Sequence alignment of Spir protein mapping the S456 and S636 phosphorylation sites. Sequence alignment of Spir proteins focusing the linker region between the WH2 domain and Spir Box, containing the monophosphorylated peptide SF[pS]EHDLAQLR with Ser 456 residue (Upper panel) and the Spir-FYVE domain with the S636 in monophosphorylated peptide FGHIPVYTLGFE[pS]PQR highlighted in red. Both the residues are found to be specific only for mammalian Spir-2 proteins. The green asterisk represent the corresponding positions of phosphorylated Ser residues. The sequences were aligned by a ClustalW mutiple sequence alignment and manually realigned when necessary. Abbreviations : SB, Spir-box; FYVE, FYVE Zn-finger domain; S, Serine

LC-MS/MS analysis revealed the presence of S136 only in the JNK-MKK7 induced condition where as the other two phosphorylated residues, S456 and S636 were present both in the presence and absence of the kinase (Table 2).

Table 2. Specificity of JNK-MKK7 on phosphorylation residues

Kinase (JNK-MKK7)	Phosphorylation sites		
	S136	**S456**	**S636**
1. – JNK-MKK7	**–**	**+**	**+**
2. + JNK-MKK7	**+**	**+**	**+**

4.1.1.6. Phosphatase treatment abrogated the phosphorylation of Spir-2

As shown by the aforementioned datas, Spir is phosphorylated and to an extent it clarifies that the phosphorylation is induced by JNK-MKK7. In order to further characterize the up-shifted band of Spir-2 in the SDS-PAGE, the study employs phosphatase treatment, which address the question, whether the electrophoretic mobility shift is by JNK-MKK7 induced phosphorylation.

As an opening wedge, HEK-293 cells were transfected with Spir-2 alone and together with JNK-MKK7 as described previously. The cell lysates harvested in IP buffer were undergone immunoprecipitation with anti-Myc 9E10 antibody, and incubated with Calf Intestinal Alkaline phosphatase (CIAP/CIP, 10U), that catalyzes protein dephosphorylation, for 1 hour at 37°C (→ 3.3.8).

The resulting samples with and without the treatment with CIP were subjected to Western blotting analysis with the same anti-Myc-antibody. Figure 4.1.1.6 shows an obvious up-shift of Spir-2 band induced by JNK-MKK7 (*Lane 3* and *Lane 4*) whereas CIP could effectively diminish the JNK-induced band shift of Spir-2 (*Lane 2*). Control experiments were performed with the total HEK-293 cell lysates expressing Spir-2, in the presence and absence of JNK-MKK7 (*Lane 5* and *Lane 8*) for the clear distinction of intact and phosphorylated fragments of Spir proteins.

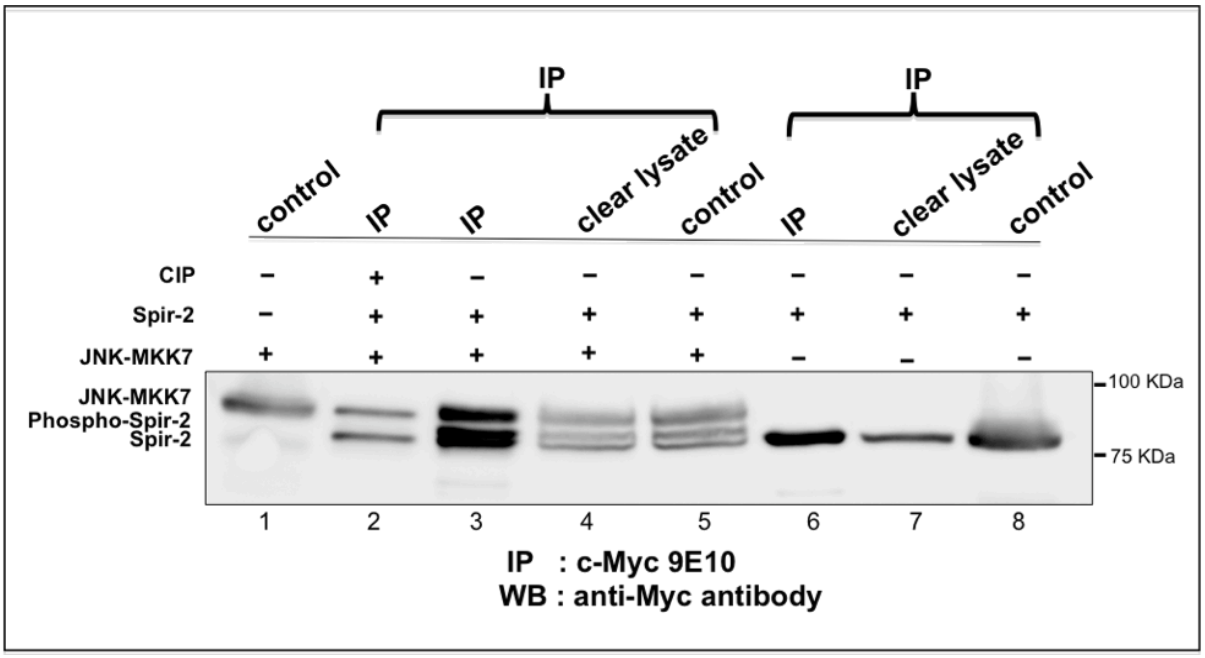

Figure 4.1.1.6 Phosphatase treatment of Spir-2 protein. HEK 293 cells transfected with plasmids encoding Spir-2 and JNK-MKK7 alone or together, were subjected to immunoprecipitation using c-Myc 9E10 antibody. A fraction of the immunoprecipitated sample were treated with calf intestinal alkaline phosphatase (CIAP, 10U) for 1hour at 37°C. Expression of Spir-2 protein in both phosphorylated and non phosphorylated form were determined by Western blotting using anti-Myc antibody. The electrophoretic mobility shift of Spir-2 induced by JNK-MKK7 is abolished by CIP treatment (*Lane 2*). *Lane 5* and *Lane 8*, HEK 293 total cell lysates expressing Spir-2, with and without JNK-MKK7 respectively; *Lane 6* and *Lane 7*, immunoprecipitate and clear supernatent from c-Myc immunoprecipitated Spir-2 protein; *Lane 3* and *Lane 4,* immunoprecipitate and clear supernatent from c-Myc immunoprecipitated Spir-2 protein together with JNK-MKK7 . *Lane 1*, JNK-MKK7 control.

4.1.1.7. Effect of kinase-inactive mutant on Spir-2 phosphorylation

Inorder to gain insights into the exact phosphorylation characterized by JNK-MKK7, the study utilises a kinase-inactive mutant, JNK-MKK7 KD. It is also known as kinase dead form of JNK-MKK7 in which the critical lysine residues in the ATP binding sites of JNK (K55A and K56A) and MKK7 (K76E) had been replaced by nonphosphorylatable amino acids (Otto *et al.,* 2000.

To analyse the specificity of JNK-MKK7 in the phosphorylation of Spir-2, HEK 293 cells were transfected with Spir-2 alone and together with JNK-MKK7 and/or JNK-MKK7 KD. The total proteins in the cell lysates were seperated by SDS-PAGE, blotted onto a nitrocellulose membrane and detected by immunoblotting using anti-Myc antibody. Figure 4.1.1.7 shows that JNK-MKK7-KD did not induce an electrophoretic mobility shift of Spir-2 as JNK-MKK7 does, which straighten out the finding that phopshorylation is induced by JNK-MKK7.

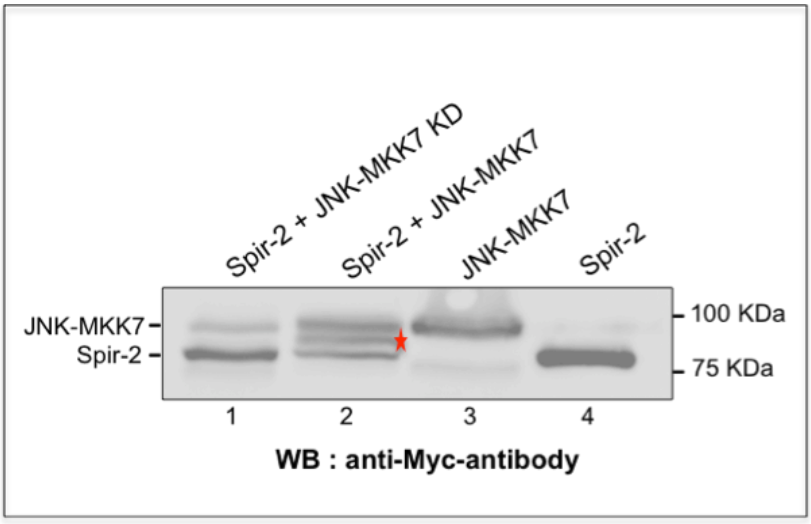

Figure 4.1.1.7. Characterization of *in vitro* Spir phosphorylation by JNK-MKK7. HEK 293 cells were transfected by with DNA vectors directing the expression of either Spir-2 alone and in combination with JNK-MKK7 or a kinase inactive mutant of JNK-MKK7 (JNK-MKK7 KD). 24 hours post-transfection, cells were lysed and the expression of total proteins were determined by Western blotting using anti-Myc antibody. The phosphorylation of Spir-2 is induced by JNK-MKK7 (*Lane 2*) where as JNK-MKK7 KD did not phosphorylate the protein (*Lane 1*). *Lane 3* and *Lane 4,* represents the total HEK 293 cell lysates of JNK-MKK7 and Spir-2 as controls. The upshifted band of Spir-2 representing the phosphorylated fragment is depicted with asterisk (red).

Together, these results demonstrated that the electrophoretic mobility shift of Spir-2 detected in the SDS-PAGE is a result of phosphorylation and the phosphorylation is induced by JNK-MKK7.

4.2. Investigation of the role of Ser136 in the biological activities of Spir proteins

Determining protein phosphorylation sites is often the primodial step in the elucidation of a regulation mechanism. Knowledge about the protein phosphorylation sites provides description of the biological events following the phosphorylation events. A prerequisite for this approach is to mutate potential phosphorylation sites and look for the functional analysis.

Upon scruitinising the interaction of two prominent actin nucleation factors, Spir and formin, a previous study revealed a high affinity Spir binding site at the very C-terminus of mammalian formins (FSI sequence) adjecant to it´s core FH2 domain which interact with the N-terminal KIND domain of Spir. The FSI sequence was found to be highly conserved only with in the Fmn subfamily of formins (Pechlivanis *et al*., 2009). Recently revealed crystal

structure of Spir-KIND/Fmn-2-FSI complex denotes that positively charged residues of Fmn-FSI peptide is mediating the interaction with acidic residues on the KIND domain (Zeth*., et al*, 2011).

Based on this identification I speculated that the physiological relevance of phosphorylation site identified in the Spir-KIND domain, Ser136, may have some effect on the interaction with formin proteins. The interesting fact on the other side was that Ser136 was also conserved in the Spir family of proteins and it fulfills the consensus sequence of JNK-MAP kinase as it is immediately succeeded by a proline residue. In order to analyse this hypothesis, mutation of Ser136 to both alanine (Ala; A) and glutamic acid (Glu; E) were performed. The S136A mutation was used as a non-phosphorylated non-serine control and the S136E mutation mimics the phosphorylated state of S136 residue. This may make out remarks in the Spir/formin cooperation with a dominant negative and a constitutively active forms with Ala and Glu mutants respectively, of the Spir proteins in parallel.

Before addressing the question of functional relevance of S136 mainly in the interaction with formins, experiments were conducted to understand whether JNK-MKK7 is inducing phosphorylation of mutants as it does with the wild type and thus provide a clarification towards the fact supporting S136 as a JNK-phosphorylation site.

4.2.1. Effect of JNK-MKK7 on the wild type and mutant forms of Spir-2 protein

Site-directed mutagenesis was done using Stratagene Quickchange Site Directed Mutagenesis Kit and the plasmids created were then sequenced through Eurofins MWG Operon for confirming the corresponding mutations (Table 3).

Table 3. Primers used for Site directed mutagenesis of S136 in Spir-2-KIND and S150 in Spir-1-KIND domain.

Mutation name	Primer sequence (5´to 3´)
S136A	gagagcgaggagcgcgaactc**gcc**cctcagctggagcggctcatc
S136E	gagagcgaggagcgcgaactc**gaa**cctcagctggagcggctcatc
S150E	aaggagaatgaagaaagggaatta**gag**cctcccctagagcagcttatc

Introduced sites of mutagenesis are in bold with underline. Mutations were done in Spir-2 and Spir-1 taking the pcDNA3-Myc-hs-Spir-2 (full length) and pGEX-4T1-NTEV-Spir-1-KIND domain as templates.

Eukaryotic expression vector pcDNA3 containing Spir-2 wild type (Spir-2,WT), Spir-2, Ala mutant (Spir-2, S136A) and Spir-2, Glu mutant (Spir-2, S136E) were transfected to HEK 293 cell line in the presence and absence of JNK-MKK7 inorder to compare the response of wild type and the mutant forms of Spir upon the coexpression with JNK-MKK7. Total cell lysates were made at 24 hours post-transfection, were subjected to SDS-PAGE followed by Western blot analysis using anti-Spir-2 antibody (4.2.1 A) and the blot was stripped for anti-Myc-antobody (4.2.1 B) as well.

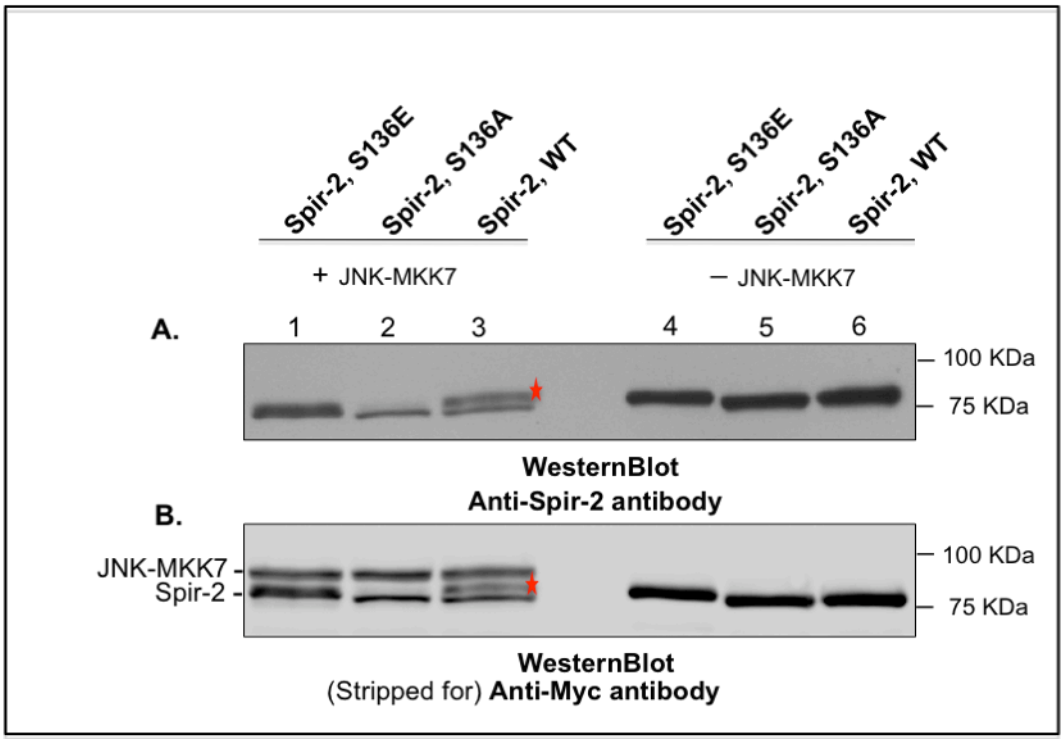

Figure 4.2.1 Effect of JNK-MKK7 on Spir-2 WT/S136A/S136E. HEK 293 cells were transiently transfected with Spir-2/WT, Spir-2/S136A and Spir-2/S136E, both in the presence and absence of JNK-MKK7. Proteins were allowed to express after 24 hours of transfection and total cell lysates were made 100µl 1X Laemmli buffer and allowed to boil for 5 mints at 90°C. The samples were subjected to SDS-PAGE followed by western blotting with a rabbit polyclonal anti-Spir-2 antibody **(A).** The blot was then stripped and reprobed against mouse monoclonal ani-Myc-antibody **(B**). The blot shows that Spir-2 wt is phopshorylated by JNK-MKK7 (*Lane 3*) but the Ala and Glu mutants not (*Lane 2* and *Lane 1*). Asterisk indicate the phospho-Spir-2. Total lysates of HEK 293 cells expressing Spir-2, wt, Spir-2, S136A and Spir-2, S136E are used as controls (*Lane 6, Lane 5* and *Lane 4*).

The finding implies that that the mutation of the conserved phosphorylated Ser136 residue in the KIND domain of Spir markedly abandoned the phosphorylation induced by JNK-MKK7 which can be easily detected by a comparison from the phosphorylation status of Spir-WT (Figure 4.2.1). *Lane 3* displays the Spir protein in both non-phosphorylated (*lower*

band) and phosphorylated fragments (*upper band*). The disappearance of phosphorylated fragment is clearly visible in the case of glutamate (*Lane 1*) and alanine (*Lane 2*) mutants when co-expressed with JNK-MKK7. *Lane 6, lane 5* and *Lane 4* represents the total HEK 293 cell lysates expressing Spir-2/WT, Spir-2/S136A and Spir-2/S136E mutants, which are used as controls.. The blot of Anti-Spir-2 antibody is stripped and reprobed against anti-Myc-antibody.

Concluding, the present finding support the previous results that Spir is phosphorylated by JNK and Ser136 is a positive target motif for JNK.

4.2.2. Mutational analysis of Serine 136 on Spir/formin interaction

4.2.2.1. GST Pull-down assay to detect the interaction between Spir-2,wt/S136A/S136E and Fmn-2

Further step to investigate the possible role of the phosphorylated S136 residue of Spir-2 in the interaction with Fmn-2 were performed with a preliminary GST pull-down assay. HEK 293 cells were transiently transfected with Spir-2 WT/S136A/S136E constructs all along with JNK-MKK7. After 24 hours of transfection, cell lysates were extracted in pull-down buffer and subjected to pull-down assay by incubating with purified GST-Fmn-2-eFSI protein coupled to GSH-Sepharose 4B beads. A fraction of the same cell lysates pulled with purified GST protein coupled to Sepharose beads in the same manner, were used a control. The pulled fractions were subjected to SDS-PAGE followed by western blot with anti-Myc-antibody (Figure 4.2.2.1).

As figured in 4.2.2.1, the interaction of the Spir-KIND-domain and Fmn-2-eFSI is not significantly affected by the phosphorylation. In a more precise way, the result points out that both the mutant variants of Spir-2, S136A and S136E, interact with the Fmn proteins as the wild type does (*Lane 3, Lane 6 and Lane 9*). Also, it seems to be intersting that phosphorylated and non-phosphorylated Spir-2 were pulled out by GST-Fmn-2-eFSI to equal amounts in cotransfection approaches with JNK-MKK7, which is highlighted in red circles (*Lane 1 and Lane 3*). This can be led to the hypothesis that both the phosphorylated and non-phosphorylated forms of Spir-2 interact with Fmn-2-eFSI with equal affinity, which indeed require further investigations to confirm. Nevertheless, one could conclude from the observation that phosphorylation does not have a signifant impact on the interaction between the mammalian Spir and mammalian Fmn subgroup of formins, since the Ala and Glu mutants of Spir-2 interact with Fmn-2, in the same manner the Spir-2 wt does.

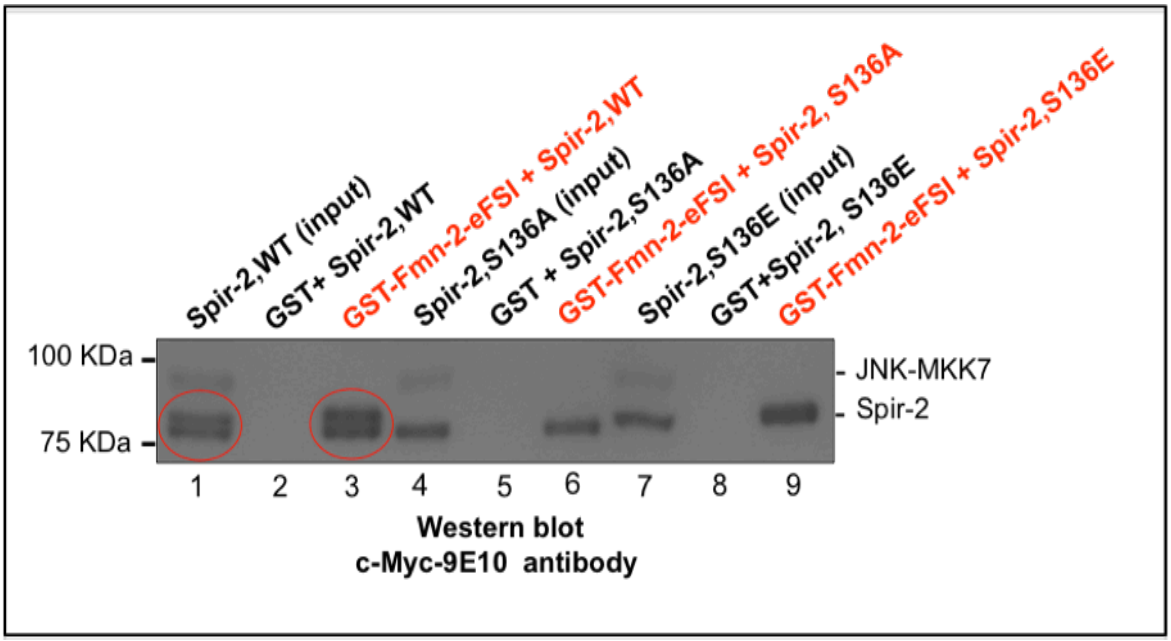

Figure 4.2.2.1 Interaction of Spir (WT,S136A and S136E) and formin proteins. Purified GST protein alone and GST-Fmn-2-eFSI have been coupled to Glutathione-Sepharose beads and incubated with HEK293 cell lysates expressing wild type Spir-2/JNK-MKK7, Spir-2, S136A/JNK-MKK7 and Spir-2,S136E/JNK-MKK7. Myc-tagged proteins expressd in the cell lysates were pulled down using GST-Fmn-2-eFSI were detected by immunoblotting with mouse monoclonal anti-Myc antibody. Spir protein fragmented equally into phosphorylated and non-phosphorylated forms is shown in the red circles (*Lane 1* and *Lane 3*). JNK-MKK7 is visible at a molecular weight of ~96 KDa. *Lane 2, Lane 5* and *Lane 8* shows the pull down of all the three constructs of Spir-2 with GST, as control. *Lane 3*, *Lane 6* and *Lane 9* are the Spir-2,S136A and Spir-2, S136E pulled form GST-Fmn-2-eFSI.

Eventhough it can not be excluded from the pull down assay that there is no apparent difference in the interaction between Spir-2, wild type as well as mutant forms, with mammalian formin-2 protein, it is worthwhile to employ a biophysical approach to measure the strength of interaction between the proteins. Fluorescence anisotropy measurements provide a very sensitive tool to detect and quantify protein interactions (Dr. Markos Pechlivanis is acknowledged for the Anisotropy measurements).

4.2.2.2. Fluorescence polarization measurement to quantify the Spir/formin interaction .

To monitor the strength of interaction between C-terminal extension of Fmn-2 (Fmn-2-eFSI) and Spir-KIND domain, flurescent BodipyFL-labeled Fmn-2-eFSI and Spir-1-KIND-WT and Spir-1-KIND-S150E were used (Figure 4.2.2.2 A and B) (The phosphorylated S150 in human Spir-1 corresponds to the S136 in human Spir-2; the difference exists in the number

of aminoacids in both proteins as, Spir-1 protein is with more aminoacid residues (756 amino acids) than Spir-2 (728 amino acids). Also, the phosphorylated Ser residue in the KIND domain, is highly conserved in both mammalian Spir proteins). From the fluorescence anisotropy measurements, the strength of interaction between Spir-1-KIND-WT and Fmn-2-eFSI as well as Spir-1-KIND-S150E and Fmn-2-eFSI was measured. The values of strength measured for the interaction of both the wild type as well as mutant variant of Spir-1 shows that, the strength of the Spir-1-KIND WT/Fmn-2-eFSI interaction (Kd~48nM) is almost similar to Spir-1-KIND-S150E/Fmn-2-eFSI (Kd~63nM). Thus the anisotropy data along with the pull-down assay validate the fact that both the wild type as well as the mutant forms of Spir interacts with Fmn-2 protein and also the mutants of Spir restore the similar strength of interaction with the the Fmn-2 protein as the wild type does.

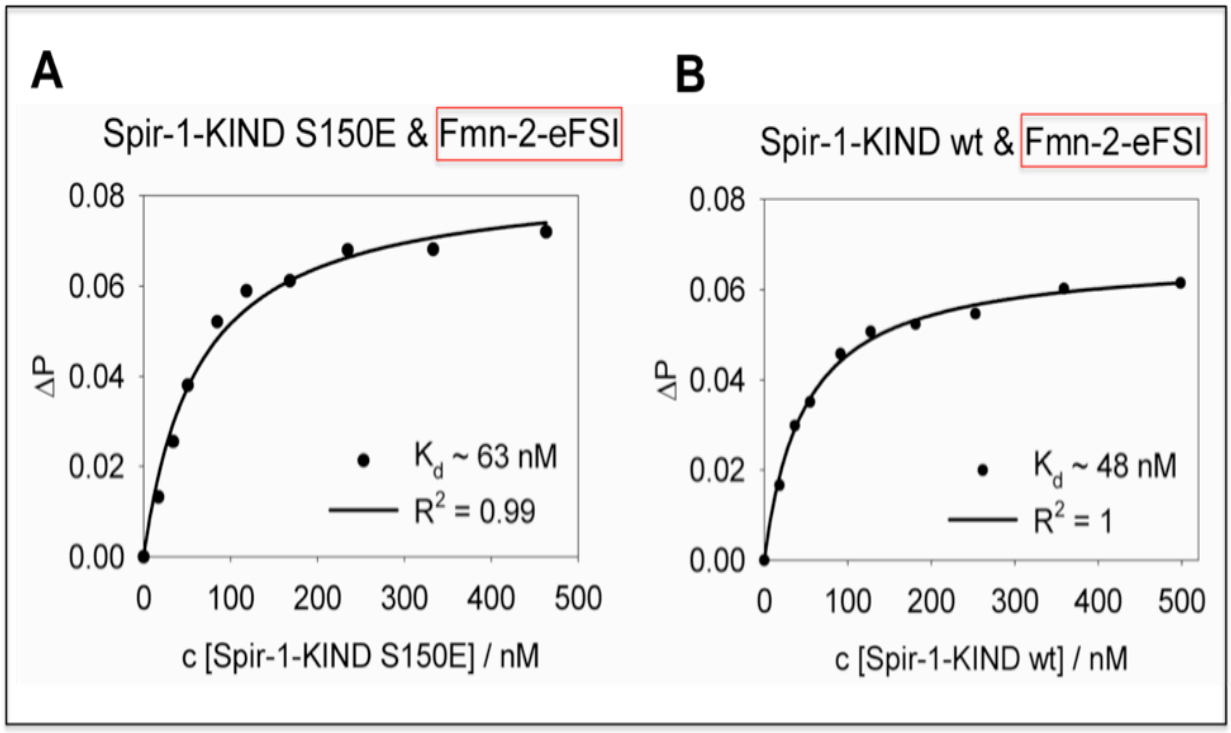

Figure 4.2.2.2. Fluorescence anisotropy/polarization measurements probing the interactions of Spir-1-KIND-wt and Spir-1-KIND-S150E with Fmn-2-eFSI. Binding of Spir-1-KIND-S150E (A) and Spir-1-KIND-wt (B) to BodipyFl-labelled Fmn-2-eFSI (100nM) is shown. The affinities of both the constructs of Spir-1-KIND, wt as well as mutant, towards the Fmn-2-eFSI reflects no visible difference, as clearly depicted by the dissociation constants. Fmn-2-eFSI protein is marked by the red boxes
Abbreviations: wt, wild type; ΔP, change in polarization; BodypyFl-labelled

4.2.3. Effect of phosphorylation on autoregulatory interaction of Spir proteins

As phosphorylation has no significant impact on the trans-regulatory interaction between mammalian Spir and mammalian Fmn proteins, further step to investigate whether the identified Ser phosphorylated residue in the KIND domain has been influencing the autoregulatory bakfolding property of the Spir proteins, a GST pull-down assay was employed. GST fusion proteins, GST-Spir-1-KIND-wt and GST-Spir-1-KIND-S150E, were tested for their ability to pull down EGFP-Spir-1-FYVE domain. The purified GST fusion proteins were incubated with HEK 293 cell extracts transiently transfected with EGFP-Spir-1-FYVE, since the interaction is mediated by the FKI (FYVE - KIND interaction sequence) residing in the FYVE domain. EGFP-Spir-1-FYVE was detected by immunoblotting using anti-EGFP antibody (α-living colors GFP) and horseradish peroxidase conjugated anti-rabbit antibody as primary and secondary antibodies respectively, and detected with Enhanced Chemiluminescence Kit. The blot shows that the band corresponding to the Spir-1-FYVE pulled from the glutamate mutant of Spir-1-KIND is stronger when compared to that pulled from the Spir-1-KIND wild type which conveys that glutamate mutant variant of Spir-1-KIND is binding more strongly to the Spir-1-FYVE domain when compared to the wild type (Figure 4.2.3 A and B). In a statistical approach, Spir-1-KIND, S150E mutant possess a 1.4 fold stronger interaction than the Spir-1-KIND, wild type towards the Spir-1-FYVE domain (4.2.3 B). But yet it has to be confirmed by a biophysical approach like fluoresence polarization measurement to quantify the strength of interaction between the corresponding N- and C-terminal domains of Spir.

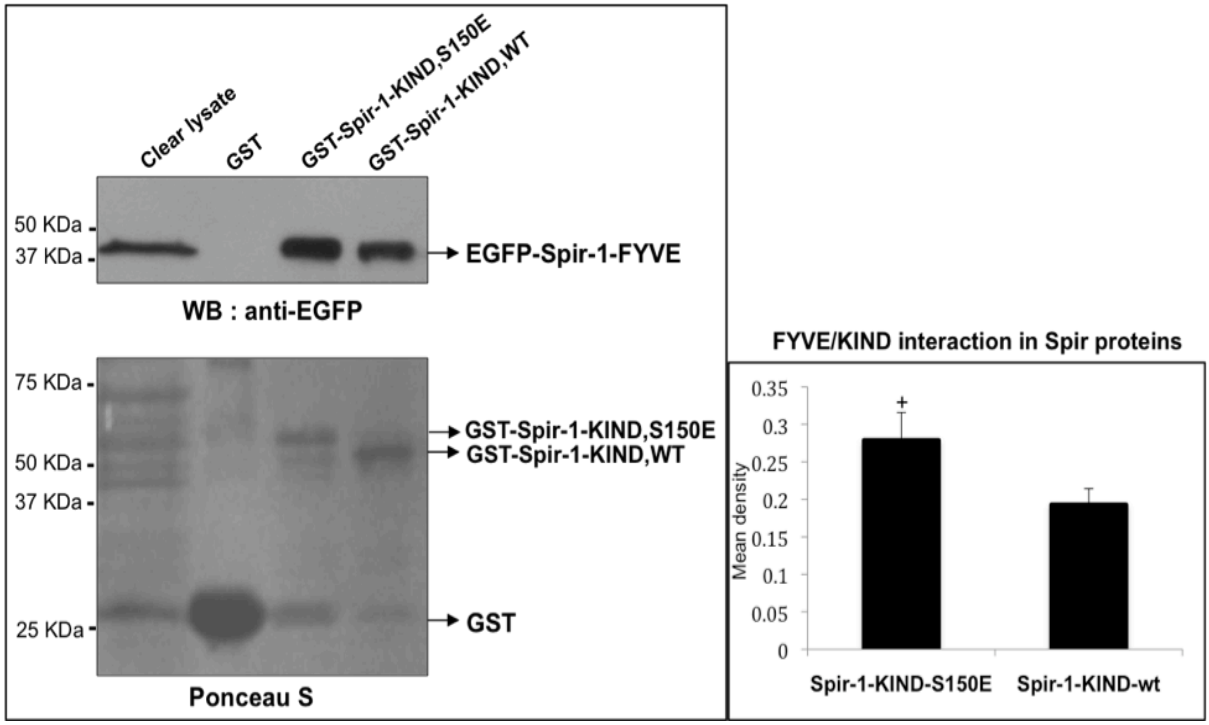

Figure 4.2.3. Interaction of Spir-KIND WT/S150E and Spir-1-FYVE domain. A. Purified GST protein alone and GST-Spir-1-KIND-wt/S150E have been coupled to Glutathione-Sepharose beads and incubated with HEK 293 cell lysates expressing EGFP-Spir-1-FYVE. The cell lysates were pulled down using GST fusion proteins were detected by immunoblotting with anti-EGFP antibody (α-living colors GFP) . Ponceau S staining of the bacterially expressed and purified GST, GST-Spir-1-KIND (wt and S150E) and immunoblots of pulled EGFP-Spir-1-FYVE proteins from HEK-293 lysates are shown. **B.** Comparison of the strength of interaction between wt and S150E mutant of Spir-1-KIND and the Spir-1-FYVE domain. The intensity if the signal is corrected by the loading control. Mean density values are estimated using the Image J programme. Data represents mean ± SD. +P = 0.045 (Pair sampled T-test). This figure is a representative of two independent experiments. SD, Standard deviation; P, probability.

5. Discussion

Spir proteins are the founding members of the emerging group of actin nucleation factors with one or multiple WH2 domains as their signature. Since their discovery (Wellington *et al*., 1999; Otto *et al*., 2000) Spir proteins have seen fruitful investigations which unveiled their prominent roles including their interaction with formin proteins (Rosales-Nieves A.E, *et al.,* 2006; Quinlan *et al.,* 2007; Pechlivanis M, *et al.,* 2009), followed by the effect of this co-operativity in *Drosophila* and mammalian oogenesis (Dahlgaard K. *et al*., 2007; Pfender, S. *et al.,* 2011). Apart from these interactions, Spir proteins provide an important link to understand the role of actin dynamics in regulating the intracellular membrane transport through their mambrane localization FYVE domain which makes them to specifically target towards the endosomal membrane (Kerkhoff *et al.,* 2001; Morel *et al.,* 2009).

The first member identified, among the Spir family of proteins, to be phosphorylated was *Drosophila* p150-Spir and it was shown that the phopshorylation is induced by JNK-MKK7, a constitutively active form of JNK (Otto *et al.,* 2000). Moreover, it´s role as a direct link between JNK and actin organization, unveiled a new proposal for regulatory mechanisms among Spir family proteins through signal cascades (Otto *et al.,* 2000). Gaining interest from this finding the current work shed light on the phosphorylation status of mammalian Spir proteins which have not been described yet.

The present study concentrate in elucidating the influence of post-translational modification on the regulatory events of Spir proteins, which is conducted in two sessions: the identification and characterization of phosphorylation sites in the mammalian Spir proteins, and later on, role of identified phosphorylation sites in the biological activities of the protein.

5.1. Analysis of phosphorylation of human Spir-2

5.1.1. Phosphorylation of Spir-2 by JNK-MKK7

On the basis of the findings observed in p150-Spir protein, phopshorylation studies were switched to mammalian homologues. A study regarding the phosphorylation of a particular protein carries us through two preliminary stages which is of utter relevance. The first attempt was to find out whether the mammalian Spir proteins are phosphorylated or not, and secondly, if there is a phosphorylation, are there any kinases involved in catalyzing the specific phosphorylation, if yes, the type of the kinase like Ser-Thr kinases or Tyr kinases.

Further step will be the identification of phosphorylated residues using the most versatile tool to identify the post-translational modifications of the protein, called Mass spectrometry.

In this study, a phosphorylation profile of human Spir-2 is described for the first time. To accomplish this, a pull-down assay with GST-fusion protein, GST-Fmn-2-eFSI was conducted. Pull-down experiments with GST-fusion proteins attached to Glutathione beads are a screening technique for the identification of protein-protein interaction. The phosphorylation studies were conducted in Myc-tagged human Spir-2 protein, with 728 amino acids. Since the previous study detected phosphorylation of p150-Spir induced by JNK-MKK7, we checked the effect of JNK kinase on mammalian Spir. Therefore, Spir-2 in presence and absence of JNK-MKK7 was expressed in HEK 293 cells and subsequently cell lysates were subjected to pull-down assay using purified GST-Fmn-2-eFSI. The first interesting observation was the finding that Spir-2 is phosphorylated by JNK-MKK7 (Figure. 4.1.1.3 B.). The pulled fragment was clearly visible in two prominent bands, corresponding to the molecular weight of phosphorylated and non-phopshorylated residues of Spir-2, in both Western blot analysis as well as in Coomassie staining (Figure. 4.1.1.4). The observation controlled by Spir-2 protein pulled without JNK-MKK7 give us a hint that it may be a target of the kinase, which is further verified using the kinase dead mutant.

The induction of phosphorylation of *Drosophila* Spir by JNK-MKK7 was already described. JNK-MKK7 is a fusion protein formed by fusing JNK 3 (rat) to it´s upstream activator MKK7 (mouse) via a linker region. A previous finding has shown an *in vitro* phosphorylation of aminoterminal c-Jun sequences by JNK-MKK7 which resulted in the electrophoretic mobility shift of c-Jun (Otto *et al.,* 2000). MKK7 activates JNK by phosphorylating a TPY motif in the central region of JNK.

In contrast to JNK-MKK7, it´s kinase inactive mutant, JNK-MKK7 KD, which is otherwise known as kinase dead mutant, failed to phosphorylate the Spir-2 protein. In JNK-MKK7 KD, critical lysine residues in the ATP-binding sites of JNK (K55A and K56A) and MKK7 (K76E) were replaced by non phosphorylatable amino acids (Otto *et al.,*2000). Supporting the phosphatase data, the migratory and immunoblot behaviour of Spir-2 was compared when coexpressed with JNK-MKK7 as well as JNK-MKK7 KD. The results showed that, kinase dead mutant did not induce the electrophoretic mobility shift of Spir-2 (Figure 4.1.1.7). The data indeed proved the role of JNK-MKK7 on Spir phosphorylation. Yet, solely taking this data under consideration the prediction of specificity of JNK-MKK7 on Spir-2 phosphorylation is impossible. One can not exclude the possibility of the existance of another kinase in the cascade through which JNK can indirectly phopshorylate the protein. If at all, this speculation open a new gateway for future studies which reveals the localization pattern as well as the actin organization. Upon stimulation, JNK kinases translocate from the cytoplasm to the nucleus where they phosphorylate a variety of transcription factors. In

analyzing the subcellular localization of both the intact and dead mutant of JNK-MKK7, it was observed that, JNK-MKK7 was found predominantly in the nucleus where as its inactive mutant form was totally excluded from the nucleus (Rennefahrt *et al.,* 2002). Based on these findings, it will be interesting to look for the localization pattern of JNK-MKK7 as well as it´s mutant form when co-expressed with Spir-2 protein. The analysis can also be performed the other way around to look for the localization of Spir together with MAP kinases. Additionally, the transient expression of JNK -MKK7 tremendously reduced or led to the complete loss of actin stress fibers, whereas the inactive form, JNK-MKK7 KD, had no such effect (Rennefahrt *et al.,* 2002). Spir proteins are prominant actin nucleation factors which elicits unbranched actin filaments. The above finding thus carry relevance in finding out the changes, if there is any, in the actin nucleation ability of Spir proteins together with the active and inactive form of the JNK kinase. These expectations are to be revealed by further studies.

MAP kinases are specifically Ser/Thr kinases and JNK MAP kinases are recruited to substrate proteins via docking sites, enabling the kinase to phosphorylate the Ser or Thr residues adjecant to prolins (S/TP motifs) (Jacobs, D *et al,* 1999). Phosphorylation of Spir-2 has to be further characterized by Mass spectrometric analysis which provide the sequence of the phosphorylated peptides as well as the precise site of phosphorylation. But before getting into the detailed sequence analysis of the protein we attempted a phosphatase assay with Calf Intestinal Alkaline Phosphatase (CIP).

5.1.2. Dephosphorylation of Spir-2 by alkaline phosphatase

Inorder to verify that the upshifted band is exactly as a result of phosphorylation, we conducted a phosphatase assay using Calf Intestinal Alkaline Phosphatase (CIP). CIP is a phosphomonoesterase purified from calf Intestinal mucosa. CIP effectively dephosphorylate proteins containing phosphoserine and phosphothreonine, which together account for > 97 % of protein bound phosphate in eukaryotic cells (Coligan *et al.,* 1997). Transiently transfected HEK 293 cell lines with Spir-2 together with JNK-MKK7 were lysed and immunoprecipitated with anti-Myc-antibody and a portion of the immunecomplex was treated with CIP. In Figure. 4.1.1.6, we found that JNK-MKK7 resulted in the appearance of phosphorylated form of Spir-2 which got erased by the CIP treatment. This observation confirmed that the upshifted band observed is resulted from phosphorylation. The GST pull-down assay together with the phosphatase treatment brings the fact that hs-Spir-2 protein as well is phosphorylated by JNK-MKK7 like the *Drosophila* homologue.

5.1.3. Determination of novel phosphorylation sites in Spir-2 protein by Mass spectrometry

Incorporation of one or more phosphate groups on specific amino acid side chains within a protein, with serine, threonine, tyrosine, and histidine being the most commonly studied, often induces significant protein conformational change and consequently profound effects on protein activity and protein–protein interactions (Cohen, P., 2002). Since phosphorylation is an important regulatory mechanism, we generated a phosphorylation mapping with human Spir-2 protein. Phosphorylation sites are identified using contemperory mass spectrometrical approach employing nano-HPLC coupled Tandem mass spectrometry. Mass spectrometry is ideally suited to the direct identification of protein phosphorylation sites. Phosphopeptides present in the mixtures can be sequenced at the femtomole level without the need for extensive purification. A great advantage of mass spectrometry is that they do not require prior labelling of the target protein with 32P. Regardless of the method used to map phosphorylation sites, it is imperative that the native phosphorylation state of the target protein be preserved during isolation.

The Coomassie staining in the Figure 4.1.1.4 showed the bands corresponding to intact and phosphorylated fragments of Spir-2 protein. To read any protein sample derived by SDS-PAGE, in mass spectrometer, special preparatory protocols are in need. The process of elution of proteins from acrylamide gels are more or less inefficient, so the most sraightforward approach to prepare gel-fractionated proteins for MS analysis is the direct digestion of protein in the gel (Shevchenko *et al.,* 2007). The fragments corresponding to non-phosphorylated and phosphorylated Spir-2 proteins are excised from the gel, digested by trypsin to get smaller peptides which were subjected to nano-HPLC-MS/MS analysis.

MS analysis allowed us to identify a total of three phosphopeptides, with three phosphorylated serine residues in each, namely S136, S456 and S636 (Figure 4.1.1.5 B/C/D). Table.1 shows each confirmed phosphorylation assignment by sequence position using QTOF-MS instrument. Out of the three identified phosphorylation sites, S136 takes the importance when compared to the two other sites because of three main facts:

- S136 is located in the N-terminal KIND domain of Spir-2 (Figure 5.1), whose role as potential protein interaction module has already unveiled in recent studies.
- S136 is conserved among the Spir family proteins and
- S136 can be considered as a positive target motif for JNK, since it satisfy the consensus sequence of JNK as it is immediately followed by Proline In mammals and it has been proved by MS analysis that the site is promisingly regulated by JNK-MKK7 (Figure 4.1.1.5 F; Table 2).

All these particulars of S136 raise the possibility that this site serve a functional guise.

The second and third phopshorylation residues, S456 and S636, are found to be situated in the C-terminus of the protein (Figure 5.1). More precisely, S456 in the linker region between the last WH2 domain and Spir-box where as S636 in the membrane binding FYVE domain (4.1.1.5 G). Eventhough S456 is outside of known domains, can not be considered as an irrelevant site. Both are found as conserved only in mammalian Spir-2 protein. From the amino acid sequence allignment it is clearly visible that S456 can not be considered as a direct target of JNK. In contrast, S636 is succeeded by Proline, in human Spir-2 only, and could be a JNK substrate, however it´s phopshorylation was not found to be upregulated by JNK-MKK7 in mass spectrometry. Still, the significance of this finding is unclear unless put in front for further investigtions.

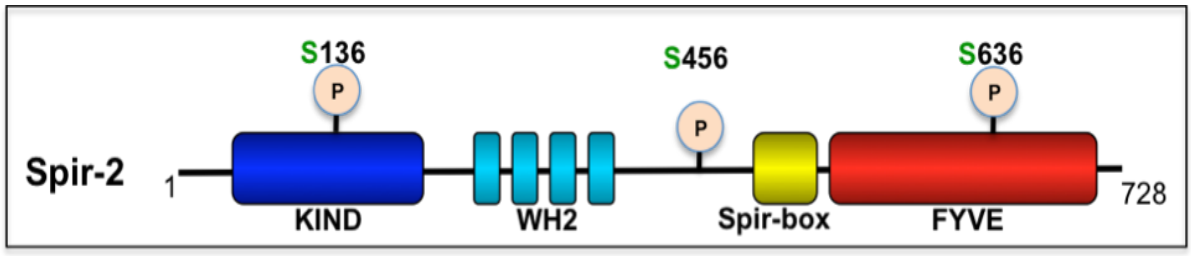

Figure 5.1. Schematic representation of phosphorylation sites in Spir-2 protein. The structure of human Spir-2 with the three newly identified phosphorylation sites, S136, S456 and S636 in defenite regions are shown.

A recent study highlighting Spir/formin synergy, presented a crystal structure of Spir-KIND domain alone and in complex with Fmn-2-FSI peptide with resolution at 2.05A° and 1.8 A° respectively (Zeth *et al*., 2011). This finding described the molecular basis of the two prominant actin nucleation factors, Spir and formin, that the large interface with conserved and positively charged residues of the Fmn-2-FSI peptide electrostatically interact with the acidic groove on the surface of KIND domain (Zeth K *et al.,* 2011). In collaboration study with Dr. Kornelius Zeth, MPI, Tubingen, we could map the phosphorylated S136 (S136 in Spir-2 correspond to S150 in Spir-1) in the crystal structure of Spir-KIND domain alone and in complex with Fmn-2-FSI peptide.

The interaction between mammalian Spir and mammalian Fmn subfamily of formins was already anatomized, which revealed a new formin Spir interaction (FSI) sequence in the very C-terminus of Fmn proteins, which interact with the KIND domain of Spir proteins. (Pechlivanis *et al,* 2009). Since Spir/formin interactions studies are heading in the current days, S136 has been selected for further investigation to examine it´s functional relevance.

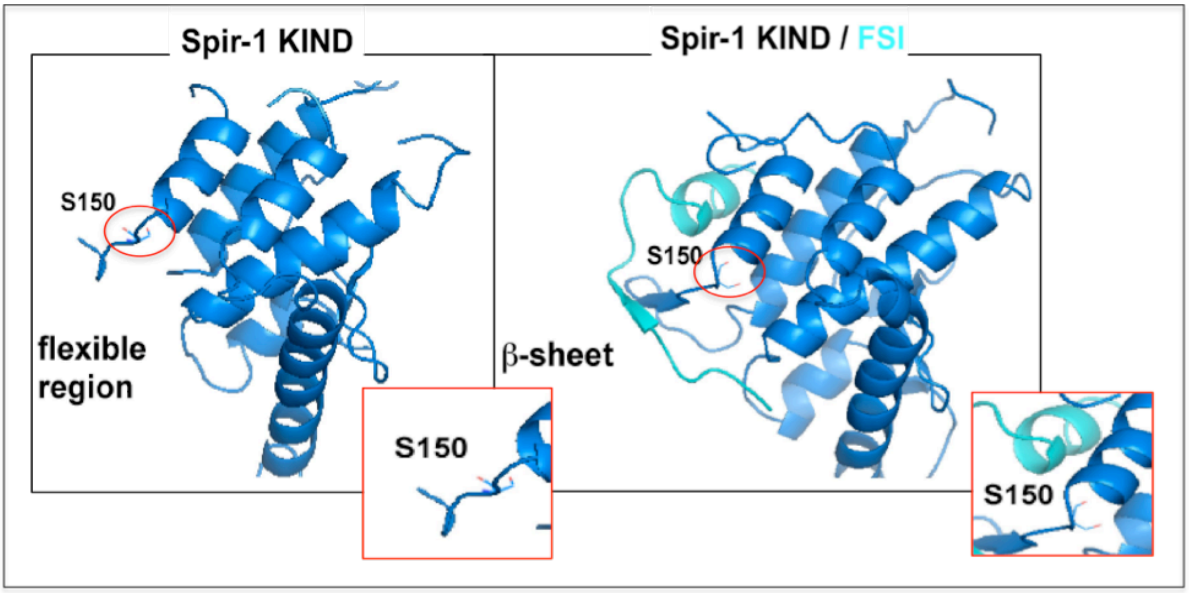

Figure 5.2. Crystal structure of Spir-1-KIND domain alone and in complex with Fmn-2-FSI mapping the S150* phosphorylation site in the KIND domain: The structure of KIND domain shows a dominance of α-helices with very few β-sheets. The S150 residue seems to be accessible in the KIND domain alone, but turn towards the inner portion of the structure when complexed with FSI peptide which again not accessible to the Fmn-2-FSI. The position of S150 in the structure of Spir-1-KIND alone and in complex with Fmn-2-FSI peptide is shown in red circles, which is highlighted in the boxes.

* The phopshorylated residue S136 in Spir-2 protein correspond to the S150 residue in Spir-1 protein. The difference in number results from the length of the two proteins as hs-Spir-1 is with 756 aminoacids and hs-Spir-2 with 728 aminoacids.

5.2. Functional relevance of phosphorylated Ser136 in Spir-KIND domain

To establish that phosphorylation of a given protein plays a crucial role in a process under study is the evaluation of the effect of non-phosphorylatable mutations in the candidate substrate. Therefore inorder to observe the possible functional role of the phosphorylated S136 site in Spir proteins, phosphodeficient and phosphomimic mutants of S136 were generated, such as S136A and S136E. The effect of JNK-MKK7 on Spir-2 wildtype (wt) and mutant variants were undertook. We found that JNK-MKK7 induces the phosphorylation of only the wt type protein and none of the mutants (Figure 4.2.1). This observation make us to hypothesise that Spir activity might be regulated by JNK kinases which phosphorylate S136. The peptide ^{134}EL[pS]PQLER^{141} contains mitogen-activated protein kiinase (MAPK) phosphorylation site and a SP motif (Proline-directed Ser) which is conserved among Spir family proteins.

5.2.1. Influence of phosphorylation on Spir/formin cooperation

S136 was found in the KIND domain of Spir, which is typically involved in the protein-protein interactions, which made us to suspect that the phosphorylation site in this domain may regulate the ability of Spir to bind to its interaction partners. The prominent interaction partner being formins, we examined how the phosphorylation on Spir protein influence the transregulatory interaction with the formins. GST pull-down assay to screen the interaction followed by fluorescent polarization measurements for quantifying the strength of interaction were undertaken. Spir-2 wt, Spir-2, S136A and Spir-2, S136E together with JNK-MKK7 were pulled down using GST-Fmn-2-eFSI (Figure 4.2.2.1). The data pointed out two remarkable observations, first one being, both the phosphorylated as well as the non-phosphorylated fragments of Spir protein was pulled by the formin protein, which indirectly conveys that both the fragments are interacting with formin proteins. But it has to be still confirmed and clarified that whether both the fragments are interacting with the formins with equal strength or not. The second observation was that, mutation on S136 does not affect the interaction with Fmn-2 protein, which clears that phosphorylation in the KIND domain has no significant impact on the interaction between mammalian Spir and mammalian formin proteins.

In accordance with this, we quantified the strength of interaction between the Spir-1-KIND domain and the Fmn-2-eFSI peptide, using both the wild type as well as the phosphomimicing mutant, S150E. From the dissociation constants obtained, we could conclude the above finding that the wt as well as the mutant form of Spir-KIND interact with the Fmn-2-eFSI with similar strength.

The interaction between mammalian Spir and mammalian formins were previously validated already by the pull-down assay and colocalization experiments. The colocalization between Fmn-2-eFSI and a membrane targeted Myc-Spir-1-KIND-CAAX were observed in Hela cells. Cytoplasmically expressed Fmn-2-eFSI relocated to the plasma membrane along with the Spir-1-KIND (Pechlivanis *et al.,* 2009). Obvious visualization studies are in need to investigate the difference in localization pattern of Fmn-2-eFSI when co-expressed with Spir-1-KIND wt and Spir-1-KIND-S150E.

Like the Fmn subfamily of formins have the FSI domain at the very C-terminus, some of the members of formin superfamily contain an autoregulatory peptide in their C-termini called Diaphanous autoregulatory domain (DAD) (Giggs H N, 2005). DAD interacts with the Diaphanous inhibitory domain (DID) located in the N-termini of the same proteins. This intramolecular DID/DAD interaction results in an autoinhibited conformation of the formin proteins. This inhibited confirmation must be released by the Rho small G- protein for the acivation of formin proteins (Li and Giggs, 2005; Otomo *et al.,* 2005). Homologous DAD/DID sequences could not be found in the Fmn subfamily members (Pechlivanis *et al.,* 2009). This conveys that the Fmn subfamily of formins may not be potentially regulated by an

autoinhibitory backfolding interactions but can be through a transregulatory interaction with Spir-KIND domain utilising their FSI module. More studies have to be added to understand the effect of kinase mediated phopshorylation on the Spir/formin complex.

5.2.2. Phosphorylation on autoregulatory backfolding of Spir

Apart from the intermolecular interaction with Fmn subgroup of formins, we also performed experiments to look for the effect of phosphorylation on the autoregulatory interaction of Spir protein which is mediated by the N-terminal KIND and C-terminal FYVE domain. The specific sequence mediating this binding is FYVE/KIND interaction sequence (FKI) located in the FYVE domain (Tittel, Dietrich, Pechlivanis, Samol, Pleiser, Schwille and Kerkhoff., manuscript in preparation). We conducted the experiment in which EGFP tagged Spir-1-FYVE was pulled from the purified GST-tagged Spir-1-KIND wt and th Spir-1-KIND S150E. The data figured in 4.2.3, shows that Spir-1-KIND S150E possess more intensive binding with the Spir-FYVE domain rather than the wt. Even though, the finding must be validated through a quantitative assay like flurescence anisotropy, the data shows that phosphomimicing mutant of Spir interact more strongly to the membrane binding FYVE domain. It raises a possibility that autoinhibition of Spir proteins through backfolding is regulated by phosphorylation. This finding must be validated by a biophysical approach which enable the quantification of the strength of FYVE/KIND interaction

FYVE domains are important zinc finger domains which recruite a subset of proteins to the endosomal membrane by binding to phosphatidylinositol-3-phosphate (PI(3)P) (Stenmark, 2005). Spir consists of a modified FYVE domain, lacking the basic cluster between cysteines 2 and 3, mediating the PI(3)P binding and having a loop insertion between cysteines 6 and 7. Fyve domain form a ´turret loop´ to penetrate the membrane. Membrane binding property of the Spir proteins depends on the integrity of Spir-box and FYVE domain (Kerkhoff *et al.,* 2001). If the above finding clarifies the intensive binding if the mutant when compared to the wild type form of Spir, which is to be studied in detail, then we could hypothesise that the phopshorylation alters the membrane localization of Spir. More precisely, when the KIND domain interact with the FYVE domain more strongly, it will result in pulling the FYVE from the intracellular membranes making the domain more accessible for binding with the KIND domain. It remains to be determined in future studies.

6. Conclusion and perspectives

The identification of sites of post-translational modification is crucial for fully deciphering the biological roles of any given protein. The study has demonstrated the power of combining biochemical and mass spectrometrical analysis in precise identification of phosphoresidues and provides an essential foundation in elucidating the biological events following phosphorylation.

The current study generated a phosphorylation profile of mammalian Spir protein using nano-LC-MS/MS analysis, which revealed three new serine phosphorylation residues, in human Spir-2 protein. One among the three phosphorylated serine residue, S136, residing in the N-terminal KIND domain, a protein interaction module, was conserved in both mammalian Spir proteins, Spir-1 and Spir-2, Drosophila p150-Spir and Spir Ciona savignyi (Pem-5). Apart from the fact that the sequence following S136 satisfy the JNK consensus sequence (ST/P motif), mass spectrometrical approaches could ascertain that this site could be assigned as a positive target motif for JNK,. The other two sites, S456 and S636, residing in the C-terminus of the Spir-2 protein was not found to be conserved among the Spir family of proteins. Since KIND domain is a potential protein interaction module, inorder to gain insights into the functional relevance of conserved S136 in the N-terminal KIND domain, mutational analysis was performed. Emerging data indicated that phosphorylation has no significant impact on the interaction between Spir and formin proteins. Moreover, the mutants restore the similar strength of interaction as the wild type does. Further verification in understanding the influence of phosphorylation on the autoregulatory interaction between N-terminal N-terminal KIND and C-terminal FYVE domains of Spir proteins revealed that the glutamate mutant possess a strong binding affinity towards Spir-FYVE in contrast to the wt, which has to be verified by a biophysical approach like fluorescence anisotropy measurements.

Further research should focus on the studies incorporating localization patterns of Spir proteins under, both phosphorylated and non-phosphorylated conditions. Immunostaining followed by Fluorescence microscopy will shed light to get an idea whether phosphorylation inhibit or augment the membrane targeting property of the protein. It also carries interest to look for the alterations in the localization of Spir protein under serum starvation, if at all, examining the capability of Spir proteins to induce actin filaments under serum deprived conditions will open efficacious avenues for future studies.

APPENDIX

Appendix -I- Abbreviations and acronyms

APS	Ammonium persulfate
Arp2/3	actin-related protein 2 and 3
ADP	adenosin diphosphate
ATP	adenosin triphosphate
bp	base pairs
BSA	Bovine serum albumin
C_c	Critical concentration
Capu	Cappuccino
cDNA	complementary DNA
Co-IP	co-immunoprecipitation
Cobl	Cordon-bleu
Cdc42	Cell division cycle 42
CE	capillary electrophoresis
CID	Collision-induced dissociation
DAAM	dishevelled-associated activator of morphogenesis
DAD	diaphanous autoregulatory domain
Dia	diaphanous
DID	diaphanous inhibitory domain
DMEM	Dulbecco's modified Eagle's medium
DMSO	Dimethyl Sulfoxide
DNA	Deoxyribonucleic acid
dSpir	*Drosophila* Spir
eGFP	enhanced green fluorescent protein
E. coli	*Escherichia coli*
ECL	enhanced chemiluminescent light detection
EDTA	Ethylenediaminetetraacetic acid
EEA1	early endosome antigen 1
ERK-1	extracellular-signal-regulated kinase 1
ESI	Electrospray ionisation
FYVE	Fab1p, YOTB, Vac1p, EEA1
FH1	formin homology 1

FH2	formin homology 2
FHOD	formin homology domain-containing protein
FRL	formin-related gene in leukocytes
FSI	formin-Spir Interaction site
FKI	FYVE-KIND Interaction site
Fmn	formin
F-actin	filamentous actin
FCS	fetal calf serum
G proteins	guanine nucleotide-binding proteins
G-actin	globular actin
GDF	GDI-displacement factor
GDI	GDP-dissociation inhibitor
GDP	Guanosine diphosphate
Glu	Glutamic acid
GST	glutathione S-transferase
GTP	Guanosine-5'-triphosphate
GC	Gas chromatography
HEK 293	human embryonic kidney 293 cells
His	Histidine
HRP	horseradish peroxidase
HPLC	High-performance liquid chromatography
IgG	Immunoglobulin G
IP	Immunoprecipitation
IPTG	Isopropyl beta-D-1-thiogalactopyranoside
JMY	junction-mediating regulatory protein
JNK	c-Jun N-terminal kinase
kb	kilo bases
kDa	kilo Dalton
kV	Kilovolt
KIND	kinase non-catalytic C-lobe domain
L-3	linker region 3
LB	Luria Bertani
Lmod-2	Leiomodin-2
mA	milliampere
mAbp1	mammalian actin-binding protein 1
MCS	multiple cloning site

ml	milliliter
mM	millimolar
µM	micromolar
M	molar
MWCO	molecular-weight cutoff
MreB	Murein formation cluster E B
MAPKKK	Mitogen activated protein kinase –kinase-kinase
MAPKK	Mitogen activated protein kinase –kinase
MAPK	Mitogen-activated protein kinase
m/z	mass to charge ratio
MS	Mass spectrometer/Mass spectrometry
MS/MS	Tandem mass spectrometry
MALDI	Matrix-assisted laser desorption/ionisation
NPF	nucleation promoting factor
OD	Optical density
Par M	Partitioning M
PA	phosphatidic acid
PAGE	Polyacrylamide gel electrophoresis
PBS	phosphate buffered saline
PCR	polymerase chain reaction
Pen	Penicillin
PEM-5	Posterior end mark-5
PTM	Post-translational modification
pSer	phosphorylated Ser
pThr	phosphorylated Thr
pTyr	phosphorylated Tyr
Pfu	*Pyrococcus furiosus*
Q-TOF	Quadrapole-Time-of-flight
rpm	rounds per minute
RPLC	Reversed phase liquid chromatography
SCAR	suppressor of cAMP receptor
SDS	Sodium dodecyl sulfate
Strep	Streptomycin
SB	Spir-Box
Ser	serine
s	seconds

TARP	translocated actin recruiting phosphoprotein
TEMED	Tetramethylethylenediamine
TGN	trans-Golgi network
Thr	Threonine
Tyr	Tyrosine
tRNA	transfer RNA
VSV-G	Vesicular stomatitis virus glycoprotein
WASP	Wiskott-Aldrich syndrome protein
WH2	WASP homology domain 2
WAVE	WASp family verprolin homologous protein
WASH	WASP and SCAR homologue
WB	Western Blot
WHAMM	Wiskott Aldrich syndrome protein homologue associated with actin, golgi membranes and microtubules
WHIF1	WH2 domain-containing formin 1
wt	wild type
ºC	degree Celsius
α	Alpha
β	Beta
γ	Gamma

Appendix -II- Human Spir-2 sequence

(NCBI Accession: CAD19439.1)

```
atg gac gcg ggt cgg cgc gcg gga ggc gat gac ggc ccc gcc atg gcc cgg gcg ggc agc  < 60
M   D   A   G   R   R   A   G   G   D   D   G   P   A   M   A   R   A   G   S    < 20

tgc ggc ggc gcc gcg gca ggc gca ggg cgg ccg gag ccc tgg gag ctg tcc ctg gag gag  < 120
C   G   G   A   A   A   G   A   G   R   P   E   P   W   E   L   S   L   E   E    < 40

gtg ctg aag gcc tac gag cag ccg ctc aac gag gag cag gcg ttg gcc gtg tgc ttc cag  < 180
V   L   K   A   Y   E   Q   P   L   N   E   E   Q   A   L   A   V   C   F   Q    < 60

ggc tgc cgc ggg ctg cgg ggc tcg ccg ggc cgg cgc ctg cgg gat acc ggg gac ctc ctg  < 240
G   C   R   G   L   R   G   S   P   G   R   R   L   R   D   T   G   D   L   L    < 80

ctg cgc ggg gac ggc tcg gtc ggg gcg cgg gag ccc gag gcc gcg gaa cct gca acc atg  < 300
L   R   G   D   G   S   V   G   A   R   E   P   E   A   A   E   P   A   T   M    < 100

gtc gtg cca cta gcc agc tcg gaa gcc cag acc gtg cag tcc ctc ggc ttc gcc atc tac  < 360
V   V   P   L   A   S   S   E   A   Q   T   V   Q   S   L   G   F   A   I   Y    < 120

cgc gcg ctg gac tgg ggg ctg gac gag agc gag gag cgc gaa ctc agc cct cag ctg gag  < 420
R   A   L   D   W   G   L   D   E   S   E   E   R   E   L   S   P   Q   L   E    < 140

cgg ctc atc gac ctc atg gcc aac aac gac agc gag gac agc ggc tgc ggt gcc gcc gat  < 480
R   L   I   D   L   M   A   N   N   D   S   E   D   S   G   C   G   A   A   D    < 160

gag ggc tac ggg ggt ccc gag gag gag gag gag gcc gag ggc gta ccc cgc agc gtg cgc  < 540
E   G   Y   G   G   P   E   E   E   E   E   A   E   G   V   P   R   S   V   R    < 180

acc ttt gcc cag gcc atg cgg ctg tgc gcg gcg cgg ctg acc gac ccc cgg ggc gca cag  < 600
T   F   A   Q   A   M   R   L   C   A   A   R   L   T   D   P   R   G   A   Q    < 200

gcg cat tac cag gcc gtg tgc cgc gcg ctc ttc gtg gag acg ctg gag ctg cgg gcc ttc  < 660
A   H   Y   Q   A   V   C   R   A   L   F   V   E   T   L   E   L   R   A   F    < 220

ctg gcc agg gtc cgg gag gcc aag gag atg ctg cag aag ctt cgg gag gac gag ccg cat  < 720
L   A   R   V   R   E   A   K   E   M   L   Q   K   L   R   E   D   E   P   H    < 240

ctg gag acg cct cgg gca gag ctg gac agc ctg ggt cac aca gac tgg gcc cga ctg tgg  < 780
L   E   T   P   R   A   E   L   D   S   L   G   H   T   D   W   A   R   L   W    < 260

gtt cag ctc atg cgg gag ctc cgc cgc gga gtg aag ctg aag aag gtg caa gag cag gag  < 840
V   Q   L   M   R   E   L   R   R   G   V   K   L   K   K   V   Q   E   Q   E    < 280

ttc aac ccc ctc ccc acc gag ttc cag ctc acg ccc ttc gag atg ctg atg cag gac atc  < 900
F   N   P   L   P   T   E   F   Q   L   T   P   F   E   M   L   M   Q   D   I    < 300

cgg gcc cgg aac tac aag ctg cgc aag gtc atg gtg gat ggg gac atc ccg ccc cgg gtg  < 960
R   A   R   N   Y   K   L   R   K   V   M   V   D   G   D   I   P   P   R   V    < 320

aag aag gac gct cac gag ctc atc ctg gac ttt atc cgc tca cgg cct cca ctg aag cag  < 1020
K   K   D   A   H   E   L   I   L   D   F   I   R   S   R   P   P   L   K   Q    < 340

gtc tct gag agg cgg ctg cgc ccg ttg cca cca aag caa agg tcc ctg cat gag aag atc  < 1080
V   S   E   R   R   L   R   P   L   P   P   K   Q   R   S   L   H   E   K   I    < 360

ctg gag gag atc aag cag gag cgg agg ctg cgc ccg gtg cgg ggc gag ggc tgg gct gcc  < 1140
L   E   E   I   K   Q   E   R   R   L   R   P   V   R   G   E   G   W   A   A    < 380

cgc ggg ttt ggc tct ctg ccc tgc atc ctc aac gcc tgc tcc gga gat gcc aag tcc acc  < 1200
R   G   F   G   S   L   P   C   I   L   N   A   C   S   G   D   A   K   S   T    < 400

tcc tgc atc aac ctg tca gtc aca gat gct ggg ggc agc gcc cag cgc ccg cgg ccc cgc  < 1260
S   C   I   N   L   S   V   T   D   A   G   G   S   A   Q   R   P   R   P   R    < 420

gtg ctg ctc aag gcg cct acc ttg gct gaa atg gaa gag atg aat aca tct gag gaa gaa  < 1320
V   L   L   K   A   P   T   L   A   E   M   E   E   M   N   T   S   E   E   E    < 440


gag tct ccg tgt ggg gag gtg acg ctg aaa cgg gac cgc tcc ttc tca gag cat gac ctg  < 1380
 E   S   P   C   G   E   V   T   L   K   R   D   R   S   F   S   E   H   D   L    < 460
```

```
gcc cag ctc cga agt gag gtg gcc tct ggc ctg cag tcg gcc acc cac ccc cca gga ggg  < 1440
  A   Q   L   R   S   E   V   A   S   G   L   Q   S   A   T   H   P   P   G   G    < 480

  acg gag cca cca cgg ccc cga gct ggc agt gcg cat gtg tgg agg ccc ggc tcc cga gac  < 1500
  T   E   P   P   R   P   R   A   G   S   A   H   V   W   R   P   G   S   R   D    < 500

  cag ggt acc tgt ccc gcg agt gtc tct gac ccc agc cac ccc cta ctc agc aac cgg ggc  < 1560
  Q   G   T   C   P   A   S   V   S   D   P   S   H   P   L   L   S   N   R   G    < 520

  tcc tcg ggg gac aga ccc gag gcc tcc atg acc ccc gat gcc aaa cac ctg tgg ctg gag  < 1620
  S   S   G   D   R   P   E   A   S   M   T   P   D   A   K   H   L   W   L   E    < 540

  ttc agc cac ccc gtg gag agc ctg gcg ctg act gtg gaa gag gtg atg gac gtg cgc cgt  < 1680
  F   S   H   P   V   E   S   L   A   L   T   V   E   E   V   M   D   V   R   R    < 560

  gtg ctg gtg aag gcc gag atg gaa aag ttt ttg cag aac aag gag ctc ttc agc agt ctg  < 1740
  V   L   V   K   A   E   M   E   K   F   L   Q   N   K   E   L   F   S   S   L    < 580

  aag aag ggg aag att tgc tgc tgc tgc cgg gcc aag ttc ccg ctg ttc tcg tgg ccg ccc  < 1800
  K   K   G   K   I   C   C   C   C   R   A   K   F   P   L   F   S   W   P   P    < 600

  agc tgt ctc ttc tgc aag aga gcc gtc tgc act tcc tgt agc ata aag atg aag atg cct  < 1860
  S   C   L   F   C   K   R   A   V   C   T   S   C   S   I   K   M   K   M   P    < 620

  tct aag aaa ttt gga cac atc cct gtc tac aca ctg ggc ttt gag agt cct cag agg gta  < 1920
  S   K   K   F   G   H   I   P   V   Y   T   L   G   F   E   S   P   Q   R   V    < 640

  tca gct gcc aaa acc gcg cca atc cag aga aga gac atc ttt cag tct ctg caa ggg cca  < 1980
  S   A   A   K   T   A   P   I   Q   R   R   D   I   F   Q   S   L   Q   G   P    < 660

  cag tgg cag agc gtg gag gag gcg ttc ccc cac atc tac tcc cac ggc tgt gtc ctg aag  < 2040
  Q   W   Q   S   V   E   E   A   F   P   H   I   Y   S   H   G   C   V   L   K    < 680

  gat gtc tgc agt gag tgc acc agc ttt gtg gca gac gtg gtg cgt tcc agc cgc aag agc  < 2100
  D   V   C   S   E   C   T   S   F   V   A   D   V   V   R   S   S   R   K   S    < 700

  gtg gac gtc ctc aac act acg cca cga cgc agt cgc cag acc caa tcc ctc tac atc cct  < 2160
  V   D   V   L   N   T   T   P   R   R   S   R   Q   T   Q   S   L   Y   I   P    < 720

  aac acc agg act ctt gac ttc aag tga  < 2187
   N   T   R   T   L   D   F   K   *    < 728
```

Appendix -III- Construct overview

Construct	Description	Restriction sites	Purpose
pcDNA3-Myc-hs-Spir-2	Myc-Spir-2 f.l (full length)	BamHI / HindIII	GST pull-down, Mass spectrometry, Immunoprecipitation.
pGEX- 4T1- NTEV-mFmn-2-eFSI	GST-Fmn-2-eFSI	EcoRI / SalI	GST pull-down; Anisotropy
pcDNA3-Myc-JNK-MKK7	Myc-JNK-MKK7	BamHI / XbaI	GST pull-down, Immunoprecipitation
pcDNA3-Myc-hs-Spir-2-S136A	Myc-Spir-2-S136A	BamHI / HindIII	Mutation analysis; GST pull-down
pcDNA3-Myc-hs-Spir-2-S136E	Myc-Spir-2-S136E	BamHI / HindIII	Mutation analysis; GST pull-down
pGEX- 4T1- NTEV-hs-Spir-1-KIND	GST-Spir-1-KIND	BamHI / XhoI	GST pull-down
pGEX- 4T1- NTEV-hs-Spir-1-KIND-S150E	GST-Spir-1-KIND-S150E	BamHI / XhoI	GST pull-down
pEGFP-C1-hs-Spir-1-FYVE	EGFP-Spir-1-FYVE	XhoI / BamHI	GST pull-down
pProExHtb-hs-Spir-1-KIND	His-Spir-1-KIND	BamHI / XhoI	Anisotropy
pProExHtb-hs-Spir-1-KIND-S150E	His-Spir-1-KIND-S150E	BamHI / XhoI	Anisotropy

Acknowledgements

With immense pleasure, I am taking this opportunity to express my heartfelt thanks to all, outside and inside the work circle, for their invaluable contributions to make this voyage possible and enjoyable. Without these supporters, especially, the select few I am about to mention, I may not have reached to where I am today.

I must begin by thanking my supervisor, Prof. Dr. Eugen Kerkhoff, for his sincere assistance and guidance throughout the tenure of my thesis, for making time even when there was little to spare. Above all, for giving an opportunity to carry out my Ph.D in his lab.

I am perpetually greatful to Prof. Dr. Daniela Männel, Institute of Immunology, for her encouragements, constructive criticisms and all time expert and wise advices. Boundless thanks for bringing sunshines and courage to withstand in my tough situations. A` Thank you` means a lot to me....

I owe a special debt of gratitude to Prof. Dr. Jens Schlossmann, Department of Pharmacology and Toxicology, for generously accepting my mentorship, for being a part of my thesis jury and for valuable suggestions and precious support rendered to me.

My hearfelt respect and gratitude goes to Prof. Dr. Oliver Reiser, Institute for Organic Chemistry, for helping me in the enrollment of my Ph.D thesis.

I am indebted to Prof. Dr. Peter Oefner and Prof. Dr. Anja Bosserhoff, for their kindness and constant readiness to help me.

I extend my sincere gratitude to Bayerische Forschungsstiftung for their scintillating scientific and financial support.

I deeply thank Dr. Markos Pechlivanis, for the motivations and timely advices whenever I was in need of.

I am greatful to Dr. Joerg Reinders, Proteomics group, for introducing the world of Mass spectrometry. Thank you for your excellent support for carrying out the mass spectometrical analysis.

Dr. Kornelius Zeth is warmly acknowledged for his collaboration in crystalographic studies.

Thanks to my labmates, Annette Samol, Sandra Pleiser, Sabine Weiß, Dr. Agnes Pawelec and Dr. Susanne Dietrich for their support. I remember, my former colleague, Martin Beusch, for making the ambience fresh and funny with his presence.

Many thanks to Nevels-Paulus Lab, for moulding me to get started with my Ph.D life. Without daubt I will look back with fond memories and nostalgia on my time in your lab. Thank you Christina for being a wonderful teacher and friend.

I am thankful to Tanja Janoschek, for helping me to get cleared with the administration stuffs.
Thank you Denise, for being with me whenever there was computer emergencies.
Petra Leukel is thanked for her all time helps with Image J programme..
Sylvia Moeckel, thank you for being with me while I work with Excel.

My friends....
Ines Tschertner, words fail to express my thanks to you. You added much colours to my life in Germany. Simply, You are Wonderful!
Tina, for being there for me, making my life smooth and funny.
Stefan Benecke and family for their gentle support during tough circumstances.
Anja Thomas, for being a nice and supportive friend.

My family....
My wonderful parents, Mr.Gopalakrishnan and Mrs.Valsala Gopalakrishnan, and my brother, Manikandan, for their unconditional love and support which always makes me to step forward- specially, my mother for being my ardent hand and for her contagious enthusiasm for academia.
The most profoud thanks I owe to my husband, Preetham, it would have been impossible without his support.
My daughter, Prarthana, for her lovely kicks instigating me to stick to the timetables, to complete this thesis work on schedule, and above all, for making my life more beautiful.
..... and to the Almighty, under his watchful eyes, I gained strength and perseverence to tackle challenges head on.

Sreeja Lakshmi, Regensburg, 2011

Bibliography

Alberto, P. and Juan, P. A. (2008). Advances in the analysis of protein phosphorylation. *J. Proteome Res. 7*, 1809-1818.

Azoury, J., Lee, K. W., Georget,V., Rassinier, P., Leader, B. and Verlhac, M. H. (2008) Spindle positioning in mouse oocytes relies on a dynamic meshwork of actin filaments. *Curr. Biol.18*, 1514-1519.

Ahuja, R., Pinyol, R., Reichenbach, N., Custer, L., Klingensmith, J., Kessels, M. M. and Qualmann, B. (2007). Cordon-Bleu Is an Actin Nucleation Factor and Controls Neuronal Morphology. *Cell*. *131*, 337–350.

Blanchoin, L. and Pollard, T. D. (2002). Hydrolysis of ATP by polymerized actin depends on the bound divalent cation but not proline. *Biochemistry. 41*, 597-602.

Baum, B. and Kunda, P. *(2005).* Actin nucleation: spire-actin nucleator in a class of its own. *Curr. Biol. 15,* R305-R308.

Blanchoin, L. and Robinson, R.C., (2000). Phosphorylation of *Acanthamoeba* actophorin (ADF/cofilin) blocks interaction with actin without a change in atomic structure. *J. Mol. Biol. 295*, 203-211.

Chalkley, R. (2010). Instrumentation for LC-MS/MS in proteomics. *Methods. Mol. Biol. 658,* 47-60.

Chesarone, M. A., DuPage, A. G and Goode, B. L. (2010). Unleashing formins to remodel the actin and microtubule cytoskeletons. *Nat. Mol. Cell. Biol.11*, 63-74.

Carlier, M. F. (1998). Control of actin dynamics. *Curr. Opin. Cell. Biol.10*, 45-51.

Chesarone, M. A. and Goode, B. L. (2009). Actin nucleation and elongation factors: mechanisms and interplay. *Curr. Opin. Cell. Biol 21*, 28-37.

Campellone, K. G. and Welch, M. D. (2010). A nucleator arms race: cellular control of actin assembly. *Nat. Rev. Mol. Cell. Biol. 11,* 237-251.

Conley, C. A., Fritz-Six, K. L., Almenar-Queralt, A. and Fowler, V. M. (2001). Leiomodins: larger members of the tropomodulin (Tmod) gene family. *Genomics 73*, 127-139.

Chereau, D., Boczkowska, M., Maruszewska, A.S., Fujiwara, I., Hayes, B. H., Rebowski, G., Lappalainen, P., Pollard, T. D. and Dominguez, R. (2008). Leiomodin is an actin □filament nucleator in muscle cells. *Science, 320*, 239-243.

Chereau, D., Ker, F., Grace, P., Grabarek, Z., Langsetmo, K. and Dominguez, R. (2005). Actin-bound structures of Wiskott-Aldrich syndrome protein (WASP)- homology domain 2 and the implications for □lament assembly. *Proc Natl Acad Sci* U S A, *102*, 16644-16649.

Chhabra, E. S. and Higgs, H. N. (2007). The many faces of actin: matching assembly factors with cellular structures. *Nature. Cell. Biol. 9*, 1110-1121.

Carroll, A. E., Gerrelli, D., Gasca, S., Berg, E., Beier, D. R., Copp, A. J. and Klingensmith, J. (2003). Cordon-bleu is a conserved gene involved in neural tube formation. *Dev. Biol. 262*, 16-31.

Ciccarelli, F. D., Bork, P. and Kerkhoff, E. (2003). The KIND module: a putative signalling domain evolved from the C lobe of protein kinase fold. *Trends. Biochem. Sci. 28*, 349-352.

Cohen, P. (2002). The origins of protein phosphorylation. *Nat. Cell. Biol.4,* E127–E130.

Dos Remedios, C. G., Chhabra, D., Kekic, M., Dedova, I. V., Tsubakihara, M., Berry, D.A. and Nosworthy, N. J. (2003). Actin binding proteins: regulation of cytoskeletal microfilaments. *Physiol. Rev. 83*, 433-473.

Domon, B. and Aebersold, R. (2006). Mass spectrometry and protein analysis. *Science*. *312,* 212-217.

Dominguez, R. and Holmes, K. C. (2011). Actin structure and function*. Annu. Rev. Biophys.*40, 169-186.

Dahlgaard, K., Raposo, A. A., Niccoli, T. and St Johnston, D. (2007). Capu and Spire assemble a cytoplasmic actin mesh that maintains microtubule organization in the *Drosophila* oocyte. *Dev. Cell. 13*, 539 –553.

Davis, R. J. (2000) Signal transduction by the JNK group of MAP kinases. *Cell.* 103, 239-252.

Dumont, J., Million, K., Sunderland, K., Rassinier, P., Lim, H., Leader, B. and Verlhac, M. H. (2007). Formin-2 is required for spindle migration and for the late steps of cytokinesis in mouse oocytes. *Dev Biol. 301*, 254-265.

Duncan, M.C., Cope, M.J., Goode, B. L., Wendland, B. and Drubin, D. G. (2001). Yeast Eps15-like endocytic protein, Pan1p, activates the Arp 2/3 complex. *Nat. Cell. Biol*. *3*, 687-690.

Estes, J. E., L. A. Selden, and L. C. Gershman. (1987). Tight binding of divalent cations to monomeric actin. Binding kinetics support a simplified model. *J. Biol. Chem. 262*, 4952-4957.

Emmons, S., Phan, H., Calley, J., Chen, W., James, B. and Manseau, L. (1995). Cappuccino, a Drosophila maternal effect gene required for polarity of the egg and embryo, is related to the vertebrate limb deformity locus. *Genes Dev. 9,* 2482-2494.

Firat-Karalar, E. N. and Welch, M. D. (2011). New mechanisms and functions of actin nucleation. *Curr. Opin. Cell. Biol. 23*, 4-13.

Fletcher, D. A. and Mullins, R. D. (2010). Cell mechanics and the cytoskeleton. *Nature. 463,* 485-92.

Faix, J. and Grosse, R. (2006). Staying in shape with formins. *Dev. Cell 10*, 693–706.

Foltz, I. N., Gerl, R. E., Wieler, J.S., Luckach, M., Salmon, R.A. and Schrader, J. W. (1998). Human mitogen-activated protein kinase kinase 7 (MKK7) is a highly conserved c-Jun N-terminal kinase/stress-activated protein kinase (JNK/SAPK) activated by environmental stresses and physiological stimuli. *J Biol Chem. 273*, 9344-9351.

Goley, E. D., Rammohan, A., Znameroski, E. A., Firat-Karalar, E.N., Sept, D. and Welch, M. D. (2010). An actin-filament-binding interface on the Arp2/3 complex is critical for nucleation and branch stability. *Proc. Natl. Acad. Sci. U S A.107*, 8159-8164.

Goley, E. D. and Welch, M. D. (2006). The ARP2/3 complex: an actin nucleator comes of age. *Nat. Rev..Mol..Cell..Biol. 7*, 713-726.

Goode, B. L., Rodal, A. A., Barnes, G. and Drubin, D. G. (2001). Activation of the Arp2/3 complex by the actin filament binding protein Abp1p. *J. Cell Biol. 153*, 627–634.

Goode, B. L. and Eck, M. J. (2007). Mechanism and function of formins in the control of actin assembly. *Annu.Rev.Biochem.76,* 593-627.

Higgs, H.N. and Peterson, K.J. (2005). Phylogenetic analysis of forming homology 2 domain. *Mol.Biol. Cell 16*, 1-13.

Higgs, H.N. and Pollard, T.D. (2000). Activation by Cdc42 and PIP2 of Wiskott-Aldrich Syndrome protein (WASp) stimulates actin nucleation by Arp2/3 complex. *J. Cell Biol. 150*, 1311–1320.

Holmes, K. C., Popp, D., Gebhard, W. and Kabsch, W. (1990). Atomic model of the actin filament. *Nature*, *347*, 44-49.

Hjerrild, M. and Gammeltoft, S. (2006). Phosphoproteomics toolbox: computational biology, protein chemistry and mass spectrometry. *FEBS Lett. 580*, 4764-4770.

Higgs, H.N. (2005). Formin proteins: a domain-based approach. *Trends. Biochem. Sci. 30*, 342–353.

Ito, T., Narita, A., Hirayama, T., Taki, M., Iyoshi, S., Yamamoto, Y., Maéda, Y. and Oda, T. (2011). Human Spire interacts with the barbed end of the actin filament. *J. Mol. Biol. 408,* 18–25.

Jewett, T. J., Fischer, E.R., Mead, D.J. and Hackstadt, T. (2006). Chlamydial TARP is a bacterial nucleator of actin. *Proc. Natl. Acad. Sci. U S A.103,* 15599-15604.

Johnson, H. and Eyers, C. E. (2010). Analysis of post-translational modifications by LC-MS/MS. *Methods. Mol. Biol. 658,* 93-108.

Jacobs, D., Glossip, D., Xing, H., Muslin, A. J. and Kornfeld, K. (1999). Multiple docking sites on substrate proteins form a modular system that mediates recognition by ERK MAP kinase. *Genes Dev. 13,* 163-175.

Kabsch,W., Mannherz, H. G., Suck, D., Pai, E. F. and Holmes, K.C.(1990.) Atomic structure of the actin:DNase I complex. *Nature*, *347*, 37-44.

Kerkhoff, E. (2006). Cellular functions of the Spir actin-nucleation factors. *Trends. Cell. Biol. 16,* 477- 483.

Kerkhoff, E., Simpson, J.C., Leberfinger, C.B., Otto, I.M., Doerks, T., Bork, P., Rapp, U.R., Raabe, T. and Pepperkok, R. (2001). The Spir actin organizers are involved in vesicle transport processes. *Curr. Biol. 11*, 1963-1968.

Kerkhoff, E. (2006). Cellular functions of the Spir actin-nucleation factors. *Trends Cell Biol 16,* 477- 483.

Katoh, M. and Katoh, M. (2004). Identification and characterization of human FHDC1, mouse Fhdc1 and zebrafish fhdc1 genes in silico. *Int. J. Mol. Med. 6,* 929–934.

Kerkhoff E. (2010) Actin dynamics at intracellular membranes: The Spir/formin nucleator complex. *Eur.J. Cell. Biol.* 90, 922-925.

Kovar, D.R. (2006). Molecular details of formin-mediated actin assembly. *Curr. Opin. Cell Biol. 18*, 11–17.

Kerkhoff, E., Simpson, J. C., Leberfinger, C. B., Otto, I. M., Doerks, T., Bork, P., Rapp, U. R., Raabe, T. and Pepperkok, R. (2001). The Spir actin organizers are involved in vesicle transport processes. *Curr. Biol. 11*, 1963-1968.

Le Goff, C., Laurent, V., Le Bon, K., Tanguy, G., Couturier, A., Le Goff, X. and Le Guellec, R. (2006). pEg6, a spire family member, is a maternal gene encoding a vegetally localized mRNA in Xenopus embryos. *Biol Cell. 98*, 697-708.

Li, F. and Higgs, H. N. (2003). The mouse Formin mDia1 is a potent actin nucleation factor regulated by autoinhibition. *Curr. Biol, 13*, 1335-1340.

Li, H., Guo, F., Rubinstein, B. and Li, R. (2008). Actin-driven chromosomal motility leads to symmetry breaking in mammalian meiotic oocytes. *Nat. Cell. Biol,10*, 1301-1308.

Leader, B. and Leder, P. (2000). Formin-2, a novel formin homology protein of the cappuccino subfamily, is highly expressed in the developing and adult central nervous system. *Mech Dev, 93*, 221-31.

Lammers, M., Rose, R., Scrima, A. and Wittinghofer, A. (2005). The regulation of mDia1 by autoinhibition and its release by Rho GTP. *EMBO J. 24,* 4176–4187.

Leader, B., Lim, H., Carabatsos, M. J., Harrington, A., Ecsedy, J., Pellman, D., Maas, R. and Leder, P. (2002.) Formin-2, polyploidy, hypofertility and positioning of the meiotic spindle in mouse oocytes. *Nat. Cell. Biol, 4,* 921-928.

LeClaire, L. L 3rd., Baumgartner, M., Iwasa, J. H., Mullins, R. D. and Barber, D. L. (2008). Phosphorylation of the Arp2/3 complex is necessary to nucleate actin filaments. *J. Cell. Biol.182*, 647-54.

Liverman, A. D., Cheng, H. C., Trosky, J. E., Leung, D. W., Yarbrough, M. L., Burdette, D. L., Rosen, M. K. and Orth, K. (2007). Arp2/3- independent assembly of actin by *Vibrio* type III effector VopL. *Proc Natl Acad Sci USA. 104,* 17117–17122.

Mooney, L. M and Whitmarsh, A. J. (2004). Docking interactions in the c-Jun N-terminal kinase pathway. *J. Biol. Chem. 279*, 11843-11852.

Mann, M. and Jensen, O. N. (2003). Proteomic analysis of post-translational modifications. *Nat. Biotechnol*. 21, 255-61.

Moseley, J.B., I. Sagot., A. L. Manning., Y. Xu., M.J. Eck., D. Pellman, and B.L.Goode . (2004). A conserved mechanism for Bni1- and mDia1-induced actin assembly and dual regulation of Bni1 by Bud6 and profi lin. *Mol. Biol. Cell . 15*, 896 – 907.

Manseau, L. J. and Schüpbach,. T. (1989). Capuccino and spire: two unique maternal-effect loci required for both the anterioposterior and dorsoventral patterns of the Drosophila embryo. *Genes Dev. 3,* 1437-1452.

Molecular Biology of the Cell. Fifth Edition.

Morel, E., Parton, R. G., Gruenberg, J. (2009). Annexin A2-dependent polymerization of actin mediates endosome biogenesis. *Dev. Cell 16,* 445-457.

Otto, I.M., Raabe, T., Rennefahrt, U.E., Bork, P., Rapp, U.R. and Kerkhoff, E. (2000). The p150- Spir protein provides a link between c-Jun N-terminal kinase function and actin reorganization. *Curr. Biol. 10*, 345-348.

Ostermeier, C. and Brünger, A.T. (1999) Structural basis of Rab effector specificity: crystal structure of the small G protein Rab3A complexed with the effector domain of rabphilin-3A. *Cell*, *96*, 363–374.

Oda, T. and Maeda, Y. (2010). Multiple Conformations of F-actin. *Structure, 18*, 761-767.

Oda, T., Iwasa, M., Aihara, T., Maeda, Y. and Narita, A. (2009). The nature of the globular- to fibrous- actin transition. *Nature. 457*, 441-5.

Olsen, J. V., Ong, S. E. and Mann, M. (2004). Trypsin cleaves exclusively C-terminal to Arginine and lysine residues. *Mol. Cell. Proteomics*.*3,* 608-614.

Otomo, T., D.R. Tomchick, C. Otomo, S.C. Panchal, M. Machius, and M.K.Rosen. (2005). Structural basis of actin filament nucleation and processive capping by a formin homology 2 domain. *Nature. 433,* 488–494.

Otterbein, L. R., Grace, P. and Dominguez, R. (2001). The crystal structure of uncomplexed actin in the ADP state. *Science. 293*, 708-711.

Paul, A. S. and Pollard, T.D. (2009). Review of the mechanism of processive actin filament elongation by formins. *Cell. Motil. Cytoskeleton*. *66*, 606-617.

Paradela, A. and Albar, J. P. (2008). Advances in the analysis of protein phosphorylations. *J. Proteome Res. 7*, 1809-1818.

Pring, M., Evangelista, M., Boone, C. and Zigmond, S. (2003). Mechanism of formin-induced nucleation of actin filaments. *Biochemistry. 42*, 486-496.

Pollard, T D., Blanchoin, L., and Mullins, R. D. (2000). Molecular mechanisms controlling actin fiament dynamics in nonmuscle cells. *Annu. Rev. Biophys. Biomol. Struct. 29*, 545-576.

Pollard, T. D. and Borisy, G.G. (2003). Cellular motility driven by assembly and disassembly of actin filaments. *Cell*. *112*, 453-465.

Pleiser, S., Rock, R., Wellmann, J., Gessler, M. and Kerkhoff, E. (2010). Expression patterns of the mouse Spir-2 actin nucleator. *Gene. Expr. Patterns. 10*, 345–350.

Pechlivanis, M., Samol, A., and Kerkhoff, E. (2009). Identification of a short Spir interaction sequence at the C-terminal end of formin subgroup proteins. *J. Biol. Chem 284*, 25324-25333.

Pollard, T.D. (2007). Regulation of actin filament assembly by Arp2/3 complex and formins. *Annu Rev Biophys Biomol Struct 36*, 451-477.

Perrin, B. J. and Ervasti, J. M. (2010). The actin gene family: function follows isoform. *Cytoskeleton. 67*, 630-634.

Page, R., Lindberg, U. and Schutt, C. E. (1998). Domain motions in actin. *J. Mol. Biol. 280*, 463-474.

Pfender, S., Kunzetsov, V., Pleiser, S., Kerkhoff, E. and Schuh, M. (2011). Spir-type actin nucleators co-operate with Formin-2 to drive asymmetric oocyte division. *Curr. Biol*. *21*, 955-960.

Paunola, E., Mattila, P. K. and Lappalainen, P. (2002). WH2 domain: a small, versatile adapter for actin monomers. *FEBS Lett, 513*, 92-97.

Quinlan, M.E., Heuser, J.E., Kerkhoff, E. and Mullins, R.D. (2005). Drosophila Spire is an actin nucleation factor. *Nature*. *433,* 382-388.

Quinlan. M.E., Hilgert, S., Bedrossian, A., Mullins, R.D., and Kerkhoff, E. (2007). Regulatory interactions between two actin nucleators, Spire and Cappuccino. *J. Cell. Biol 179*, 117-128.

Quinlan, M.E., and Kerkhoff, E. (2008). Actin nucleation: bacteria get in-Spired. *Nat. Cell. Biol 10*, 13-15.

Qualmann, B. and Kessels, M. M. (2009). New players in actin polymerization- WH2-domain-containing actin nucleators. *Rev. Trends. Cell. Biol.19*, 276-285.

Qualmann, B. and Kessels, M. M. (2008). Actin nucleation: Putting the breaks on Arp2/3 complex. *Curr.Biol.18*, R420-422.

Reinders, J. and Sickmann, A. (2005). State-of-the-art in phosphoproteomics. *Proteomics. 5,* 4052-4061.

Renault, L., Bugyi, B. and Carlier MF. (2008). Spire and Cordon-bleu: multifunctional regulators of actin dynamics. *Trends. Cell. Biol. 18*, 494-504.

Robinson, R. C., Turbedsky, K., Kaiser, D. A., Marchand, J. B., Higgs, H. N., Choe, S. and Pollard, T. D.(2001). Crystal structure of Arp2/3 complex. *Science*. *294*, 1679-1684.

Rennefahrt, U. E., Illert, B., Kerkhoff, E., Troppmair, J. and Rapp, U. R. (2002). Constitutive JNK activation in NIH 3T3 fibroblasts induces a partially transformed phenotype. *J. Biol. Chem. 277*, 29510-29518.

Rosales-Nieves, A. E., Johndrow, J. E., Keller, L. C., Magie, C. R., Pinto-Santini, D. M. and Parkhurst, S. M. (2006). Coordination of microtubule and microfilament dynamics by Drosophila Rho1, Spire and Cappuccino. *Nat. Cell. Biol*. *8,* 367-376.

Shevchenko, A., Wilm, M., Vorm, O. and Mann, M.(1996). Mass spectrometric sequencing of proteins silver-stained polyacrylamide gels. *Anal. Chem*. *68,* 850-858.

Sept, D. and McCammon, J A. (2001). Thermodynamics and kinetics of actin filament nucleation. *Biophys J, 81*, 667-674.

Schumacher, N., Borawski, J. M., Leberfinger, C. B., Gessler, M. and Kerkhoff. E. (2004). Overlapping expression pattern of the actin organizers Spir-1 and formin-2 in the developing mouse nervous system and the adult brain. *Gene. Expr Patterns*.4, 249-255.

Stenmark, H., Aasland, R., Toh, B. H. and D'Arrigo, A. (1996). Endosomal localization of the autoantigen EEA1 is mediated by a zinc-binding FYVE finger. *J. Biol. Chem, 27*, 24048-24054.

Stenmark, H. (2005). The FYVE finger: A Phosphoinositide Binding Domain. Chapter 19, Zinc-finger proteins: From Atomic Contact to cellular Function.

Steen, H. and Mann, M. (2004). The ABC's (and XYZ's) of peptide sequencing. *Nat Rev Mol Cell Biol. 5*, 699-711.

Schuh, M. and Ellenberg, J. (2008). A new model for asymmetric spindle positioning in mouse oocytes. *Curr Biol.18,* 1986-1992.

Shevchenko, A., Tomas, H., Havlis, J., Olsen, J. V. and Mann M. (2006). In-gel digestion for mass spectrometric characterization of proteins and proteomes. *Nat Protoc.1*, 2856-2860.

Small, J. V., Rottner, K. and Kaverina, I. (1999). Functional design in the actin cytoskeleton. *Curr. Opin. Cell. Biol.11*, 54-60.

Schmidt, A. and Hall, M.N. (1998). Signaling to the actin cytoskeleton. *Annu. Rev. Cell. Dev. Biol.14,* 305-338.

Schonichen, A. and Geyer, M. (2010). Fifteen formins for an actin filament: a molecular view on the regulation of human formins. *Biochem Biophys Acta. 1803*, 152-163.

Schüler, H. (2001). ATPase activity and conformational changes in the regulation of actin. *Biochem. Biophys.Acta.1549,* 137–147.

Theurkauf, W. E. (1994). Premature microtubule-dependent cytoplasmic streaming in cappuccino and spire mutant oocytes. *Science. 265*, 2093-2096.

Tournier, C., Dong, C., Turner, T.K., Jones, S. N., Flavell, R. A. and Davis, R. J. (2001). MKK7 is an essential component of the JNK signal transduction activated by proinflammatory cytokines. *Genes Dev. 15*, 1419-1426.

Tam, V.C., Serruto, D., Dziejman, M., Brieher, W. and Mekalanos, J.J. (2007). A type III secretion system in *Vibrio cholerae* translocates a formin/spire hybrid-like actin nucleator to promote intestinal colonization. *Cell. Host. Microbe 1,* 95–107.

Vertommen, D., Rider, M., Ni. Y., Waelkens, E., Merlevede, W., Vandenheede, J. R.and Van Lint, J. (2000). Regulation of protein kinase D by multisite phosphorylation. Identification of phosphorylation sites by mass spectrometry and characterization by site-directed mutagenesis. *J. Biol. Chem. 275*, 19567-19576.

Wellington. A., Emmons. S., James, B., Calley. J., Grover, M., Tolias, P. and Manseau, L. (1999). Spire contains actin binding domains and is related to ascidian posterior end mark-5. *Development. 126,* 5267-5274.

Wilm. M., Shevchenko, A., Houthaeve, T., Breit, S., Schweigerer, L., Fotsis, T. and Mann, M. (1996). Femtomole sequencing of proteins from polyacrylamide gels by nano-electrospray mass spectrometry. *Nature. 369,* 466-469.

Wang, X., Destrument, A. and Tournier, C. (2007). Physiological roles of MKK4 and MKK7: insights from animal models. *Biochem. Biophys. Acta. 1773,* 1349-1357.

Weston, C. R. and Davis, R. J. (2007). The JNK signal transduction pathway. *Curr Opin Cell Biol. 19,* 142-149.

Wallar, B.J., Stropich, B.N., Schoenherr, J.A., Holman, H.A., Kitchen, S.M., and Alberts, A.S. (2006). The basic region of the diaphanous autoregulatory domain (DAD) is required for autoregulatory interactions with the diaphanous-related formin inhibitory domain. *J. Biol.Chem. 281*, 4300–4307.

Weber, A. (1999). Actin binding proteins that change extent and rate of actin monomer-polymer distribution by different mechanisms. *Mol. Cell. Biochem. 190*, 67–74.

Winckler, B. and D.A. Schafer. (2007). Cordon-bleu: a new taste in actin nucleation. *Cell. 131,* 236–238.

Welch, M. D. and Mullins, R. D. (2002). Cellular control of actin nucleation. *Annu. Rev. Cell. Dev. Biol, 18*, 247- 288.

Weaver, A. M., Karginov, A. V., Kinley, A. W., Weed, S. A., Li, Y., Parsons,J. T. and Cooper, J. A. (2001). Cortactin promotes and stabilizes Arp2/3-induced actin filament network formation. *Curr. Biol. 11*, 370-374.

Wang, R.W., Yang, C.Y., Zhao, G.F. and Yang, J.X. (2005) Fragmentation effects on diversity of wasp community and its impact on fig/fig wasp interaction in *Ficus racemosa* L. *Journal of Integrative Plant Biology*. *47*, 20–26.

Wallar, B. J. and Alberts, A.S. (2003). The formins: active scaffolds that remodel the cytoskeleton. *Trends. Cell. Biol. 13*, 435-446.

Witze, E. S., Old, W. M., Resing, K. A. and Ahn, N. G. (2007). Mapping protein post-translational modifications with mass spectrometry. *Nature methods*. *4*, 798-806.

Xu, Y., Moseley, J.B., Sagot, I., Poy, F., Pellman, D., Goode, B.L. and Eck, M.J. (2004) Crystal structures of a Formin Homology-2 domain reveal a tethered dimer architecture. *Cell 116*, 711–723.

Yao, Z., Diener, K., Wang, X. S., Zukowski, M., Matsumoto, G., Zhou, G., Mo, R., Sasaki, T., Nishina, H., Hui, C. C., Tan, T. H., Woodgett, J. P. and Penninger, J. M. (1997). Activation of stress-activated protein kinases/c-Jun N-terminal protein kinases (SAPKs/JNKs) by a novel mitogen-activated protein kinase. *J. Biol. Chem. 272,* 32378-32383.

Yi, K., Guo, C., Chen, D., Zhao, B., Yang, B. and Ren, H. (2005). Cloning and functional characterization of a formin-like protein (AtFH8) from Arabidopsis. *Plant. Physiol. 138,* 1071-1082.

Zeth, K., Pechlivanis, M., Samol, A., Pleiser, S., Vonrhein, C. and Kerkhoff E. (2011). Molecular Basis of Actin Nucleation factor Cooperativity: CRYSTAL STRUCTURE OF THE SPIR-1 KINASE NON-CATALYTIC C-LOBE DOMAIN (KIND).FORMIN-2 FORMIN SPIR INTERACTION MOTIF (FSI) COMPLEX. *J Biol Chem*.*286*, 30732-30739.

Zigmond, S. H. (2004). Formin-induced nucleation of actin filaments. *Curr Opin Cell Biol. 16*, 99-105.